

The Influence of Water Table Oscillations on Pyrite Weathering and Acidification in Open Pit Lignite Mines

*Column Studies and Modelling of Hydrogeochemical and Hydraulic Processes
in the LOHSA Storage System, Germany*

Dissertation zur Erlangung des Doktorgrades

des Fachbereichs Geowissenschaften

der Freien Universität Berlin

vorgelegt von

Claus Kohfahl

Berlin 2003

Kohfahl, Claus:

The Influence of Water Table Oscillations on Pyrite Weathering and Acidification in Open Pit Lignite Mines : Column Studies and Modelling of Hydrogeochemical and Hydraulic Processes in the LOHSA Storage System, Germany

Claus Kohfahl. – Als Ms. gedr.. –

Berlin : dissertation.de – Verlag im Internet GmbH, 2004

Zugl.: Berlin, Freie Univ., Diss., 2003

ISBN 3-89825-774-6

Umschlagbild: Gestaltung: Susana Piñar Alvarez

Bibliografische Information Der Deutschen Bibliothek

Die Deutsche Bibliothek verzeichnet diese Publikation in der Deutschen Nationalbibliografie; detaillierte bibliografische Daten sind im Internet über <http://dnb.ddb.de> abrufbar.

Copyright dissertation.de – Verlag im Internet GmbH 2004

Alle Rechte, auch das des auszugsweisen Nachdruckes, der auszugsweisen oder vollständigen Wiedergabe, der Speicherung in Datenverarbeitungsanlagen, auf Datenträgern oder im Internet und der Übersetzung, vorbehalten.

Es wird ausschließlich chlorfrei gebleichtes
Papier (TCF) nach DIN-ISO 9706 verwendet.
Printed in Germany.

dissertation.de - Verlag im Internet GmbH
Pestalozzistraße 9
10 625 Berlin

URL: <http://www.dissertation.de>

Preface

The present study was conducted within the scope of the project “Influence of changing water levels and capillary fringes on the hydrogeochemical evolution of flooded lignite mines in the Lusatian Zone”, which was funded by the LAUSITZER MITTELDEUTSCHE BERGBAUVEREINIGUNG (LmbV) and the BUNDESMINISTERIUM FÜR BILDUNG UND FORSCHUNG (BMBF).

The thesis contains the following contributions by scientists, technicians, and students:

- The geophysical and geochemical properties of sediment cores and the chemical analyses of ground- and surface water were analysed by technical staff of the Department of Geological Sciences of the Free University of Berlin
- Some of the hydraulic and geochemical data were kindly provided by the Lausitzer und Mitteldeutsche Bergbau-Verwaltungsgesellschaft mbH (LMBV) and the BRANDENBURGER TECHNISCHE UNIVERSITÄT COTTBUS (BTU)
- Some data and results documented in chapter 3.1 and 3.4 were produced as part of two Diplom Theses (Greskowiak, 2002; Hamann, 2002).

Abstract

During and after the process of remediation by flooding of former pit mines, oscillations of the water level, caused by seasonal effects or management strategies, are often inevitable. In the study area LOHSA in the new eastern federal states of Germany, annual water oscillations due to management strategies are predicted to range between 5 and 8 m. This leads to oxygen input by air during the period of descending water levels, which causes pyrite oxidation in the surrounding sediments. When the water level is rising freshwater of the lake infiltrates into the groundwater and leads to additional input of oxygen. The resulting weathering products of the partly oxidized unsaturated zone are flushed into the groundwater and are discharged into the flooded lakes later. Also, acid builders, which originated in the elution zone at the lake front are transported into the flooded lake during the periods of falling water levels. To investigate the effect of water oscillations on acidification processes, different studies of the storage system LOHSA were combined. The aim of this research is to gain a better quantitative understanding of the hydrogeochemical system using model-based interpretations, which can be applied to other similar environments and which allow some first estimates with regard to the future acidification of the flooded lakes.

The first part of our research focuses on the quantitative effects of different moisture contents in the sediment with respect to acidification (chap.3.1). The objective of this study is the investigation of hydrogeochemical processes occurring in pyrite bearing sediments, which are dewatered due to falling groundwater levels. To quantify acidification by oxygen diffusion a column experiment was set up. The anoxic material used for this column experiment was taken from a core drilled in the southern periphery of the study area. After packing the column under anaerobic conditions it was drained and maintained in an unsaturated state for a period of one hundred days to allow oxygen delivery and pyrite weathering. During this period oxygen breakthrough curves were measured. These curves were modelled using SAPY, a one-dimensional reactive transport code based on the mixed cell approach, taking kinetics into consideration. To fit the measured breakthrough curves of oxygen the algorithm for the calculation of the tortuosity implemented in the source code of SAPY had to be adjusted. The experiment yielded comparatively high tortuosities for even small moisture contents, which is likely due to the strong heterogeneity of the sediment and the high proportions of silty material. Based on the modelling results an empirical equation was derived, describing the dependence of the effective coefficient of diffusion on the moisture content of the sediment. This equation was developed to assist in upscaling the laboratory results to field conditions for predicting the effects of ongoing processes of pyrite weathering in the unsaturated zone during a period of falling groundwater levels.

The objective of the second part of our research is to study the possibility of applying the results of the column study to field conditions. Therefore SAPY was upscaled to field conditions using the adjusted dependency of tortuosity on water content and verified by a measured oxygen and sulphate profile of the heap (chap. 3.2). The calculated results of the upscaled model did not fit the measured field data because tortuosities were overestimated in the model. The difficulty of upscaling is probably owing to the fact that the column study was conducted with soil moisture contents below 0.1 whereas in the field elevated moisture contents of ca. 0.2 were measured. Furthermore, high preferential pathways due to heterogeneities of the sediment structure may lead to smaller tortuosities. Also, the local variability of the sediment material in the heap may explain the mismatching between field data and laboratory data. The sediment in the observation well for the field measurements shows higher proportions of coarse grained material than the sediment of the column. The original dependency of tortuosity on moisture content implemented in the SAPY source code yielded a good fit of the measured oxygen profile in the field. Using the original source code of SAPY the input of sulphate from the unsaturated zone of the heap into the groundwater was calculated for a period of 80 years. Scenarios for a period of 80 years were simulated for different distances of the groundwater level to the subsurface and the mass input of sulphate from the unsaturated zone into the groundwater was calculated in terms of specific fluxes for different times. In future work the calculated source terms may be implemented in a regional three-dimensional groundwater model to predict the future evolution of the ground- and surface water in the study area.

Another aspect of our research (chap. 3.3) reports the hydrogeochemical modelling of reactions that take place during the uptake of weathering products by a rising water table into a partly oxidized, pyrite bearing sediment in a column study. The experiment is the continuation of the column study documented in chap. 3.1. After draining the column over a period of 100 days the column was flooded with distilled anoxic water from the bottom to the top with an average velocity of 5 cm per day. The water contents, oxygen contents, and the chemical composition were monitored over the profile of the column. The compositions of the water samples at different depths of the column were modelled with PHREEQC, a hydrogeochemical one-dimensional transport model. The measured concentrations could be reproduced with the model using the dual-porosity module, chemical equilibria, exchange reactions, and kinetic expressions for source terms of acids and acid builders. The aim of this study is to obtain a deeper understanding of the hydrogeochemical processes going on during uptake of weathering products due to rising water levels in the heaps of decommissioned pit mines.

In a final approach a two-dimensional vertical hydraulic model was built up using PROCESSING MODFLOW to obtain a rough initial estimate for the influence of water oscillations on acidification (chap. 3.4). The strong lateral migration of the shoreline due to a low morphologic gradient was simulated by the reservoir package. The modelled transient water fluxes were used to estimate the discharge of acid builders from the water-saturated part of the heap into the lake. The contribution of water oscillations to acidification was taken into account by a separate calculation of the release of weathering products in the unsaturated zone. The modelled scenarios indicate that the contribution to acidification by release of weathering products from the unsaturated zone is small in comparison to the mass input by acid mine drainage from the saturated zone of the heap.

Zusammenfassung

Während und nach der Durchführung von Rekultivierungsmaßnahmen an ehemaligen Braunkohletagebauen kann es betriebsbedingt oder saisonabhängig zu Wasserspiegelschwankungen kommen. In dem Untersuchungsgebiet des gefluteten ehemaligen Braunkohletagebaus LOHSA bei HOYERSWERDER liegen die Prognosen zukünftiger jährlicher Oberflächenwasserschwankungen zwischen 5-8 m. Dies führt während der Absenkphasen zu Sauerstoffeintrag in die angrenzenden Sedimente durch Luft und somit zur Pyritverwitterung und anschließendem Eintrag von Säurebildnern in das Grund- und Oberflächenwasser. In der Wiederanstiegsphase werden die Verwitterungsprodukte ins Grundwasser aufgenommen und gelangen mit zeitlicher Verzögerung in den Restsee. Zusätzlich kommt es während der Wiederanstiegsphasen durch infiltrierendes Restseewasser zu Sauerstoffeintrag ins Grundwasser und damit zur Freisetzung von Säurebildnern. Zur Untersuchung der Auswirkungen und Effekte der jährlichen bewirtschaftungsinduzierten Wasserspiegelschwankungen auf die hydrogeochemischen Versauerungsprozesse wurden Säulenversuche sowie geochemische und hydraulische Modellierungen durchgeführt. Hierdurch soll auf der Basis modellgestützter Interpretationen zunächst ein tieferes Verständnis für die hydrogeochemischen und hydraulischen Systemzusammenhänge im Untersuchungsgebiet gewonnen werden, welche dann generalisiert und auf andere Regionen übertragen werden können. Desweiteren sollen prognostische Abschätzungen im Hinblick auf die zukünftige Entwicklung der Wasserbeschaffenheit ermöglicht werden.

Der erste Teil der Forschungsarbeit untersucht Versauerungsprozesse, die mit sinkenden Grundwasserspiegeln in Verbindung stehen (Kap. 3.1). Zur Quantifizierung der Versauerung durch Diffusion von atmosphärischem Sauerstoff in entwässerte pyrithaltige Sedimente wurde ein Säulenversuch mit einer 2 m langen Säule durchgeführt. Das anaerobe Sedimentmaterial der Säule wurde aus einem Bohrkern im südlichen Anstrom des Speicherbeckens LOHSA II entnommen und wassergesättigt unter anaeroben Bedingungen in die Säule eingebaut. Nach der Entwässerung der Säule wurden die Durchbruchkurven des Sauerstoffs gemessen und mit dem Fortran Code SAPY, einem eindimensionalen reaktiven Transportmodell simuliert, welches kinetische Prozesse der Pyritverwitterung berücksichtigt. Zur Anpassung der gerechneten Sauerstoffdurchbruchkurven an die Messwerte musste die programminterne Berechnungsvorschrift der Tortuosität in SAPY angepasst werden. Die Versuchsergebnisse ergaben relativ hohe Tortuositäten selbst bei geringen Wassergehalten, was auf die schlechte Sortierung des Sediments und den hohen Feinkornanteil zurückgeführt werden kann. Ausgehend von Simulationsergebnissen der Modellkalibrierung wurde eine für das untersuchte Sediment charakteristische empirische Beziehung zwischen der Tortuosität und

dem Wassergehalt abgeleitet. Mit Hilfe dieser Gleichung soll eine Übertragung der im Labor beobachteten Verwitterungsprozesse auf Geländeverhältnisse im Speicherbecken LOHSA II ermöglicht werden.

Zur Untersuchung der prinzipiellen Anwendbarkeit der Ergebnisse des Säulenversuchs auf Geländeverhältnisse wurde das kalibrierte SAPY-Modell auf Geländeverhältnisse übertragen und mit einem Sulfat- und Sauerstoffprofil abgeglichen, welches an einer nur wenige Meter vom Bohrstandort der Säulensedimente entfernten Sickerwasser-Grundwasser-Messstelle gemessen wurde. Hierbei konnte die in dem Säulenversuch neu kalibrierte Beziehung zwischen Tortuosität und Wassergehalt nicht verifiziert werden, wohingegen die gemessenen Sauerstoff- und Sulfatprofile der Kippe mit der ursprünglich in dem Programmcode enthaltenen Beziehung zufriedenstellend nachgebildet werden konnten. Die Diskrepanz der Ergebnisse aus dem Säulenversuch und der Geländemessung kann durch mehrere Ursachen begründet sein. Zunächst liegen die Bodenwassergehalte des Säulenversuchs im Sediment unter 0.1, während die Geländewerte ca. 0.2 betragen, weshalb eine Extrapolation der Laborergebnisse auf Geländeverhältnisse problematisch ist. Weiterhin können bevorzugte Eintragspfade des Sauerstoffs entlang lagerungsbedingter Sedimentstrukturen im Gelände die Tortuositäten deutlich verringern. Ein weiterer Grund kann die lokale Variabilität des Kippenmaterials sein, welches an der Sickerwasser-Grundwassermessstelle höhere Anteile grobkörnigen Sedimentmaterials auswies, als das in der Säule verwendete Material. Der Sulfateintrag aus der ungesättigten Zone wurde deshalb mit dem ursprünglichen Programmcode für einen Zeitraum von 80 Jahren für verschiedene Flurabstände berechnet. Mit Hilfe dieser berechneten Quellterme können regionale Studien auf der Basis dreidimensionaler Grundwassermodelle durchgeführt werden.

Eine weitere Studie (Kap. 3.3) dokumentiert die hydrogeochemische Modellierung von beobachteten Reaktionen während des Aufsättigens ungesättigter, teilweise oxidierter Kippensedimente in einem Säulenversuch. Das anaerobe Sedimentmaterial entspricht dem Material des in Kap. 3.1 dokumentierten Säulenversuchs und hat einen anfänglichen Pyritgehalt von 0.04 Gew. %. Nach dem Packen der Säule wurde diese über einen Zeitraum von 100 Tagen drainiert und anschließend mit destilliertem anaerobem Wasser von unten nach oben geflutet. Während der gesamten Versuchsdauer wurden der Sauerstoffgehalt, der Wassergehalt sowie die hydrochemische Zusammensetzung des Flutungswassers analysiert. Die gemessene hydrochemische Entwicklung des Flutungswassers konnte mit PHREEQC, einem eindimensionalen reaktiven Transportcode unter Berücksichtigung von Kinetik, chemischen Gleichgewichten, Ionenaustauschprozessen und einem doppelt porösen Medium nachgebildet werden. Das Ziel dieser modellgestützten Interpretation des Säulenversuchs ist

das Erlangen eines tieferen und quantitativeren Verständnisses der bei der Aufsättigung von Kippensedimenten ablaufenden Prozesse.

In einer letzten Forschungsarbeit (Kap. 3.4) wurde ein zweidimensionales vertikales Grundwassermodell mit dem Simulator PROCESSING MODFLOW aufgebaut, um eine Abschätzung des quantitativen Beitrags der Wasserspiegelschwankungen auf die gesamte Versauerung im Untersuchungsgebiet vornehmen zu können. Die starke durch die Wasserschwankungen bedingte laterale Wanderung des Seeufers wurde durch das Modul RESERVOIR PACKAGE berücksichtigt. Auf der Grundlage der über die Strömungsbilanzen ermittelten instationären Volumenströme wurden die resultierenden Stofffrachten der Säurebildner aus dem gesättigten Kippenbereich in das Oberflächenwasser berechnet. Der Beitrag zur Versauerung durch den Säureeintrag aus der ungesättigten Zone wurde mittels separater Berechnungen berücksichtigt. Die simulierten Szenarien ergeben, dass der Beitrag wasserinduzierter Grundwasserschwankungen gering ist im Vergleich zum Eintrag der Säurebildner aus dem gesättigten Kippenbereich.

Content

Figures	XVII
----------------------	-------------

1 Introduction	1
-----------------------------	----------

1.1 Decommission of lignite mines	1
1.2 Study area	1
1.3 Major tasks	3

2 Previous studies	5
---------------------------------	----------

2.1 Geological setting.....	5
2.2 Hydrogeology of the study area	7

3 Methods and results	11
------------------------------------	-----------

3.1 Modelling oxygen diffusion and acidification for extremely heterogeneous pyrite bearing sediments based on a column study.....	11
--	----

3.1.1 Abstract	11
3.1.2 Introduction	11
3.1.3 Theory	13
3.1.3.1 Pyrite weathering	13
3.1.3.2 Overview of diffusion.....	14
3.1.4 Column experiment	16
3.1.5 Numerical Modelling	19
3.1.5.1 The program SAPY	19
3.1.5.1.1 General aspects	19
3.1.5.1.2 Diffusion coefficients.....	20
3.1.5.1.3 Kinetics	21
3.1.5.2 Calibration	23

3.1.5.3	Calculated sulphate and pyrite contents.....	27
3.1.6	Conclusions and Outlook	29
3.2	Deriving source terms of sulphate input for a hydraulic model using an upscaled reactive transport model	30
3.2.1	Abstract	30
3.2.2	Introduction	30
3.2.3	The reactive transport code SAPY	32
3.2.3.1	Program description	32
3.2.3.2	Calibration of tortuosity to moisture content	33
3.2.4	Upscaling and verification	34
3.2.4.1	Available data	34
3.2.4.2	Upscaling and verification	38
3.2.4.3	Sensitivity studies	41
3.2.5	Derivation of source terms	42
3.2.5.1	General aspects	42
3.2.5.2	Scenario simulation.....	43
3.2.5.3	Resulting source terms	46
3.2.6	Conclusions and Outlook	48
3.3	A reactive transport model for a flooding experiment using a column containing partly oxidized pyrite bearing sediments	50
3.3.1	Abstract	50
3.3.2	Introduction	50
3.3.3	Theory	52
3.3.3.1	Oxydation of pyrite and buffering	52
3.3.4	Methodology	53
3.3.4.1	Sediment parameters.....	53
3.3.4.2	Set up of the column	54

3.3.4.3	Initial conditions of the flooding experiment.....	56
3.3.4.4	Flooding of the column and sampling	58
3.3.5	Results	59
3.3.5.1	Column experiment.....	59
3.3.5.2	Boundary conditions and input parameters of the geochemical model	63
3.3.5.2.1	General aspects	63
3.3.5.2.2	Transport.....	65
3.3.5.2.3	Dual porosities	66
3.3.5.2.4	Solutions	66
3.3.5.2.5	Ion exchange	67
3.3.5.2.6	Dissolution and precipitation	67
3.3.5.2.7	Uptake of weathering products and oxygen.....	68
3.3.5.3	Calibration	70
3.3.5.4	Simulated results.....	73
3.3.6	Conclusions and Outlook	74
3.4	Estimating the effect of water table oscillations on acidification using a hydraulic model	76
3.4.1	Abstract	76
3.4.2	Introduction	76
3.4.3	Hydrogeological frame.....	78
3.4.4	Volumes of exfiltrating water	79
3.4.4.1	The hydraulic model	79
3.4.4.2	Model structure, boundary conditions and flow parameters.....	79
3.4.4.3	Calibration	82
3.4.4.4	Scenarios.....	82
3.4.4.5	Evaluation of the scenarios with respect to discharge of elution water and AMD .	83

3.4.4.6	Comparative calculations with respect to the elution zone.....	86
3.4.5	Acid charges of the exfiltrating water	87
3.4.6	Input of acids from the unsaturated zone	90
3.4.6.1	Uptake of weathering products	91
3.4.6.2	Diffusive oxygen delivery in the gas phase	92
3.4.6.3	Convective delivery of oxygen in gas phase.....	94
3.4.6.4	Oxygen delivery by seepage water	95
3.4.7	Conclusions and outlook	96
4	Combined conclusions and outlook	97
4.1	Field studies	97
4.2	Main results concerning column studies and geochemical modelling.....	98
4.3	Main results concerning hydraulic modelling	99
4.4	Outlook.....	100
	References	101

Figures

Fig. 1.1: Study area.	2
Fig. 1.2: Storage system Lohsa.	3
Fig. 2.1: Geologic map of the Lusatian zone (Nowel et al., 1994).	5
Fig. 2.2: Schematized profile of Tertiary and Quaternary sediments and the corresponding aquifers (GWL) before the start of mining activities (LMBV, 1997).	6
Fig. 2.3: Heap areas and Tertiary proportions (data provided by LmBV).	7
Fig. 2.4: Sulphate concentrations of ground- and surface water in the study area (data provided by LmBV).	8
Fig. 2.5: pH values of ground- and surface water in the study area (data provided by LmBV).	9
Fig. 3.1: Measured breakthrough curves of oxygen.	18
Fig. 3.2: Measured and calculated breakthrough curves of oxygen before calibration.	24
Fig. 3.3: Measured and calculated breakthrough curves of oxygen after calibration.	25
Fig. 3.4: Dependence of tortuosity on waterfilled porosity.	26
Fig. 3.5: Dependencies of effective diffusion on airfilled porosity (compiled from literature).	27
Fig. 3.6: Calculated sulphate and pyrite contents.	28
Fig. 3.7: Dependence of the tortuosity on water-filled porosity.	34
Fig. 3.8: Study area.	35
Fig. 3.9: Measured volumetric water fraction in the heap (data provided by the Faculty of Environmental Sciences and Process Engineering of the University of Cottbus)	36
Fig. 3.10: Measured partial pressure of oxygen in 2002 in the observation well (data provided by the Faculty of Environmental Sciences and Process Engineering of the University of Cottbus).	37
Fig. 3.11: Measured sulphate concentrations in the pore water (data provided by the Faculty of Environmental Sciences and Process Engineering of the University of Cottbus).	38

Fig. 3.12: Measured and calculated oxygen profiles (measured data provided by the Faculty of Environmental Sciences and Process Engineering of the University of Cottbus).....	40
Fig. 3.13: Measured and calculated sulphate concentrations after 30 years (measured data provided by the Faculty of Environmental Sciences and Process Engineering of the University of Cottbus).	41
Fig. 3.14: Sensitivity studies (measured data provided by the Faculty of Environmental Sciences and Process Engineering of the University of Cottbus).	42
Fig. 3.15: Simulated oxygen saturation for a period of 80 years.	44
Fig. 3.16: Calculated sulphate concentrations using a recharge of 190 mm/a.	45
Fig. 3.17: Calculated sulphate concentrations using a recharge of 100 mm/a.	46
Fig. 3.18: Source terms for sulphate at different depths assuming a natural recharge of 190 mm/a. (Source terms at 2.5 m are too small for visualization in this scenario).	47
Fig. 3.19: Source terms for sulphate at different depths assuming a natural recharge of 100 mm/a.	48
Fig. 3.20: Set up of the column for the flooding experiment.	55
Fig. 3.21: Measured oxygen breakthrough curves of column 1 before flooding.....	56
Fig. 3.22: Modelled evolution of pyrite contents with SAPY using calibrated tortuosities.	57
Fig. 3.23: Analyzed Ca^{2+} - and SO_4^{2-} -concentrations of the uppermost part of the water column during flooding.	59
Fig. 3.24: Analyzed Na^+ - Cl^- and $\text{Fe}^{2+/3+}$ concentrations of the flooding front at different heights in the column.	60
Fig. 3.25: Analyzed molar $\text{Ca}^{2+}/\text{SO}_4^{2-}$ ratios at different times and sampling points.	61
Fig. 3.26: Normalized concentrations of sulphate, Ca^{2+} , Na^+ and $\text{Fe}^{2+/3+}$ at 83 cm column height.	62
Fig. 3.27: Relative amounts of cations analyzed after 25 and 32 days of flushing at 63 cm height of column.	63
Fig. 3.28: Observed and calculated pH values.	70
Fig. 3.29: Observed and calculated sulphate concentrations.	71
Fig. 3.30: Observed and calculated iron concentrations.	72
Fig. 3.31: Observed and calculated concentrations of Na.	72

Fig. 3.32: Observed and calculated Ca^{2+} concentrations.	73
Fig. 3.33: Calculated breakthrough curves of sulphate at different heights of the column.....	74
Fig. 3.34: Study area.	77
Fig. 3.35: Hydrogeological sketch.	78
Fig. 3.36: Location of the vertical hydraulic model.....	80
Fig. 3.39: Water discharge from the heap into the lake.	85
Fig. 3.40: schematic sketch of the simulated evolution of distant groundwater levels.....	86
Fig. 3.41: Annual acid charges of the groundwater.	90
Fig. 3.42: Compiled amounts of acid input due to groundwater discharge and ongoing weathering processes.....	95

Tables

Tab. 3.1: Sediment parameters	17
Tab. 3.2 Input parameters.....	23
Tab. 3.3: Input parameters for the upscaled model	38
Tab. 3.4: Sediment parameters of the material used in the column study.....	54
Tab. 3.5: Reactive zones of the column	64
Tab. 3.6: Transport parameters	65
Tab. 3.7: Defined mixing factors of the column for the simulation.....	66
Tab. 3.8: Initial solution defined for the column.....	66
Tab. 3.9: Compiled stoichiometries and rate laws for uptake of weathering products and oxygen (F_{O_2} [mol/m ² /s]: oxygen flux; C_s : concentration of solid species [meq/100g]; λ :dissolution constant [s ⁻¹]; D_e : effective diffusion coefficient [m ² /s]; O_2 : oxygen concentration [mol/l]; n : effective porosity; p_{O_2} : partial pressure of oxygen [atm])	68
Tab. 3.10: Neutralization potential of acid mine drainage according to eq. 3.37 using analyzed groundwater samples	89
Tab. 3.11: Assumed neutralization potential NP_2 according to eq. 3.37.....	89
Tab. 3.12: Analyzed sediment parameters	91
Tab. 3.13: Input data for calculation of oxygen diffusion.....	93
Tab. 3.14 Input parameters for convective oxygen delivery in gas phase	94

1 Introduction

1.1 Decommission of lignite mines

Brown coal surface mining pits are anthropogenically disturbed geological systems. In the new federal states of Germany, the digging of these open pits often required an extensive lowering of the water table by several tens of meters and the removal of large quantities of overburden material, which consist mostly of Quaternary and Tertiary sediments with sulphide-bearing minerals such as pyrite and marcasite. Mineral reactions such as oxidation of primary iron disulfides (pyrite, marcasite) release iron, sulphate and other minor but hazardous elements to soil, surface water and groundwater. The main source of hazard is the oxidation of iron disulfides in the dump sediments due to penetration of oxygen and oxygen-rich waters, accelerated by microorganisms. Primary oxidation of the sediments begins during dewatering of the originally layered material prior to mining. Aeration is intensified during the mining process owing to excavation, mixing and dumping activities. After deposition, secondary pyrite oxidation continues in the aerated upper part of the spoils, possibly over a period of several decades. After decommissioning a mine, standard procedure is to allow the water table to rise and to convert the pit into a lake for recreational purposes. During flooding, which often extends over several years or even decades, acid builders and other chemical contents in the groundwater are flushed into the newly formed lake (Gerke, 1998). To reduce the acid input, flooding is sometimes performed not by natural groundwater rise but by surface water.

1.2 Study area

The study area belongs to the Lusatian mining district and is situated in the new federal states of Germany (Fig. 1.1).



Fig. 1.1: Study area.

In the Lusatian region of eastern Germany, brown coal (lignite) has been extracted from large open-pit mines for over 50 years. The study area is the LOHSA lignite mine near HOYERSWERDA in Germany. Mining activities in the LOHSA storage system started in the early fifties and stopped in 1984. During this time the groundwatertable was lowered by dewatering up to ca. 40 m and the pumped groundwater was discharged into the river SPREE. After decommissioning the mine pumping activities stopped and the groundwatertable started to rise and began to replenish the three separate basins DREIWEIBERN, LOHSA II and BURGHAMMER (Fig. 1.1), whereas the discharge of the SPREE started to decrease. To avoid major acidification of these originating surface waters, flooding by natural rise of acid groundwater was combined with flooding by surface water. This has been realised by applying the concept of a “Bypass System” using the river KLEINE SPREE and SPREE. Therefore specific amounts of the discharge of the two rivers have been channelled into the respective lakes. The flow directions and the connecting passages are illustrated in (Fig. 1.2).

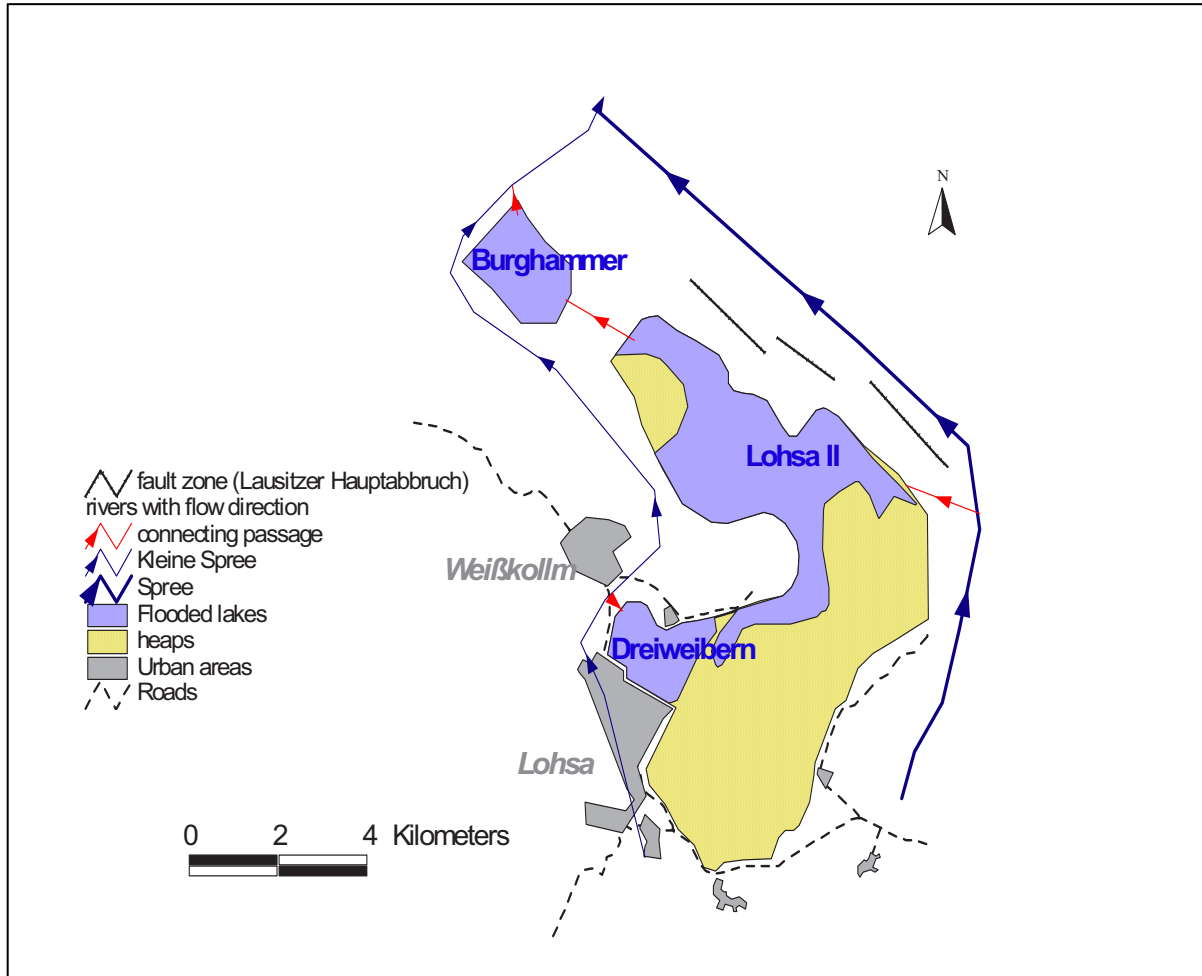


Fig. 1.2: Storage system Lohsa.

Flooding with surface water started in 1996, when part of the flow of the KLEINE SPREE was discharged into DREIWEIBERN. The flooding of LOHSA II with surface water started in 2001. Whereas the aspired water level has already been achieved in DREIWEIBERN, the basin LOHSA II is to be flooded, mainly with surface water, by 2005 and will afterwards be used as a reservoir basin to regulate the discharge of the SPREE (LMBV AND COTTBUS, 1996). To provide a certain minimum discharge of the river during the summer, present management strategies are predicting annual surface water oscillations between 5 and 8 m.

1.3 Major tasks

The bank filtrate of the SPREE is used for drinking water supply in a couple of water plants downstream of the storage system LOHSA. Therefore the water quality of the river water, which is dependent on the long-term hydrogeochemical evolution of LOHSA II, constitutes an important factor for present and future generations in this region. In this regard sulphate is of special interest because of its conservative behaviour and due to the present high sulphate concentrations in Berlin, which are already exceeding its threshold value of 240 mg/l.

Furthermore the entire hydrological system, especially with regard to the nature protection area SPREEWALD, which is also located downstream of LOHSA II, is very sensitive to changes of the water quality of the river SPREE.

The purpose of this research was to answer the following questions:

- 1 Which acidification potential can be expected in the surrounding heaps and sediments?
- 2 Which hydrogeochemical processes are going on in the heap sediments during the period of descending and rising groundwater levels?
- 3 Which are the long-term source terms of sulphate released from the unsaturated zone of the heaps?
- 4 Which are the main factors controlling the future acidification of LOHSA II?
- 5 What is the influence of water oscillations on the acidification processes?
- 6 In which amounts will acid builders be released from the heaps into the lake during the next 30 years?

Due to the complexity of this topic, in which gas-, liquid- and solid phases have to be considered, sophisticated methods and modelling approaches have to be applied. To predict the long-term hydrogeochemical evolution of the LOHSA storage system the temporal future trend of the different inflows has to be characterized with regard to its quantity and quality. The inflows are predominantly surface water from KLEINE SPREE and SPREE and the acid mine drainage from the surrounding sediments. Within this study different studies have been completed including water- and sediment-sampling, column studies and hydraulic and geochemical modelling. In future work it is planned to combine these results with regional studies and modelling approaches of the storage system LOHSA II realized at the BRANDENBURG-TECHNISCHE UNIVERSITÄT COTTBUS (BTU) in order to gain a better understanding of this complex hydrogeochemical system.

which has a max. vertical thickness of 14 m. This coal seam has been exploited in our study area (Fig. 2.2).

The Tertiary sediments are overlaid by Quaternary sediments with a thickness of 40-60 m. Due to its glacial environment these sediments are built up of marls and glaciofluvial sands. Typical Quaternary sediment structures are moraines, glacial valleys and deeply eroded channels which have been subsequently filled by fluvial sands. Fig. 2.2 shows an erosive channel structure filled with Quaternary sediments. The Quaternary basement in our study area dips stratigraphically towards the south and reaches its max. depth at the top of the second coal seam resulting in a mainly Quaternary overburden of the exploited lignite. In the northern part of the Lusatian mine district the overburden of the coal seams shows higher proportions of Tertiary sediments. Considering the fact that Tertiary sediments in this area have a higher pyrite content, it becomes evident that the acidification potential of the heaps is a direct function of its amount of Tertiary material. As the Quaternary sediments are partly built up from removed Tertiary material, its pyrite content and acidification potential still has to be taken into consideration.

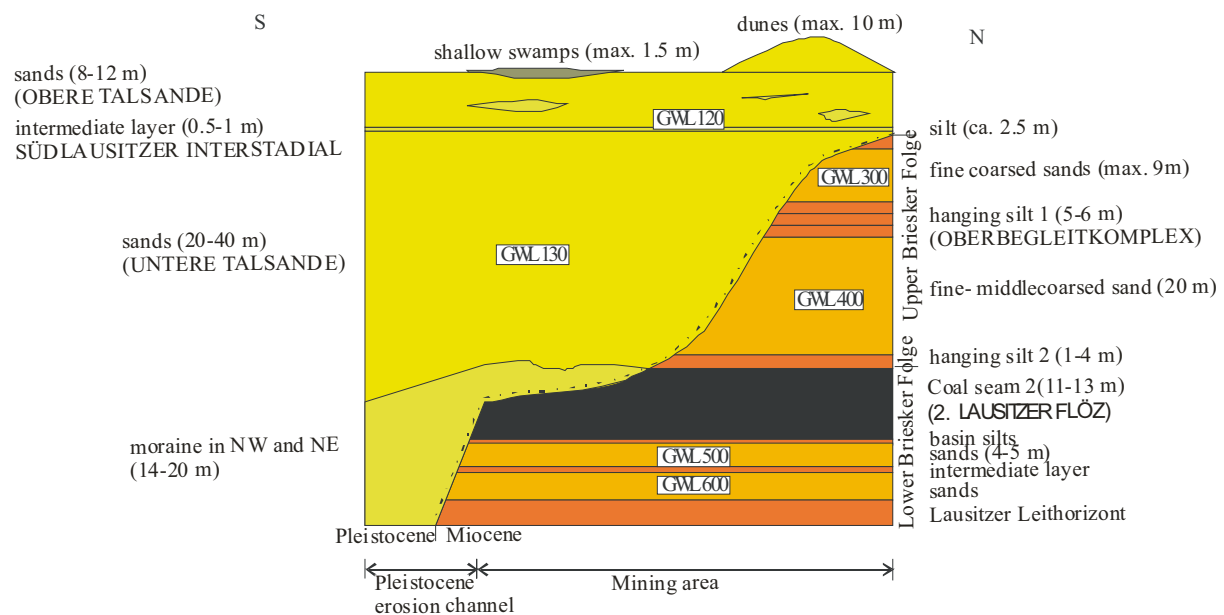


Fig. 2.2: Schematized profile of Tertiary and Quaternary sediments and the corresponding aquifers (GWL) before the start of mining activities (LMBV, 1997).

The exploited coal seam in the study area is of Lower Tertiary age and is covered by 40 to 60 m of overburden of predominantly Quaternary sediments, which mainly constitute the material of the present heaps. The original sediments of the study area are mostly Quaternary sands of the stratigraphic units OBERE TALSANDE and UNTERE TALSANDE. The fault zone LAUSITZER HAUPTABBRUCH northeast of LOHSA II (Fig. 2.3) has uplifted some

Tertiary sediments, leading to sporadic outcrops of this material, which is characterized by a high acidification potential.

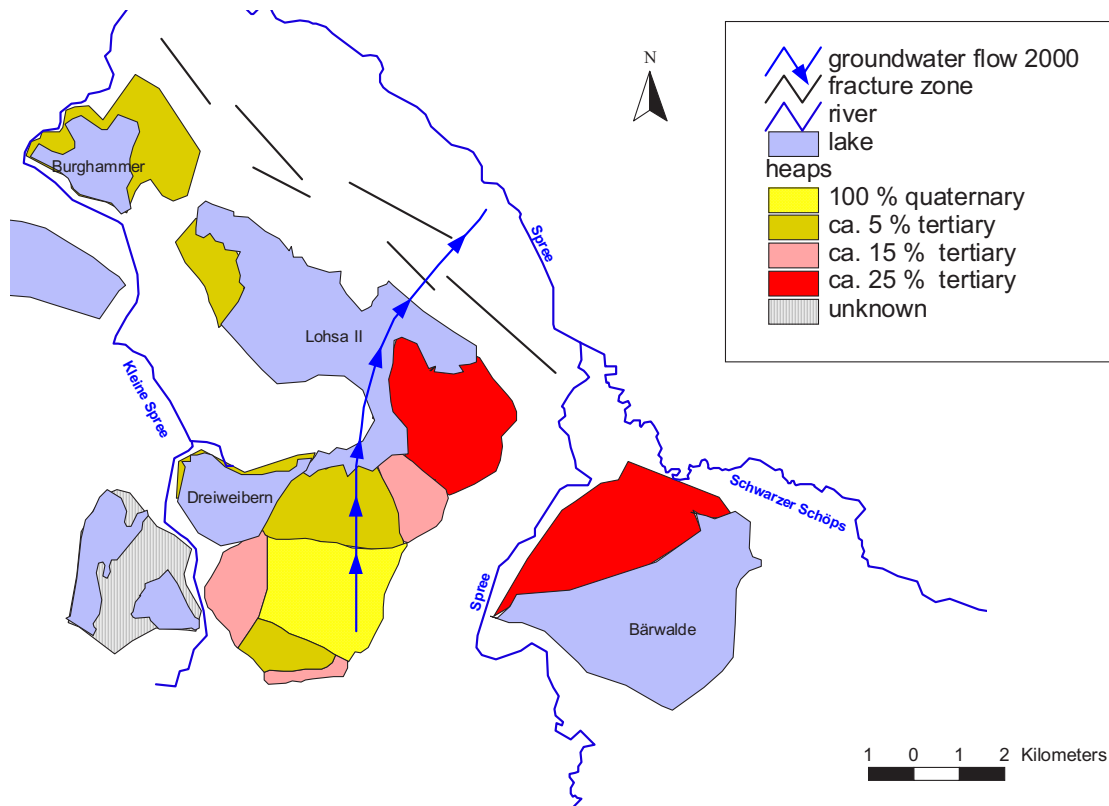


Fig. 2.3: Heap areas and Tertiary proportions (data provided by LmbV).

The biggest heap areas are south of LOHSA II and have a max. extension of 4 km from north to south (Fig. 2.3). These heaps have an average thickness of 30-40 m and are built up mainly of Quaternary material although the heaps in the southeastern part show Tertiary amounts of ca. 25 %. The white areas in Fig. 2.3 are composed mainly of original Quaternary sediments (OBERE/UNTERE TALSANDFOLGE).

2.2 Hydrogeology of the study area

Fig. 2.2 illustrates the aquifer system of our study area before mining activities started. This aquifer system can be subdivided in 6 different aquifers (Nowel et al., 1994). The most important ones, which exfiltrate directly into the surface water are the two uppermost Quaternary aquifers and the heaps. The groundwater flow in these uppermost aquifers was reconstructed using hydroisolines provided by LMBV. In the southern region it is orientated to the north. More to the north the flow direction changes to northeast towards the active

lignite mine at NOCHTEN, where the groundwater is lowered artificially by pumping (Fig. 2.3).

The hydrogeochemical parameters of our system were analysed on the basis of sampling data from 1991-2000 provided by LMBV and are illustrated by the parameters sulphate and pH. The sulphate concentrations of the groundwater in Fig. 2.4 show a clear dependency on the Tertiary proportion of the surrounding sediments. The highest values - between 2500 and 4000 mg/l (50-80 meq/l) - were analysed southeast of LOHSA II, where the heap shows a Tertiary fraction of 25 %. The water quality of LOHSA II depends mainly on the proportion of surface- and groundwater used for flooding. As flooding in LOHSA II had been achieved exclusively by rising groundwater until the date of sampling, high sulphate concentrations were measured here. The lowest sulphate concentrations have been measured in DREIWEIBERN, which had been flooded with great amounts of surface water.

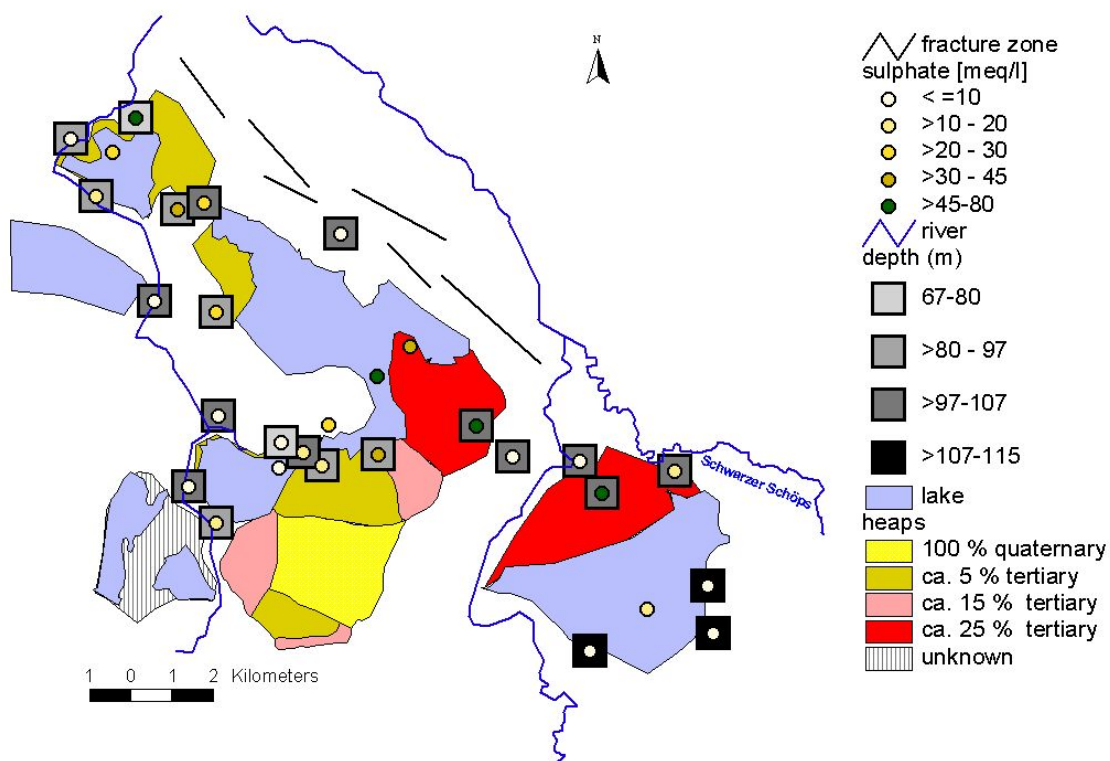


Fig. 2.4: Sulphate concentrations of ground- and surface water in the study area (data provided by LmbV).

The analysed pH values can be interpreted analogously to the sulphate concentrations (Fig. 2.5). The pH of groundwater shows a high dependency on the Tertiary amount of the surrounding sediments and the pH of the surface water depends on the amount of SPREE water used during flooding. The pH of the surface water in LOHSA II is lower than in the

groundwater of the catchment area owing to the release of protons during the formation of Fe-oxyhydroxides in aerobic surface water.

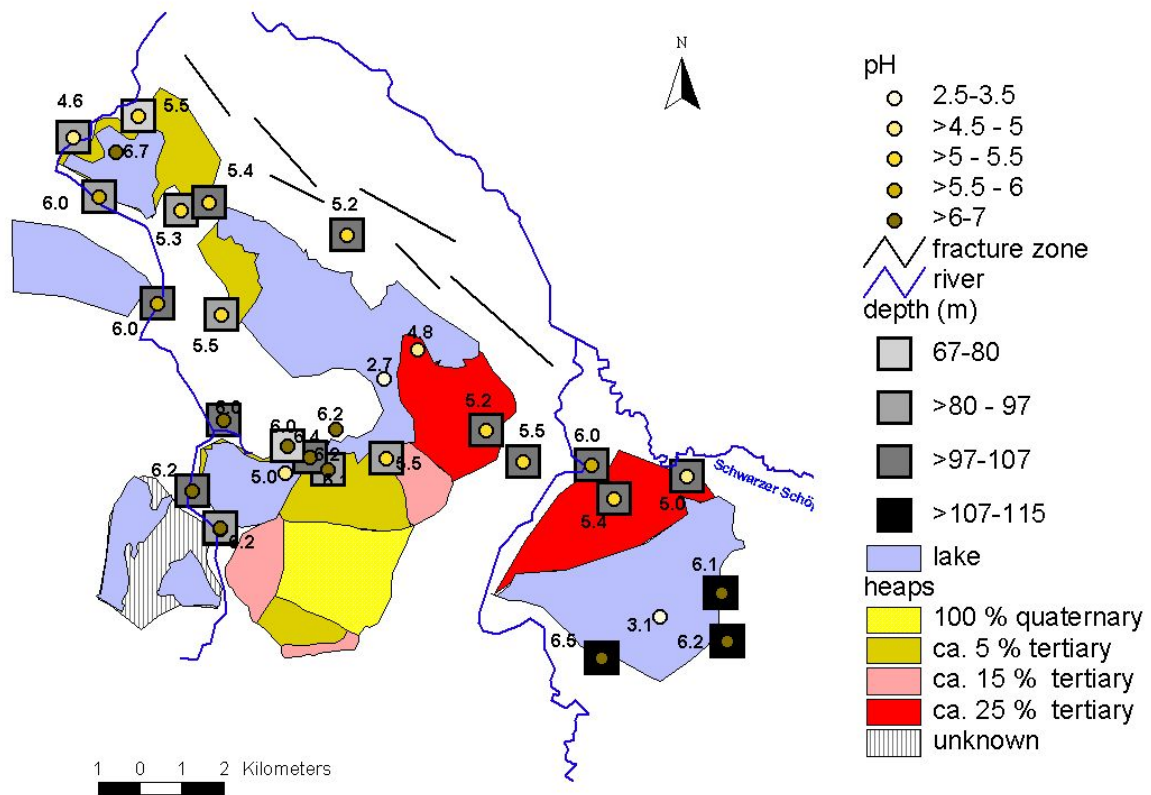


Fig. 2.5: pH values of ground- and surface water in the study area (data provided by LmBV).

3 Methods and results

3.1 Modelling oxygen diffusion and acidification for extremely heterogeneous pyrite bearing sediments based on a column study

3.1.1 Abstract

Our research focuses on the quantitative effects of different moisture contents in the sediment with respect to acidification. To quantify acidification by oxygen diffusion into pyrite bearing, very heterogeneous dump sediments, a column experiment was set up and oxygen saturation and moisture content were monitored over 100 days. The anoxic material used for the column experiment was taken from a core drilled in the southern periphery of the study area. The measured oxygen breakthrough curves were modelled using SAPY, a one-dimensional reactive transport code based on the mixed cell approach, taking kinetics into consideration. Based on the modelling results for the extremely heterogeneous sediments an empirical equation was derived, describing the dependence of the effective coefficient of diffusion on the moisture content of the sediment. This equation was developed in order to provide a helpful means for upscaling laboratory results to field conditions.

3.1.2 Introduction

Major environmental problems of abandoned lignite mines are caused by weathering of sulphide minerals within the aerated zone of the heaps. Mineral reactions such as oxidation of primary iron disulfides (pyrite, marcasite) release iron, sulphate and other minor but hazardous elements to soil, surface water and groundwater. The main source of hazard is the oxidation of iron disulfides in the dump sediments due to penetration of oxygen and oxygen-rich waters, accelerated by microorganisms as *Thiobacillus ferrooxidans* (Kleinmann and Crerar, 1979). During dewatering of the originally layered material prior to mining primary oxidation of the sediments begins. Aeration is intensified during the mining process owing to excavation, mixing and dumping activities. After deposition, secondary pyrite oxidation continues in the aerated upper part of the spoils, possibly over a period of several decades. The acidification caused by ongoing oxidation of sulphides is limited mainly by the delivery of oxygen, which is controlled predominantly by the tortuosity of the unsaturated zone. The

tortuosity depends on the moisture content as well as on the specific soil geometry and is of major concern in this problem. A general dependency on the moisture content applicable to all types of sediments cannot be formulated.

For long-term predictions, the flux of oxygen from the ground surface is therefore a limiting factor (Davis and Ritchie, 1986; Schwan et al., 1988). Most models to date consider one-dimensional vertical diffusion of oxygen within the heap based on Fick's first law (Bronswijk et al., 1993). The representation of oxygen consumption is normally based on either first-order kinetics (Elberling et al., 1994) or on a shrinking core model (Davis and Ritchie, 1986). Some further models also include O₂ diffusion and transport reactions (Hecht et al., in press; Prein and Mull, 1995; Wunderly et al., 1996). Refsgaard developed an oxygen transport and consumption model as a submodel to a general numerical model for solute transport in the unsaturated zone (Refsgaard et al., 1991).

Long term predictions of the hydrogeochemical evolution in abandoned lignite mine environments have been mostly based on homogeneous distributions of hydraulic and geochemical properties (Rogowski et al., 1977) and on aqueous-phase chemistry in batch experiments (Karathanasis et al., 1990; Kleinmann et al., 1981). Two- and three-dimensional reactive transport simulations from mine waste sites were also performed (Brand, 1996; Walter et al., 1994a; Walter et al., 1994b).

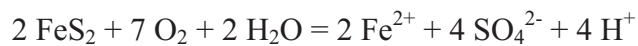
In this study we use a one-dimensional numerical simulator of the oxidation process which couples the diffusive delivery of oxygen with geochemical reaction kinetics. To provide a first quantitative estimate of acidification due to ongoing pyrite weathering in the unsaturated zone of the heap sediments a column experiment was set up measuring oxygen and moisture contents. The ongoing processes were interpreted by the simulation of the measured oxygen breakthrough curves with the numerical reactive transport code SAPY (Prein and Mull, 1995). The model was calibrated on the basis of the effective coefficients of diffusion at various depths of the column, and a dependency of the diffusion coefficient on the moisture content was derived for these sediments.

3.1.3 Theory

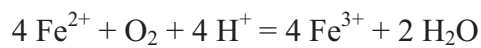
3.1.3.1 Pyrite weathering

The following equations show the generally accepted sequence of pyrite reactions (Stumm and Morgan, 1996):

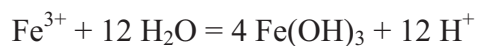
eq. 3.1



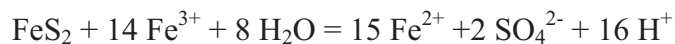
eq. 3.2



eq. 3.3



eq. 3.4



In the initial step, pyrite reacts with oxygen and water to produce ferrous iron, sulphate and acidity (eq. 3.1). The second step involves the conversion of ferrous iron to ferric iron (eq. 3.2). This second reaction is the rate determining step for the overall sequence and depends on the available amount of oxygen. At lower pH the reaction is catalyzed biologically. As oxygen delivery in sediments is mainly controlled by diffusion, reaction time is strongly reduced in sediments that are not exposed to the atmosphere. The third step involves the hydrolysis of ferric iron with water to form the solid ferric hydroxide (ferrihydrite) and the release of additional acidity (eq. 3.3). This third reaction is pH dependent and normally does not take place if pyrite is present. Under very acid conditions of less than about pH 3.5, the solid mineral does not form and ferric iron remains in solution. The fourth step (eq. 3.4) involves the oxidation of additional pyrite by ferric iron and represents the most important reaction. The ferric iron is generated by the initial oxidation reactions in steps one and two depending on the oxygen supply. This cyclic propagation of acid generation by iron takes place very rapidly and continues until the supply of ferric iron or pyrite is exhausted. Oxygen is not required for the fourth reaction to occur.

The main buffering reactions are carbonate and silicate buffering and sorption by clay minerals. Carbonate buffering neutralizes pH-values and results in low iron and heavy metal concentrations, while sulphate concentrations are limited to some thousands mg/l controlled by the solubility of gypsum. Clay minerals retard the pollutants, thus resulting in decreased concentrations spread out over longer emission times.

Oxidation of pyrite and subsequent secondary reactions may result in large concentrations of sulphate, Fe and Al in solution and pH values of less than 2 (Wisotzky, 1996). Secondary reactions under aerobic conditions, the generation of acid mine drainage (AMD) and buffer reactions during leaching have already been studied intensively by X-ray diffractometry (XRD) (Bigham et al., 1996; Nordstrom, 1982; van Breemen and Harmsen, 1975).

Oxidation of pyrite is limited by the specific grain surface, by the availability of oxygen and by the maximum seepage water concentration. The dissolution rate at the surface of the pyrite grain is linearly dependent on the quantity of grain surface available (Kölling and Schüring, 1994). The pyrite weathering rates decrease significantly in seepage water with pH values below 2 (Kölling, 1990). Also there is a pH dependent limitation of the solubility of sulphate and iron in water. The availability of oxygen depends on the delivery through the sediment and occurs in the gas phase via convection and molecular diffusion. Additionally oxygen can be delivered by percolating water in the unsaturated zone of the sediment.

3.1.3.2 Overview of diffusion

Since large amounts of oxygen are needed for pyrite weathering, oxygen recharge within the sediment body is critically important. Gaseous diffusion in the sediment occurs through the air porosity and is considered to be the most important process causing gaseous interchange between sediment and atmosphere (Troeh et al., 1982).

Experimental data in the literature show that diffusive gas transport is directly proportional to a diffusion coefficient D_0 , and to the gas concentration gradient. The general equation for open gaseous flow can be formulated by Fick's Law:

eq. 3.5

$$F = D_0 * \frac{\Delta C}{z}$$

with:

$F =$	oxygen flux in $\text{mol s}^{-1} \text{m}^{-2}$
$D_0 =$	molecular coefficient of diffusion in gas in $\text{m}^2 \text{s}^{-1}$ (for standard conditions)
$C =$	concentration of oxygen in mol m^{-3}
$z =$	distance in m

Applied to the diffusion through a porous medium Fick's Law may also be written as (Troeh et al., 1982):

eq. 3.6

$$F = D_0 * n_a * \frac{\Delta C}{z} * \frac{1}{Tort^2}$$

where n_a stands for airfilled porosity and $Tort$ represents tortuosity.

The tortuosity is defined as the ratio of the actual path length taken by a particle in a porous medium, over the straight line distance. It is a material parameter and depends on the sediment structure and the moisture content. The actual path length usually cannot be measured directly but it can be calculated by other measurements.

Currie (Currie, 1970) formulated the following analytical expression to relate the variable D/D_0 to soil structure parameters:

eq. 3.7

$$D/D_0 = n_a/Tort^2$$

where D [$\text{m}^2 \text{s}^{-1}$] represents the effective diffusion coefficient, which corresponds to the molecular diffusion coefficient corrected for airfilled porosity (n_a) and tortuosity ($Tort$).

Usually the complex geometries of soils and other similar materials make it necessary to use equations that empirically relate the variable D/D_0 to soil structure parameters. Two equations widely used in technology are (Troeh et al., 1982):

eq. 3.8

$$D/D_0=a(n_a-b)$$

and:

eq. 3.9

$$D/D_0=K n_a^m$$

where a and b as K and m are determined by fitting curves to experimental data. Marshall, Millington and Penman derived different empirical solutions using eq. 3.9 as illustrated in Fig. 3.5 (Marshall, 1959; Millington, 1960; Penman, 1940).

3.1.4 Column experiment

The material used for the column experiments was taken from a core of a heap in the southern periphery of the former open-pit mine LOHSA II. The anoxic sediment was taken from the water saturated zone in a depth of 23-25 m below subsurface and has been conserved under anoxic conditions in an airtight plastic liner. The site is located in an existing dump of dominantly Quaternary material with a thickness of about 40 m. The material consisted of fine sands and lignite fragments. The chemical characteristics of the material are compiled in Tab. 3.1.

Tab. 3.1: Sediment parameters

Parameters	Values	Analytical Method
Pyrite content [weight-%]	0.04	iodometric
Organic carbon content [weight-%]	0.50	LECO
Anorganic carbon [weight-%]	0.10	LECO
[H ⁺] (mM/kg)	25.00	Batch experiment with H ₂ O ₂
H _{CEC} (mM/kg)	0.05	CEC (diluted with BaCl ₂)
CEC (meq/kg)	20.00	CEC (diluted with BaCl ₂)

[H⁺] (mM/kg) is the concentration of protons per kg dry soil, which has been diluted by H₂O₂ (30 %). H_{CEC} (meq/kg) is the concentration of adsorbed protons per kg dry soil. The sediment has a relatively low pyrite content. The small content of anorganic carbon indicates a low buffer capacity.

A plexiglass column (200 cm length, 10 cm i.d.) was prepared along the profile with 10 suction cups, 10 TDR-probes for measuring moisture content, and 20 fiber optic oxygen probes. The technique for construction of the oxygen probes was developed by H. HECHT and M. KÖLLING (Hecht and Kölling, 2001). To allow discharge and control of water level a lower outlet was prepared below the column. The water level was controlled by a transparent tube connected with the lower outlet. At the bottom of the column a 3 cm thick filter-layer of inert quartz sand was placed to distribute flow and to prevent obstruction by smaller particles. The column was packed with the homogenized sediment adding a small amount of anoxic distilled water to minimize contact with atmospheric oxygen. After packing the column, water was discharged from the lower outlet until a hydraulic head of 50 cm measured from the bottom of the column was reached.

Over a hundred-day period oxygen saturation and moisture content were measured at different depths of the unsaturated zone in the column. The moisture contents stayed more or less constant during the experiment and ranged between 7 vol-% in the upper TDR-probes and 30 vol-% in the lower probes of the unsaturated zone. To make the system as simple as possible,

the experiment has been performed without irrigation of the column; thus no water samples have been taken.

The measured breakthrough curves are shown in Fig. 3.1.

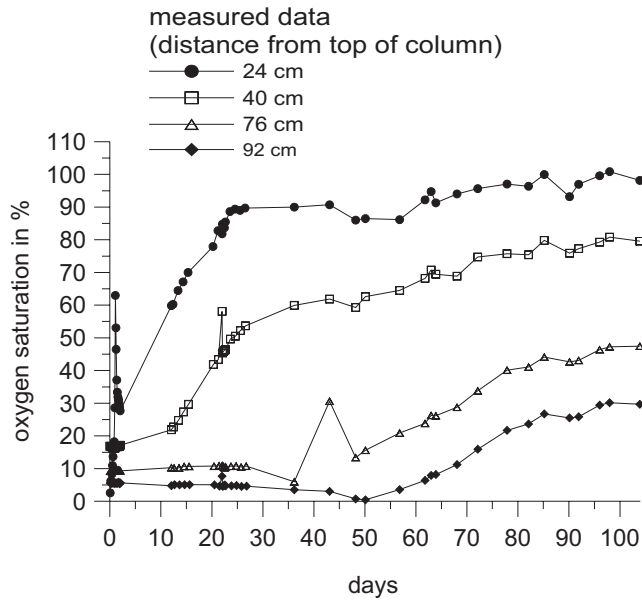


Fig. 3.1: Measured breakthrough curves of oxygen.

The oxygen saturation increased from nearly 0 % in all oxygen probes to full saturation in the upper probes and 20-30 % in the lower parts of the column. The measured breakthrough curves show an immediate sharp increase of oxygen saturation from the beginning of the experiment in the uppermost part of the column. The lower probes indicate an increasing delay of oxygen rise due to the presence of pyrite, whose oxidation constitutes a sink term for oxygen. As soon as all pyrite has been oxidized, the oxygen saturation begins to increase due to delivery of oxygen by primarily molecular diffusion. Thus the rise of the breakthrough curves shows the propagation of the depyritization depth. The propagation of the depyritization depth leads to smaller gradients of oxygen concentration in the column and causes flattening slopes of the breakthrough curves. The velocity of the propagation of the depyritization depth also decreases with time.

To achieve a quantitative understanding of the ongoing processes and to obtain an instrument to upscale these results to field conditions in LOHSA, the column experiment has been modelled with SAPY (Prein, 1993).

3.1.5 Numerical Modelling

3.1.5.1 The program SAPY

3.1.5.1.1 General aspects

The experimental results were modelled using SAPY (Prein, 1993), a one-dimensional reactive transport mixed cell model, which has been developed especially for the simulation of pyrite weathering. The numerical algorithm couples transport of the reactants by diffusion and advection in water and air with chemical reactions of pyrite weathering as source/sink terms including biological catalysis.

For each cell the following phases are differentiated:

- gas phase calculating convective transport of air, diffusion of oxygen and nitrogen
- water saturated phase where diffusive and convective transport of oxygen and reaction products (SO_4^{2-} , Fe^{2+} and H^+) are calculated
- solid phase with kinetical controlled chemical reactions of pyrite weathering

Diffusive and convective transport of oxygen and weathering products are calculated by the mixed cell approach of eq. 3.10

eq. 3.10

$$n_e \frac{\partial c}{\partial t} = D \frac{\partial^2 c}{\partial x^2} - n_e u \frac{\partial c}{\partial x} \pm Q n_e$$

where c = concentration, u = seepage-velocity, D = effective diffusion coefficient, n_e = effective porosity and Q = source-sink term.

Distribution of oxygen between water and atmosphere is calculated according to Henry's Law. Source and sink terms of O_2 , Fe^{2+} , Fe^{3+} , SO_4^{2-} , FeS_2 and H^+ are calculated according to Stumm & Morgan (Stumm and Morgan, 1981) based on the available amount of oxygen in water. Convection in water is simulated using a constant flow velocity of seepage water.

3.1.5.1.2 Diffusion coefficients

The diffusion coefficient is corrected for temperature and pressure, moisture content and tortuosity. The influence of pressure and temperature is corrected by eq. 3.11.

eq. 3.11

$$D' = D \frac{T}{273.16K} * \left(\frac{1013hPa}{p} \right)$$

where:

D' = diffusion coefficient corrected for temperature and pressure

D = molecular diffusion coefficient in gas (25 °C and 1 atm)

T = temperature in Kelvin

p = pressure in hPa

The influence of the moisture content on the diffusion coefficient is considered by the concept of tortuosity factor according to Albertsen (Albertsen, 1977). The tortuosity factor of Albertsen corresponds to the square of tortuosity (eq. 3.12)

eq. 3.12

$$D'' = n_a * \frac{D'}{tortfac}$$

where:

n_a = airfilled porosity

D'' = effective diffusion coefficient

$tortfac$ = tortuosity factor

The tortuosity factor is calculated in SAPY for perturbed sediments as follows:

eq. 3.13

For $n_a/n > 0.2$: $\frac{1}{tortfac} = 10^{(\frac{n_a}{n} - 1.126) / 0.485}$

eq. 3.14

For $n_a/n < 0.2$: $\frac{1}{tortfac} = 10^{-4}$

where

n = total porosity

3.1.5.1.3 Kinetics

The oxidation rate from Fe^{2+} to Fe^{3+} is calculated by

eq. 3.15

$$um = k * km * pO_2 * (1 + \frac{m_{Fe}}{K_i}) * m_{Fe} * \Delta t$$

where:

um : mass of oxidized Fe^{2+}

k : abiotic reaction constant

km : biologic acceleration factor

pO_2 : partial pressure of oxygen

m_{Fe} : mass of Fe^{2+} in the solution

Δt : time interval

K_i : inhibition factor

The abiotic reaction coefficient is calculated according to Sigg & Stumm (Sigg and Stumm, 1991) as a function of pH. The biologic acceleration factor implemented in the source code of SAPY is a result of fitting experimental data of Kölling (Prein, 1993). SAPY considers the influence of temperature, pH and Fe^{3+} activity. The dependency on pH takes into account the optimal milieu conditions for microbiologic activities in these sediments and is formulated as follows:

eq. 3.16

For $\text{pH} \leq 5$: $km = 10^{0.5264 \cdot (\text{pH} - 1.6) + 6.632}$

eq. 3.17

For $\text{pH} > 5$: $km = 1$

So the acceleration of the biologic activity starts with a pH lower than 5 and accelerates the abiotic oxidation rate up to 5 magnitudes.

The influence of temperature on the biological acceleration factor considers the microbiological reproduction rate and is calculated according to Ahonen (Ahonen and Tuovinen, 1989).

eq. 3.18

$$km_T = 0.0047 \cdot (T - 6)^2 + 0.12$$

with :

km_T : acceleration factor for temperature

After calculating km_T the biological acceleration factor km is multiplied by km_T to account for temperature effects on microbiologic activity.

The inhibition of the biological acceleration due to elevated Fe^{3+} activities is taken into account by the inhibition factor K_i , which is calculated in function of temperature (Karavaiko et al., 1982).

eq. 3.19

$$T > 10^\circ\text{C}: K_i = (-5.78 \cdot T + 74.90) \cdot 1000$$

eq. 3.20

$$T < 10^\circ\text{C}: K_i = (-0.82 \cdot T + 25.25) \cdot 1000$$

3.1.5.2 Calibration

The model was calibrated based on oxygen breakthrough curves using the effective diffusion coefficient as calibration parameter. In the numerical modelling the following parameters were used (Tab. 3.2):

Tab. 3.2 Input parameters

number of cells	19
vertical grid distance, cm	10
time step, sec	1
upper boundary	Dirichlet (1 st)
lower boundary	no-flow boundary
initial pyrite content (weight-%)	0.04
initial oxygen content (%)	0
initial pH	5
recharge (mm/a)	0
total porosity, %	30
water saturation, (%)	2-100 (from top to bottom)
initial pH	5
buffering capacity	0

The initial geochemical parameters are derived from the analysis of sediments and water samples of the column experiment and were defined as start values for the simulation. The start pH of 5 was measured after filling the column. The profile of waterfilled porosities was measured by TDR-probes during the whole experiment and gave approximately time-constant values.

Within the first few days a sharp increase of the calculated oxygen saturation at the upper observation points due to oxygen diffusion can be observed. When the calculated pH falls below 3, microbiological effects start to accelerate pyrite weathering, flattening the slopes of the breakthrough curves. When all pyrite has been consumed the breakthrough curves steepen again (Fig. 3.2).

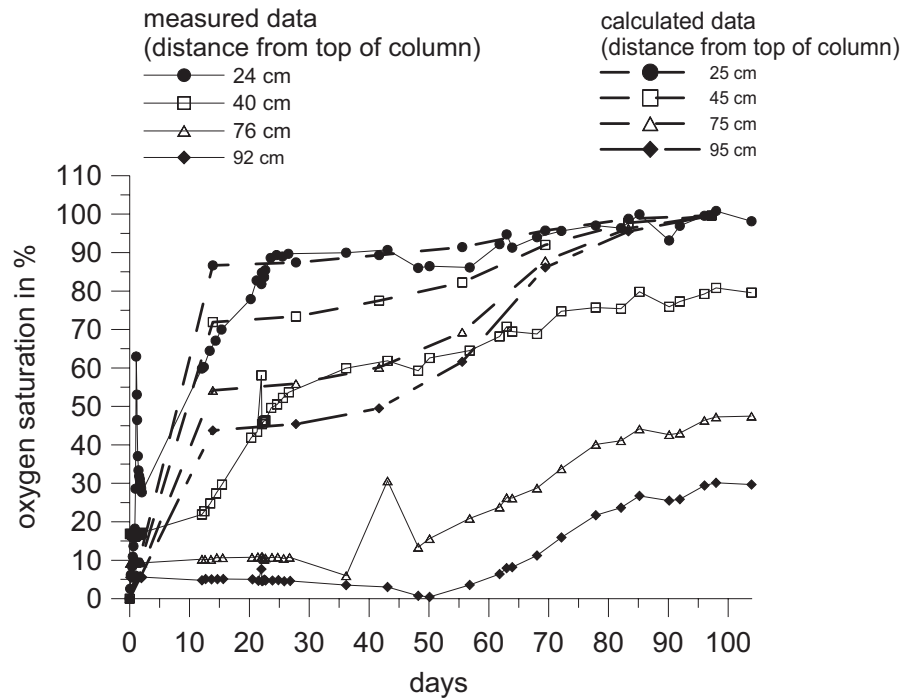


Fig. 3.2: Measured and calculated breakthrough curves of oxygen before calibration.

As the resulting calculated oxygen-breakthrough curves did not match with the measured values the model input parameters had to be adjusted. The slopes of the calculated breakthrough curves are steeper than the measured results, thus the effective diffusion coefficient seems to be overestimated in the simulation.

In general there are various possibilities to calibrate a model. Normally parameters with higher uncertainty are adjusted to fit the results. As the tortuosity factor is a parameter of high uncertainty it has been used as fitting parameter for the uppermost 16 unsaturated cells resulting in oxygen breakthrough curves shown in Fig. 3.2. The measured data could be simulated with satisfying accuracy using the calibrated model. Remaining differences between measured and calculated breakthrough curves can be observed in the two lowest breakthrough curves (75 cm and 95 cm below top of column) where biological activity in the model seems to be underestimated.

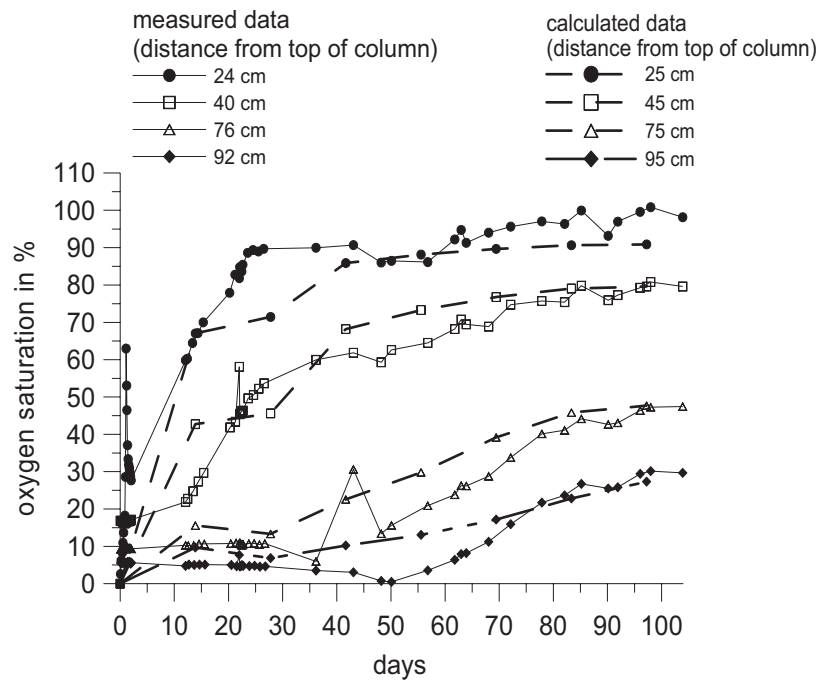


Fig. 3.3: Measured and calculated breakthrough curves of oxygen after calibration.

To fit the modelled results the initial tortuosity factor calculated by the original code of SAPY according to eq. 3.13 and eq. 3.14 had to be adjusted resulting in the following calibrated dependence of tortuosity on waterfilled porosity:

eq. 3.21

$$tort = 2.5 \cdot \ln(nw) + 12.488$$

where nw stands for waterfilled porosity and $tort$ represents tortuosity.

The original and the calibrated tortuosities are shown in Fig. 3.4.

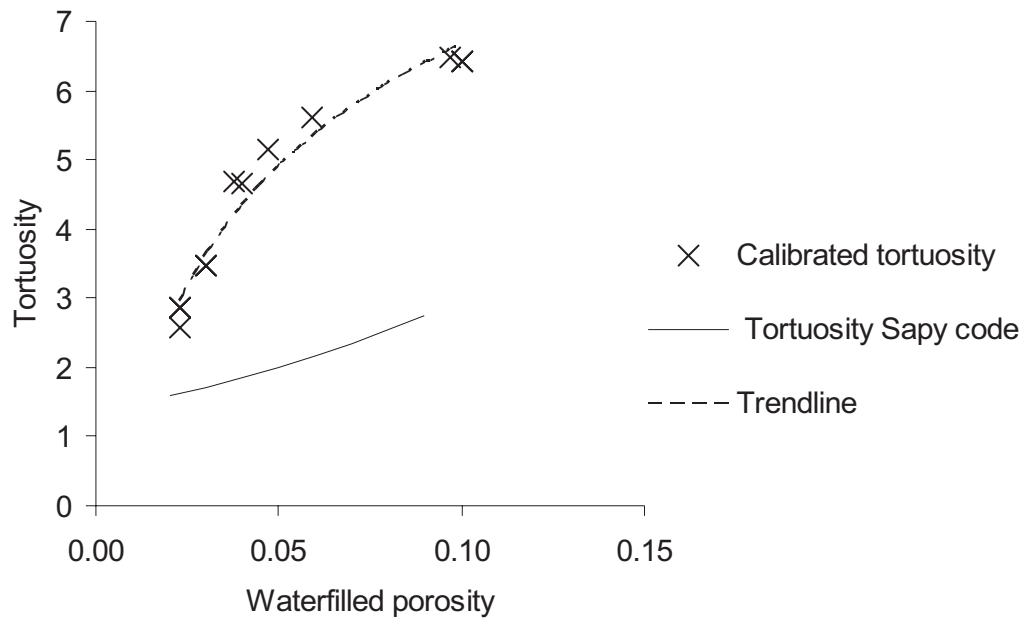


Fig. 3.4: Dependence of tortuosity on waterfilled porosity.

The calibrated logarithmic dependence of tortuosity on waterfilled porosity, which results in higher tortuosities than calculated in the original SAPY code can be used for future calculations for this type of sediment within the range of 0.02-0.1 of waterfilled porosity.

In general the value of tortuosity is difficult to calculate, because it depends strongly on pore size distribution, pore shape, degree of cementation and water content and shows great variations in natural sediments. The calculation of tortuosity applied in the original SAPY according to eq. 3.13 and eq. 3.14 was originally derived from an experiment with two types of sediments (Prein and Mull, 1995) and could not be applied to the heterogeneous sediments of our column. Furthermore there are different approaches in the literature concerning the dependence of diffusion on tortuosity, which is linear (eq. 3.12) according to Albertsen (Albertsen, 1977) but quadratic according to other authors (Dullien, 1991; Epstein, 1989).

The results of this study have been compared with different approaches characterizing the dependence of diffusion on the water content in the pores. In Fig. 3.5. the resulting values of D/D_0 for different moisture contents of our column study are plotted together with different empirical functions, which were derived in former studies by other authors.

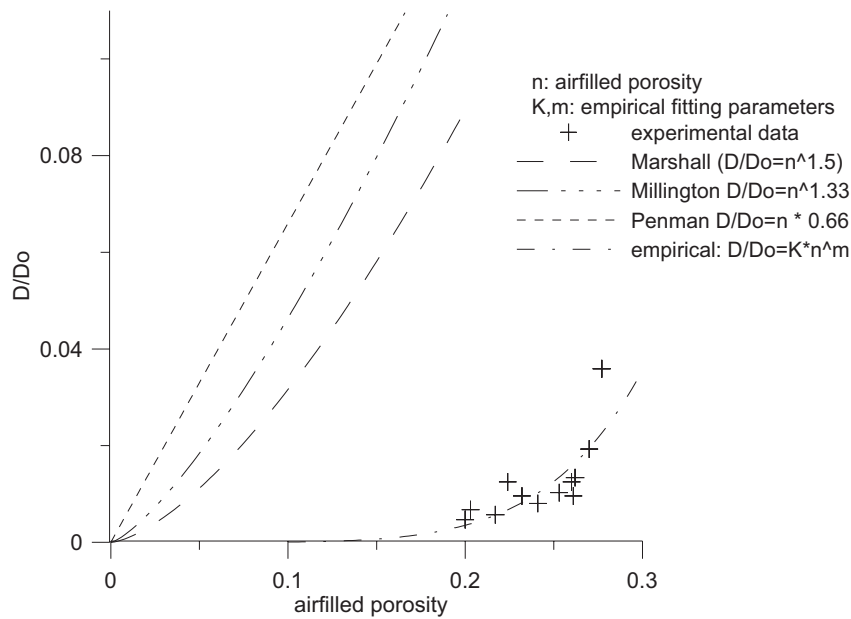


Fig. 3.5: Dependencies of effective diffusion on airfilled porosity (compiled from literature).

The compiled formulas (Marshall, 1959; Millington, 1960; Penman, 1940) overestimate the effective diffusion coefficients and cannot be applied to the sediments of our study area. This is probably due to the strong heterogeneity of the material, which shows a great variety of grain sizes causing high tortuosities. A good fit of our data could be obtained using the empirical formula eq. 3.9 (Troeh et al., 1982) with the fitting parameter $m = 5.7$ and $K = 34$. The parameter m represents pockets or incomplete passages of pore space, when diffusion ceases.

3.1.5.3 Calculated sulphate and pyrite contents

The simulation results show an immediate pH decrease to approximately 1.6 in the unsaturated zone of the column due to pyrite weathering. The calculated sulphate concentrations in the pore water increase as a function of oxygen supply until pyrite disappears (Fig. 3.6).

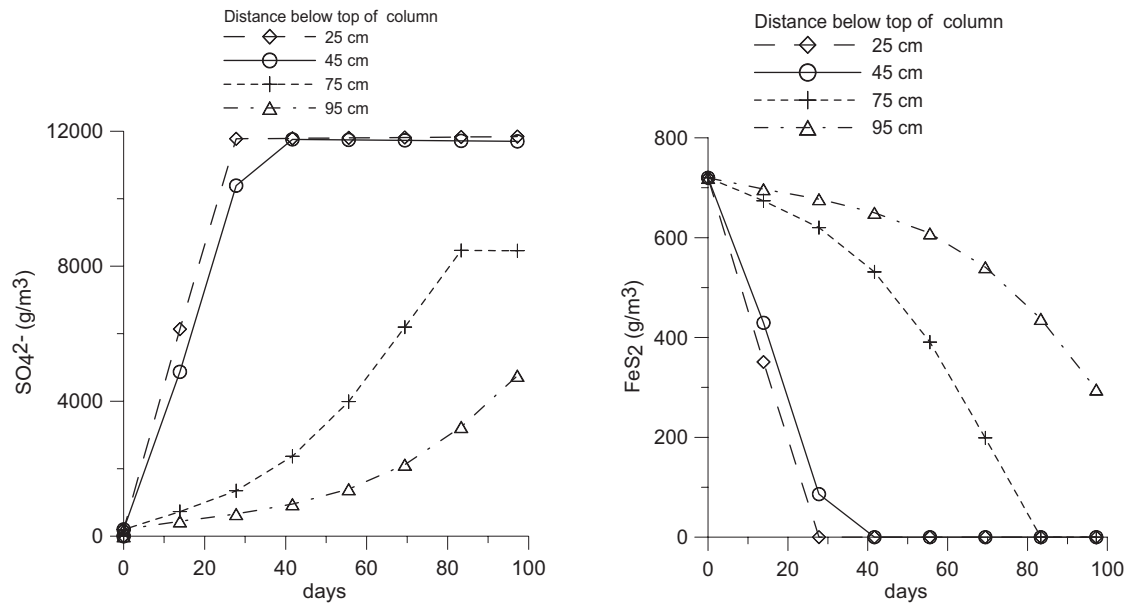


Fig. 3.6: Calculated sulphate and pyrite contents.

The different final concentrations of sulphate are a result of different waterfilled porosities in the cells. Due to the non-existing recharge in the experiment the released sulphate concentrations are not transported and remain constant after the depyritization of the surrounding sediments. As the SAPY code does not consider equilibrium of species, the saturation of sulphate which is predominantly limited by gypsum is disregarded in these simulations. Assuming a solubility of 3000g/m³ gypsum in water as a rough estimate, gypsum may be expected to precipitate in our column.

Fig. 3.6 shows that pyrite weathering is taking place in a broad zone during the entire simulation, owing to the low pyrite content of the sediments. This leads to a comparatively high production rate of weathering products. The velocity of the pyrite weathering front decreases with increasing depth, due to the decreasing oxygen flux as a result of smaller gradients.

3.1.6 Conclusions and Outlook

In this study an efficient tool was developed as a first step to predict future acidification in the LOHSA storage system. The reactive transport code SAPY (Prein and Mull, 1995) was tested based on measured oxygen breakthrough curves of a column experiment. The dependence of tortuosity on waterfilled porosity according to Albertsen (Albertsen, 1977), which is implemented in the source code of SAPY, overestimates the coefficient of effective diffusion in our heterogeneous sediments of the study area and had to be calibrated. Based on this model it was calculated that 59 % of the pyrite in the entire column was oxidized after 100 days. This corresponds to a total amount of 6300 mg oxidized pyrite in the column, leading to a production of 9954 mg sulphate and 2658 mg Fe^{2+} . The calculation of the depyritization depth gives a value around 80 cm below the top of the column after 100 days.

These results cannot be applied directly to field conditions where the unsaturated zone of the heap, which has been exposed to weathering processes since 1970, now has a thickness of about 12 m. Therefore our model has to be adapted to field conditions using the calibrated dependence of the effective diffusion coefficients on water saturation. The upscaled model has to be verified based on the present depth of the weathering front and chemical sediment analysis of the heap. Future work will focus on the derivation of source terms for acid builders released in the unsaturated zone for the next 50 years using the adapted model. These source terms will be calculated in function of the depth of the water table below surface and can be implemented in a regional three-dimensional groundwater model.

3.2 Deriving source terms of sulphate input for a hydraulic model using an upscaled reactive transport model

3.2.1 Abstract

The generation of acid mine drainage from overburden spoil piles at open-pit lignite mines is impacting the quality of groundwater and surface water bodies in large parts of the Lusatian mining area in Germany. The long-term evolution of the acidification is still largely unknown. The LOHSA study area in the new federal states of Germany was exploited until the early 1990s and is to be flooded by 2005. Afterwards it will be used as a reservoir basin for the river SPREE. Beside the release of acid builders into the surface water the future sulphate concentrations are of great interest because considerable amounts of the bank filtrate of the river SPREE are used for the drinking water supply in several communal water plants and also in the German capital Berlin, which is located 200 km downstream of the LOHSA storage system. In our study the input of sulphate from the unsaturated zone of the heap into the groundwater for a period of 80 years was calculated using the one dimensional reactive transport code SAPY. The SAPY program, which had been calibrated for effective diffusion and tortuosity using oxygen breakthrough curves of a column experiment with original heap sediments, was upscaled to field conditions and verified by a measured oxygen and sulphate profile of the heap. Scenarios for a period of 80 years were simulated for different distances of the groundwater level to the subsurface and the mass input of sulphate from the unsaturated zone into the groundwater was calculated in terms of specific fluxes for different times. It is planned to use the calculated source terms in a regional three-dimensional groundwater model to predict the future evolution of the ground- and surface water in the study area.

3.2.2 Introduction

In the new federal states of Germany large areas have been subjected to open cast lignite mining. An important production of acid builders in these mining environments is the oxidation of iron disulfides in the dump sediments due to penetration of oxygen and oxygen-rich waters, accelerated by microorganisms. Primary oxidation of the sediments starts during dewatering of the originally layered material prior to mining. Owing to the processes of mining (excavation, mixing and dumping activities) aeration is even intensified. After deposition, secondary pyrite oxidation continues in the aerated upper part of the spoils, possibly over a period of several decades. After decommissioning a mine, standard procedure

is to allow the water table to rise and to convert the pit into a lake for recreational purposes. During the flooding, which often extends over several years to decades, the acidity and other chemical contents in the groundwater are flushed into the newly formed lake (Gerke, 1998). To reduce the acid input flooding is sometimes performed by surface water, rather than by natural groundwater rise.

The study area is the lignite mine LOHSA II near HOYERSWERDA in Germany. This mine was exploited from 1970 to 1990, when its groundwater level was lowered artificially to a maximum depth of 50 m below subsurface. The pumped water was discharged into the SPREE during that period. As pumping of groundwater stopped after the mine was decommissioned, the water level of the SPREE has declined since 1990, causing problems of water quality for the drinking water supply in the downstream areas. The former lignite mine LOHSA is to be flooded, mainly with surface water, by 2005 and will afterwards be used as a reservoir basin for the river SPREE. To equilibrate the hydraulic head of the river, present management strategies are predicting annual surface water oscillations between 5 and 8 m (LmbV and Cottbus, 1996).

The ongoing weathering processes in the unsaturated zone of the surrounding, 40-m-high heaps, lead to a continuous release of acid builders into the groundwater which exfiltrates later in the newly formed lake LOHSA II and into the SPREE. As the bank filtrate of the SPREE is used for the drinking water supply in urban areas downstream of LOHSA the long-term release of sulphate and other acid builders from the unsaturated zone of the heaps has to be estimated.

To allow long term predictions of the hydrogeochemical evolution in abandoned and flooded lignite mine environments several models have already been developed (Foos, 1997; Strömberg and Banwart, 1994). All these models usually consider equilibrium reactions and additional kinetic processes. Mayer implemented kinetically controlled reactions in variably saturated porous media in a multicomponent reactive transport model (Mayer, 2002). Some models also include O₂ diffusion and transport reactions (Hecht et al., in press; Prein and Mull, 1995; Wunderly et al., 1996).

The aim of this study is to investigate in how far pyrite weathering processes, which were studied in the laboratory, may be upscaled by a model to field conditions in order to allow quantitative long term estimates concerning the release of weathering products from the aerated zone of a heap into the groundwater. To provide a first quantitative estimate the calibrated reactive transport code SAPY (Kohfahl et al., 2003; Prein and Mull, 1995) was upscaled to field conditions and verified based on in situ measurements in the heap. Using the

upscaled model simulations for different scenarios were performed to derive the temporal evolution of sulphate input into the groundwater.

3.2.3 The reactive transport code SAPY

3.2.3.1 Program description

SAPY is a one-dimensional reactive transport mixed cell model, which has been developed especially for the simulation of pyrite weathering (Prein, 1993). The numerical algorithm couples transport of the reactants by diffusion and advection in water and air with kinetics of pyrite weathering as source/sink terms, including biological catalysis.

For each cell the following phases are differentiated:

- gas phase calculating convective transport of air, diffusion of oxygen and nitrogen,
- water saturated phase where diffusive and convective transport of oxygen and reaction products (SO_4^{2-} , Fe^{2+} and H^+) are calculated,
- solid phase with chemical reactions of pyrite weathering.

The diffusive and convective transport of oxygen and weathering products are calculated by the mixed cell approach of eq. 3.22

eq. 3.22

$$n_e \frac{\partial c}{\partial t} = D \frac{\partial^2 c}{x^2} - n_e u \frac{\partial c}{\partial x} \pm Q n_e$$

where c = concentration, u = seepage-velocity, D = effective diffusion coefficient, n_e = effective porosity and Q = source-sink term.

Distribution of oxygen between water and atmosphere is calculated according to Dalton. Source and sink terms of O_2 , Fe^{2+} , Fe^{3+} , SO_4^{2-} , FeS_2 and H^+ are calculated according to Stumm & Morgan (Stumm and Morgan, 1981) based on the available amount of oxygen in water. Chemical equilibria of species distribution are not calculated in the code. Convection in water is simulated with constant flow velocities of seepage of 1 m per year.

The coefficient of effective diffusion is calculated according to Albertsen (1977):

eq. 3.23

$$D''' = n_a * \frac{D''}{tortfac}$$

where:

D''' = effective diffusion coefficient corrected for temperature, pressure, airfilled porosity (n_a) and tortuosity;

D'' = diffusion coefficient corrected for temperature and pressure;

$tortfac$ = tortuosity factor;

The tortuosity is defined as the ratio of the actual path length taken by a particle in a porous medium, over the straight line distance and is calculated in SAPY for perturbed sediments as follows:

eq. 3.24

$$\text{For } n_a/n > 0,2: \frac{1}{tortfac} = 10^{\left(\frac{n_a}{n} - 1.126\right) / 0.485}$$

eq. 3.25

$$\text{For } n_a/n < 0,2: \frac{1}{tortfac} = 10^{-4}$$

with

n = total porosity

n_a = airfilled porosity

The tortuosity factor $tortfac$ corresponds to the square of the tortuosity (Albertsen, 1977). For a more detailed description of the source code, refer to Prein (1993).

3.2.3.2 Calibration of tortuosity to moisture content

As tortuosity constitutes a material parameter the SAPY code was tested based on a column

study using unsaturated LOHSA-sediments in a previous study (Kohfahl et al., 2003). Briefly, a column experiment was set up and the diffusion of oxygen into the initially anaerobic sediment and the moisture content were monitored over 100 days. The anoxic material used for the column experiment was taken from a core drilled in the southern periphery of the study area. The measured oxygen breakthrough curves were modelled using SAPY. Based on the modelling results an empirical equation was derived, describing the dependence of tortuosity on the moisture content of the sediment. in order to provide a means for upscaling laboratory results to field conditions. To reproduce the measured oxygen breakthrough curves tortuosities for the respective water contents of the unsaturated sediment had to be elevated considerably as shown in Fig. 3.7. This is likely due to the strong heterogeneity of the sediment.

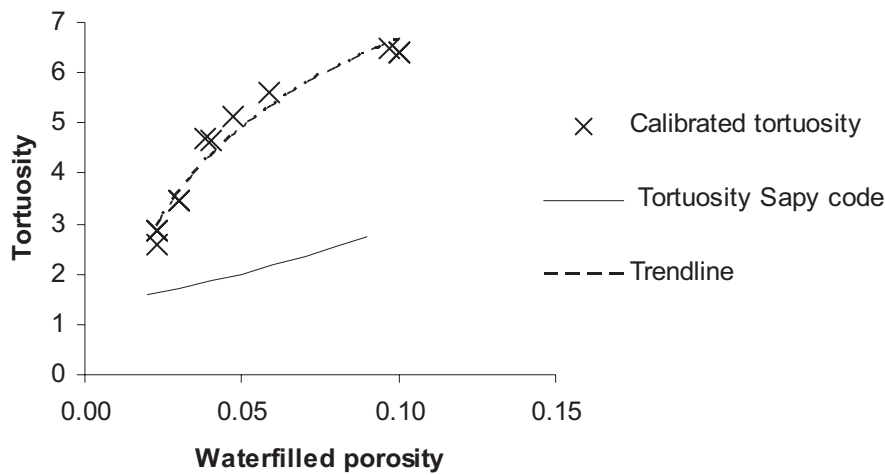


Fig. 3.7: Dependence of the tortuosity on water-filled porosity.

3.2.4 Upscaling and verification

3.2.4.1 Available data

The storage system LOHSA is partly surrounded by heaps some 40 m thick, with an unsaturated zone of 10-15 m vertical extension (Fig. 3.8).

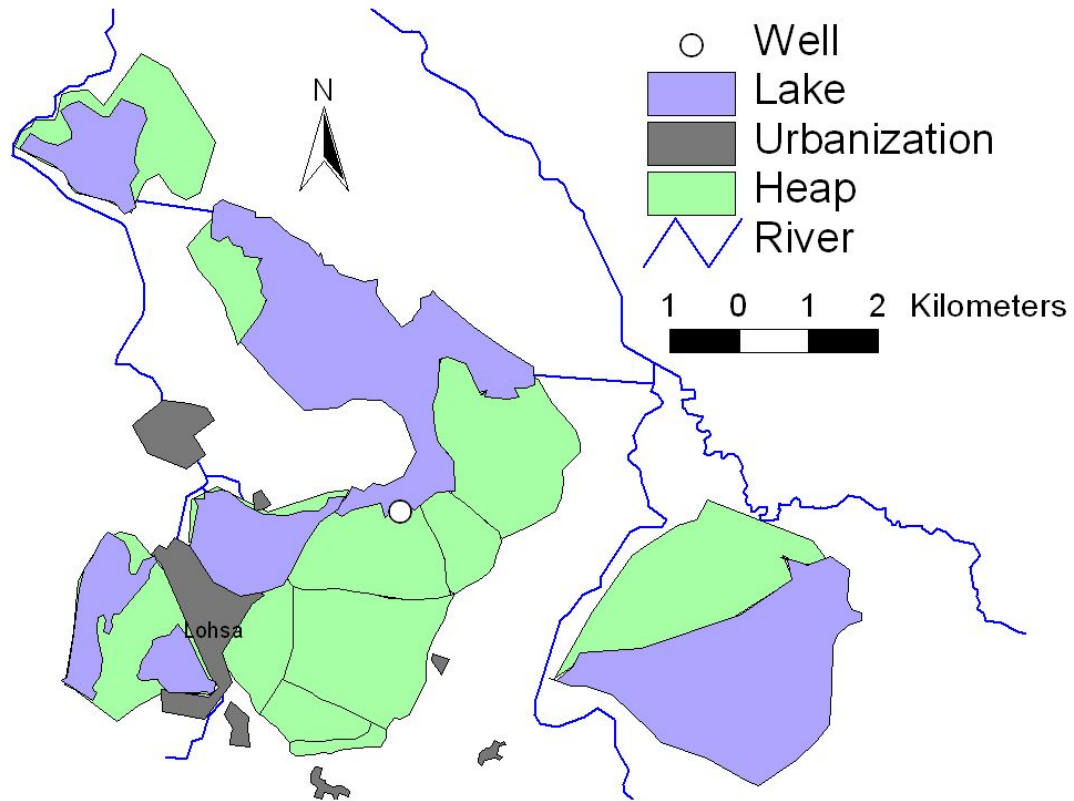


Fig. 3.8: Study area.

The field data for moisture, sulphate and oxygen profiles in the heap were provided by the Faculty of Environmental Sciences and Process Engineering of the University of Cottbus (email communication 02/2002 with B. Ehret). The data were obtained by borehole measurements in the observation well shown in Fig. 3.8, which is 10 m close to the location, where the sediment of the column study was obtained. This observation well allows measurements of porewater, groundwater and soil-gas and is located in a heap upstream of LOHSA II. The material of the heap is mainly composed of Quaternary overburden of the exploited coal seam. The level of the water table during the time of measurements ranged between 11.5 and 12.5 meters below surface (Fig. 3.9).

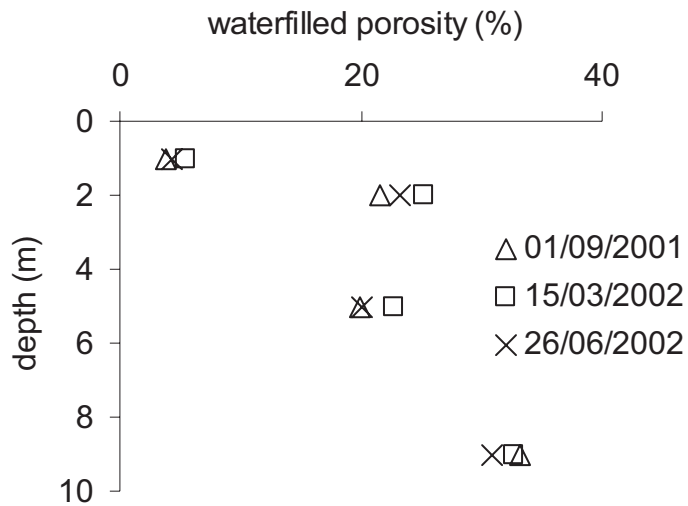


Fig. 3.9: Measured volumetric water fraction in the heap (data provided by the Faculty of Environmental Sciences and Process Engineering of the University of Cottbus)

The water contents rise from a fraction of 4 vol.-% in 1 m depth to more than 30 vol.-% at a depth of 9 m. The higher moisture content at the depth of 2 m may be due to local high contents of fineclastic sediments. The high values at 9 m depth are probably caused by the capillary fringe of the groundwater table.

The measured oxygen profile of the borehole developed from the formation of the heap in the early 1970s until 2002 is shown in Fig. 3.10.

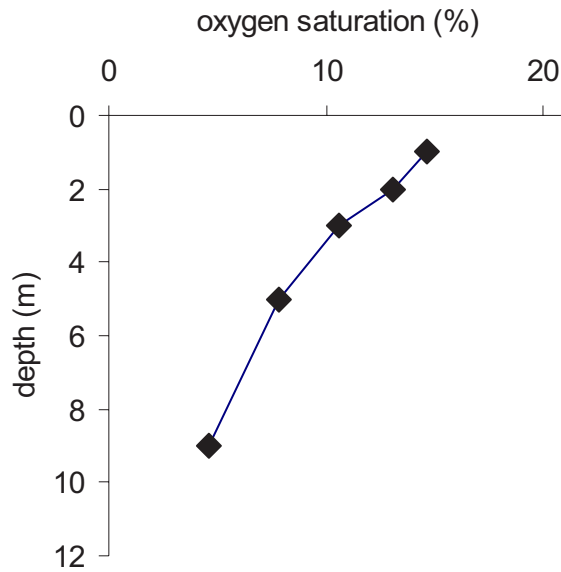


Fig. 3.10: Measured partial pressure of oxygen in 2002 in the observation well (data provided by the Faculty of Environmental Sciences and Process Engineering of the University of Cottbus).

The oxygen profile shows oxygen saturation of 15 vol.-% 1 m below subsurface, declining to 5 vol.-% at a depth of 9 m.

The measured sulphate contents in the unsaturated zone of the observation well indicate a maximum concentration of about 4000 mg/l in a depth of 10 m below surface (Fig. 3.11).

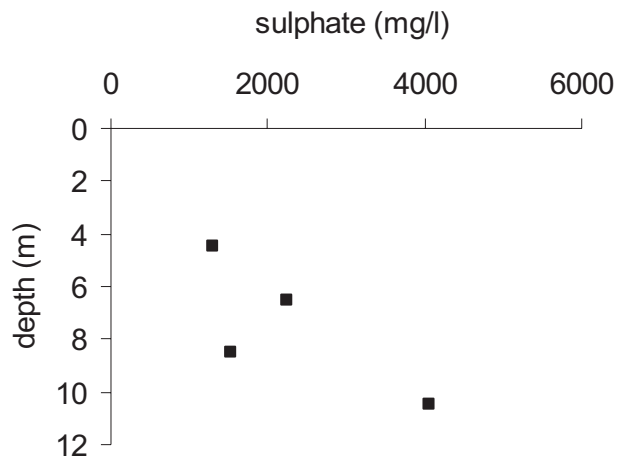


Fig. 3.11: Measured sulphate concentrations in the pore water (data provided by the Faculty of Environmental Sciences and Process Engineering of the University of Cottbus).

3.2.4.2 Upscaling and verification

To simulate the measured profiles in the field a model was set up based on the SAPY code using the following input parameters:

Tab. 3.3: Input parameters for the upscaled model

number of cells	12
vertical grid distance (m)	1
upper boundary	Dirichlet (1 st)
lower boundary for gas	no-flow boundary
lower boundary for water	Neumann (2 nd)
initial pyrite content (wt. %)	0.04
initial oxygen content (%)	0
recharge (mm/a)	100
initial pH	5
buffering capacity	0
waterfilled porosity	0.2
porosity	0.38
simulation time (a)	30

The simulations were performed using both the original and the calibrated dependency of tortuosity on water content (Fig. 3.7).

The calibrated dependency of tortuosity on water content, which yielded tortuosities about 7-8 for waterfilled porosities between 0.025 and 0.1, could not be verified on the basis of the

measured oxygen contents in the field. The calculated oxygen profiles after 30 years resulted in oxygen concentrations of nearly zero in all cells. There are a couple of possible reasons for the discrepancy between field- and laboratory data. One reason might be that the calibrated dependence of tortuosity on the moisture content of the sediment was derived for sediments with a waterfilled porosity smaller than 0.1 and can not be extrapolated to waterfilled porosities greater than 0.2 which were measured in the field. Another possible explanation is the existence of preferential pathways for gas through sedimentary structures in the field, which do not exist in our column. A further reason might be the local variability of the sediment material in the heap, which shows a higher proportion of coarse grained material at the observation well of the field measurements in comparison to the sediment material used in the column. Therefore the dependency of tortuosity on the water content originally implemented in the SAPY source code, which yielded tortuosities about 4 for the averaged observed waterfilled porosities of 0.2 in the field, was applied in all the following calculations.

The simulated results yielded a satisfying fit with the observed data (Fig. 3.12). Small deviations of higher oxygen concentrations measured at the depth of 9 meters may be due to effects of heterogeneity of the sediment structure. The heterogeneity of spoil is generally a direct consequence of the processes of waste rock disposal resulting from end-tipping and dragline spreading and lead to preferential pathways of diffusive oxygen delivery.

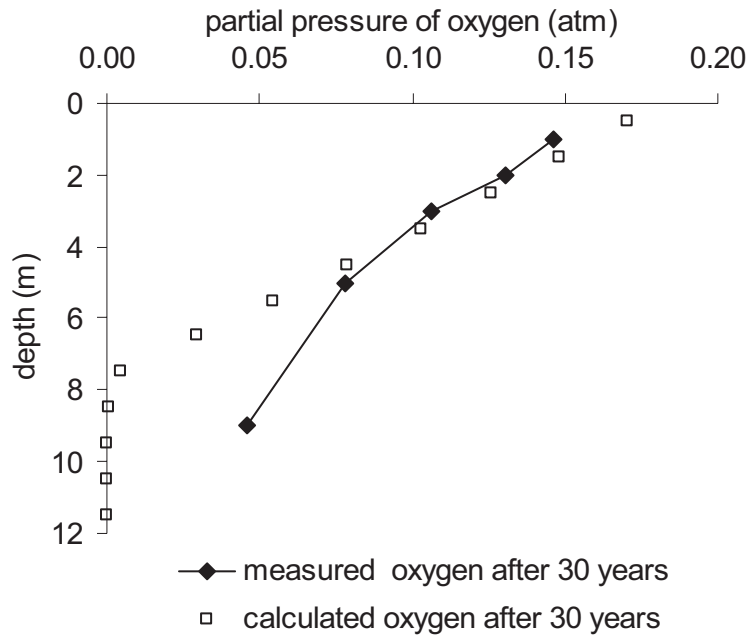


Fig. 3.12: Measured and calculated oxygen profiles (measured data provided by the Faculty of Environmental Sciences and Process Engineering of the University of Cottbus).

In addition the measured sulphate concentrations of the observation well could be reproduced in the same magnitudes with the original SAPY code, using a natural recharge of 100 mm/a (Fig. 3.13).

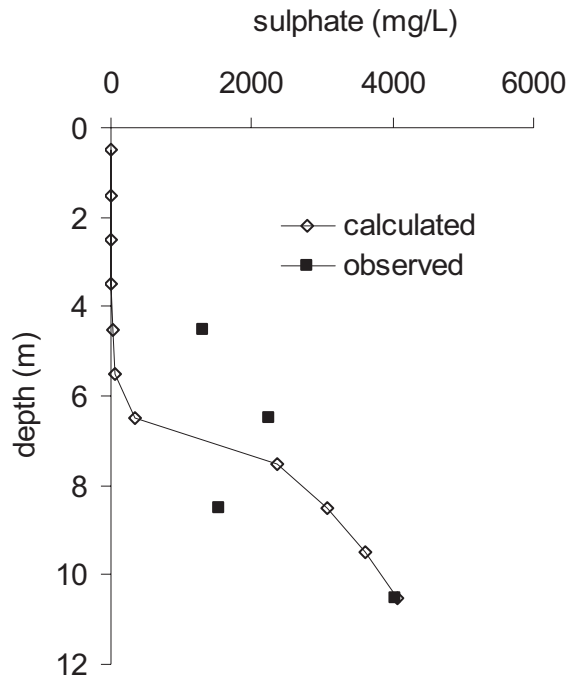


Fig. 3.13: Measured and calculated sulphate concentrations after 30 years (measured data provided by the Faculty of Environmental Sciences and Process Engineering of the University of Cottbus).

3.2.4.3 Sensitivity studies

To study the sensitivity of the model results to water-saturation and total porosity several scenarios have been simulated using different values for these parameters (Fig. 3.14).

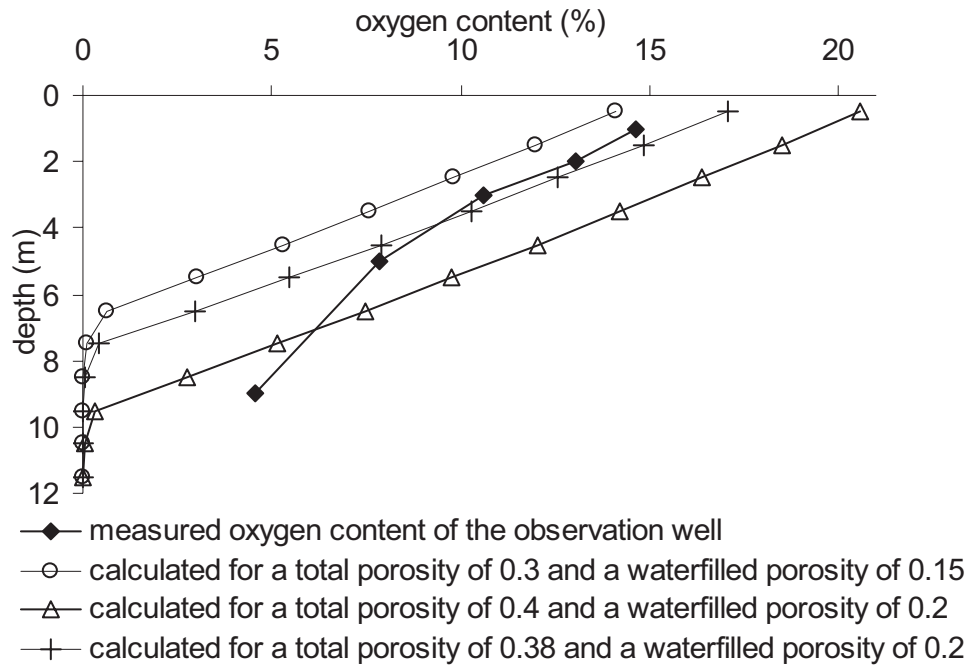


Fig. 3.14: Sensitivity studies (measured data provided by the Faculty of Environmental Sciences and Process Engineering of the University of Cottbus).

The sensitivities of the model results to different values for water-saturation and total porosities are comparatively small for the range of values used. The definition of a different vertical thickness greater than 12 m for the unsaturated zone shows no influence on the modelled results because the oxygen concentrations are almost zero at a depth of 12 m.

3.2.5 Derivation of source terms

3.2.5.1 General aspects

The derivation of source terms for acid builders aims to predict the future quality of ground- and surface water in the storage system LOHSA based on a regional groundwater model. The average flow velocity of the groundwater in the heap is estimated to range between 0.1-0.5 m per day, i.e. groundwater may be in contact with dump sediments for more than 30 years before discharging into the flooded lake. Therefore the input of acid builders from the unsaturated zone into the groundwater during the last 30 years has to be taken into account to predict future water quality in the flooded lake. The input of acid builders into the

groundwater is predominantly dependent on the vertical thickness of the covering unsaturated zone. In principle, the delivery of oxygen into the heap leads to a production of weathering products, the intensity of which decreases with time due to the declining gradient of oxygen, which is the motor of diffusion. The weathering products are transported mainly by seepage water through the unsaturated zone and reach the groundwater after a certain time, depending on the seepage velocity. Hence the source terms derived in this paper have to be defined for different distances of the groundwater table to the subsurface as a function of time.

To derive the source terms for acid building species the verified model with the input parameters defined in Tab. 3.3 was run for a simulation time of 80 years.

The measured moisture profile in Fig. 3.9 represents only a temporal condition and especially the higher values close to the present level of the groundwater table are not representative for the whole period from 1970 to 2002. Therefore the waterfilled porosity was defined with a value of 0.2 which was regarded as a reasonable approximation for the whole period of 1970 to 2002. The total porosity was set to 0.38.

For the derivation of source terms the amount of natural recharge of the groundwater implemented in the model is of great importance because it determines the vertical flow velocity of seepage water, which is calculated in the code by

eq. 3.26

$$v = Q/n_w$$

where

Q: natural recharge in (m/a)

v: flow velocity of seepage water (m/a)

n_w : water filled porosity in the unsaturated zone

3.2.5.2 Scenario simulation

To perform the prognostic simulations for a period of 80 years a model was built up using the input parameter of Tab. 3.3. The simulations were performed using a recharge of 190 mm/a (grassland) and 100 mm/a (coniferous forest), which correspond to representative values for the study area depending on the type of vegetation.

The calculated oxygen saturations of this scenario indicate that after 80 years the pyrite weathering front will have reached a depth about 13 m below subsurface. Due to the lowering oxygen gradients during the simulation the velocity of the propagating weathering front is declining with time (Fig. 3.15).

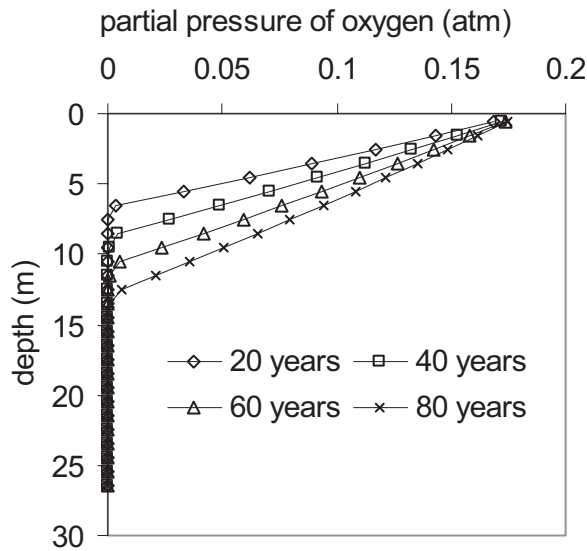


Fig. 3.15: Simulated oxygen saturation for a period of 80 years.

The calculated sulphate concentrations are controlled by the production rate the pyrite weathering front and by the seepage velocity. The displacement of the weathering front where all pyrite has been consumed is indicated by the different depths where the curves approximate to zero concentration of sulphate.

The released products are transported downwards from their point of origin by seepage water with a velocity of 0.95 m/a in this scenario (eq. 3.26), so after 20 years the maximum concentrations are at a depth of about 19 m (Fig. 3.16). The seepage water in these depths started to infiltrate into the sediment when the heap was recently formed and the oxygen delivery was very high owing to the low depth of the weathering front in that time. Later profiles show lower concentrations of sulphate, which is due to the decreasing oxygen delivery with time as a consequence of declining oxygen gradients.

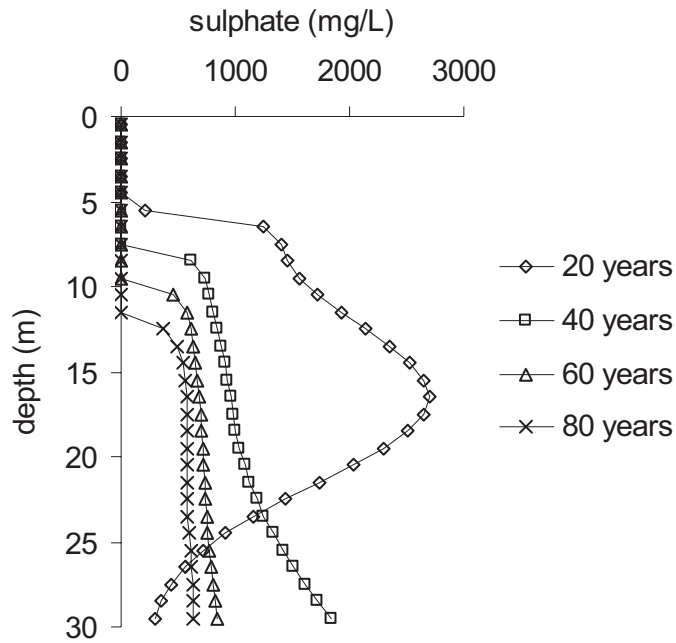


Fig. 3.16: Calculated sulphate concentrations using a recharge of 190 mm/a.

Using a natural recharge of 100 mm/a, the resulting concentrations are higher, corresponding to a lower amount of water to dissolve the released weathering products. The vertical seepage velocity is 0.5 m/a according to eq. 3.26. Fig. 3.17 shows that the greatest concentrations after 20 years are calculated for depths lower than 10 m.

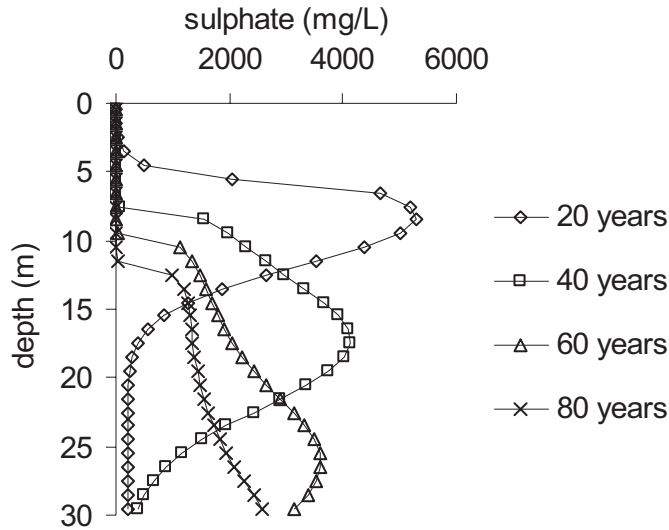


Fig. 3.17: Calculated sulphate concentrations using a recharge of 100 mm/a.

3.2.5.3 Resulting source terms

The source terms of sulphate input for a regional groundwater model can be derived based on the calculated sulphate concentrations as a function of space and time.

The mass input was calculated in terms of fluxes per m^2 to get values which are independent of the mesh discretization of the groundwater model to which these parameters will be applied. The concentrations calculated by SAPY in the respective undermost cell of the unsaturated zone was recalculated in terms of mass by:

eq. 3.27

$$m_{\text{sulphate}} = c_{\text{sulphate}} * n_w$$

where:

m_{sulphate} : mass of sulphate (mg/l)

c_{sulphate} : concentration of sulphate (mg/l)

n_w : waterfilled porosity

Considering a vertical flow velocity of 0.95 m, the mass input for the respective depths of the water tables were calculated according to

eq. 3.28

$$F_i^t = m_i^t * 0.95$$

where the indices i and t stand for the cellnumber and time respectively, F stands for the annual input of sulphate into the groundwater, m is the mass of sulphate in the undermost undersaturated cell at time t . The number of each cell corresponds to the depth of their midpoint in meters plus 0.5. The resulting mass inputs for different times and depths of the groundwatertable are documented in Fig. 3.18 using a recharge of 190 mm/a for the first scenario.

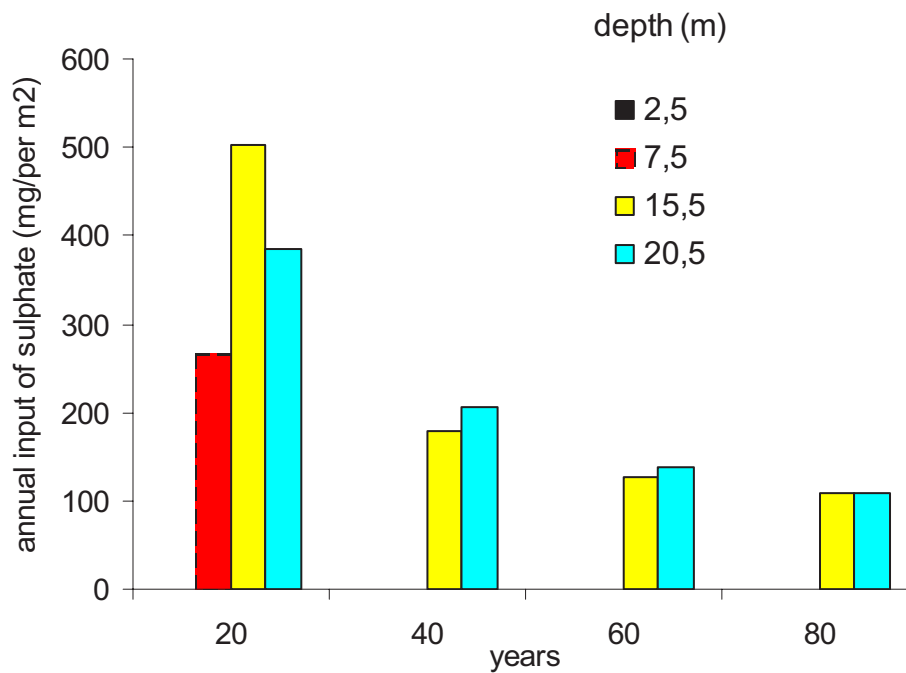


Fig. 3.18: Source terms for sulphate at different depths assuming a natural recharge of 190 mm/a. (Source terms at 2.5 m are too small for visualization in this scenario).

The annual input at different depths and times can be directly related to the calculated sulphate profiles shown in Fig. 3.16. The mass input at a depth of 2.5 m is already zero after 20 years because there is no pyrite anymore in the overlaying sediments. At depths of less than 8 meters the mass input of sulphate after 30-40 years will also tend to zero, whereas in greater depths sulphate input into the groundwater still continues.

Fig. 3.19 shows the calculated annual mass input in the second scenario using a recharge of 100 mm/a, which results in a delay of the maximum mass input. According to a flow velocity of seepage water about 0.5 m/a the maximum input at a depth of 20.5 m is calculated to occur after 40 years and not after 20 years as documented in Fig. 3.18. This leads to a slower and more dispersed discharge of weathering products from the unsaturated zone into the groundwater.

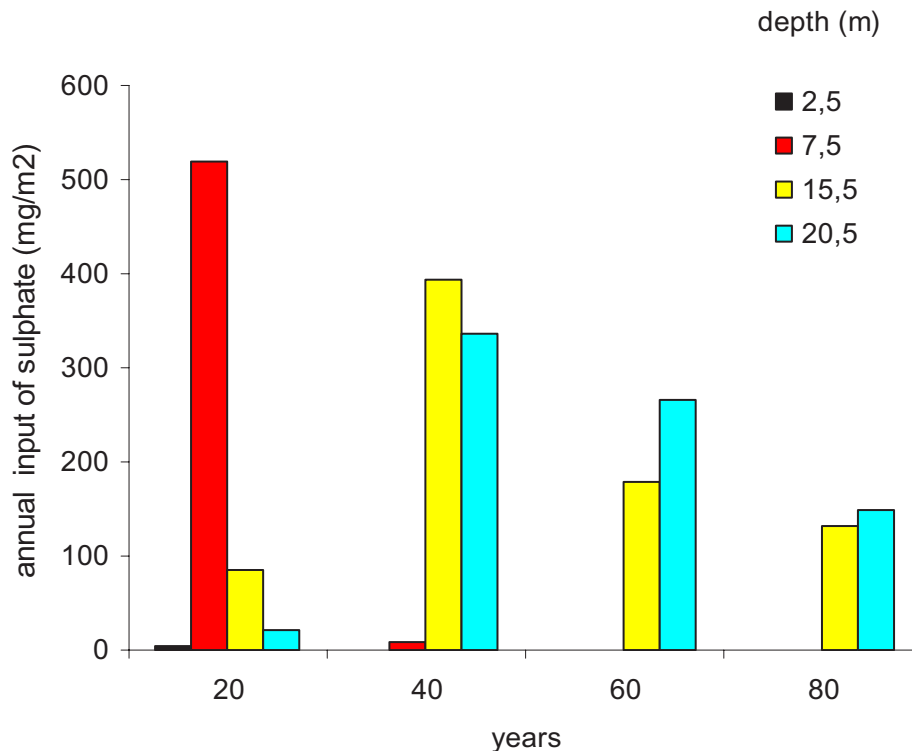


Fig. 3.19: Source terms for sulphate at different depths assuming a natural recharge of 100 mm/a.

3.2.6 Conclusions and Outlook

In this study an efficient tool was developed to predict future acidification in the storage system LOHSA. The dependencies of tortuosity on water contents for sediments of our study area, which were calibrated for low water contents in an earlier study, could not be applied to the field conditions. The original reactive transport code SAPY (Prein and Mull, 1995) was upscaled to field conditions and verified by means of measured oxygen and sulphate concentrations of a borehole in the field using measured waterfilled porosities of the unsaturated zone. Sensitivity studies showed little influence of the modeled results for the

range of used porevolumes as input parameter. Based on this model, time dependent source terms for mass input of sulphate from the unsaturated zone into the groundwater were derived for different depths of the groundwater table and for different amounts of natural recharge. The results indicate that the maximum input of sulphate into the groundwater - assuming an average depth of 12-15 m of the future groundwater table - will be between 20 and 40 years after the formation of the heap in 1970, depending on the amount of natural recharge.

The presented results do not account for geochemical equilibria of species, which is important considering the fact that the concentration of sulphate is limited by solubility of gypsum. Therefore the calculated concentrations have to be interpreted as rough initial estimates rather than exact absolute predictions of sulphate input.

Time constant levels of the groundwater table have been assumed in this study, so the effect of rising groundwater tables and annual water oscillations, which play an important role in our study area, was not taken into account. Nevertheless the model can be used as a first quantitative approach for the release of weathering products from the unsaturated zone into the groundwater. Future investigations will focus on the calculation of source terms for a regional groundwater model depending on the spatial distribution of natural recharge and the local depth of the water table. The modelled results have to be verified using measured hydrogeochemical field data of the seepage water and groundwater.

3.3 A reactive transport model for a flooding experiment using a column containing partly oxidized pyrite bearing sediments

3.3.1 Abstract

This paper reports the hydrogeochemical modelling of reactions that take place during the uptake of weathering products by a rising watertable into a partly oxidized pyrite bearing sediment. The anoxic material used for the column, which has a length of 2 m, was taken from a core of a drilling into a pyrite bearing sediment with an average pyrite content of 0.04 wt %. After packing the column it was drained and maintained in an unsaturated state during a period of hundred days to allow oxygen delivery and pyrite weathering. During this period oxygen breakthrough curves were measured. After 100 days the column was flooded with distilled anoxic water from the bottom to the top with an average velocity of 5 cm per day. The water contents, oxygen contents and the chemical composition have been monitored over the profile of the column. The compositions of the water samples at different depths of the column were modelled with PHREEQC, defining a hydrogeochemical one-dimensional transport model. The model uses the mixed cell approach for advection and the finite-differences approach for dispersion in a split operator scheme. The mixing process with the porewater of the unsaturated zone was modelled using the dual-porosity module of the transport algorithm defining a stagnant porewater and a mobile flooding water phase, which is mixed in certain amounts after each transport step. Kinetic relations were implemented to account for source terms of acids and acid builders released during the unsaturated period. The aim of this study is to obtain a deeper understanding of the hydrogeochemical processes going on during uptake of weathering products due to rising water levels in the heaps of decommissioned pit mines.

3.3.2 Introduction

In the Lusatian zone of the new federal states in Germany, lignite has been extracted from open pit mines for over half a century. The mining process requires extensive lowering of the watertable and removal of large quantities of overburden material. This overburden often contains sulphide bearing minerals, such as pyrite and marcasite. After decommissioning a mine, standard procedure is to allow the watertable to rise and to convert the pit into a lake for recreational purposes. The highly increased surface area of heap sediments as compared to naturally sedimented rocks leads to an enhanced reactivity. Subsequent to release, water

movements within the heap may cause a transport of acidity and metals to the surrounding environment through drainage systems and/or underlying aquifers. Various possible mechanisms and processes, however, may result in retention and /or immobilization of the contaminants within the heap, e.g. due to the existence of immobile water or secondary chemical reactions such as precipitation of solid phases (Erikson, 1997). Other potentially important immobilization processes are co-precipitation by, for instance, isomorphous substitution and ion-exchange (Herbert, 1996). During the flooding, which often extends over several years to decades, the acidity and other chemical contents in the groundwater are flushed in the newly formed lake (Gerke, 1998). In general, the environmental impact of the heap will be the result of complex interactions between transport and water-rock interaction.

The investigated heap of our study area was formed in the early seventies so that oxygen delivery into the sediment has been acting for more than 30 years. Sediment analysis indicates a present penetration depth of oxygen about 10 m below subsurface. The rising water levels due to the flooding of the storage system LOHSA will uptake the released weathering products, which cause a great input of acid builders into the groundwater.

To provide a first estimate of the ongoing reactions and the amount of acid inputs due to the rising water levels sophisticated modelling approaches have to be applied and they have to be verified by experimental data. Several models have already been developed to study geochemical processes at mine sites (Foos, 1997; Strömberg and Banwart, 1994) and in aquifers influenced by sulphide oxidation. All these models usually consider equilibrium reactions and additional kinetic processes. Mayer implemented kinetically controlled reactions in variably saturated porous media in a multicomponent reactive transport model (Mayer, 2002). Some models also include O₂ diffusion and transport reactions (Hecht et al., in press; Prein and Mull, 1995; Wunderly et al., 1996).

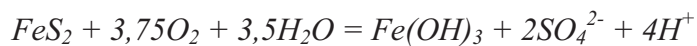
The aim of this study is to get a better understanding of the hydrogeochemical processes related to a rising groundwatertable, which enters into partly oxidized pyrite bearing sediments, using laboratory data and model based interpretation. Therefore a column experiment was set up measuring oxygen, moisture contents and the chemical composition of water in the saturated zone of the column. The experiment was interpreted using the one-dimensional reactive transport code PHREEQC (Parkhurst, 1995).

3.3.3 Theory

3.3.3.1 Oxydation of pyrite and buffering

After the formation of a heap, the pyrite bearing sediments are exposed to pyrite weathering processes which may be described according to (Stumm and Morgan, 1996):

eq. 3.29



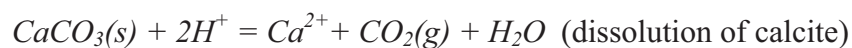
The weathering of sulfide minerals, which are thermodynamically unstable in oxidizing conditions, is driven by oxygen supply from the atmosphere, which is predominantly limited by diffusion.

The most important buffering reactions are

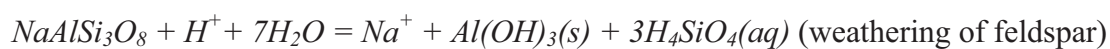
- Calcite dissolution (below and near neutral pH)
- Feldspar weathering (below neutral pH)
- Cation exchange (below neutral pH)
- Dissolution of Fe-oxyhydroxides and gibbsite (below neutral pH)

The release of protons initiates buffering reactions such as dissolution and transformation of alkalinity producing carbonates and silicates, here exemplified by calcite dissolution, weathering of feldspar and dissolution of gibbsite:

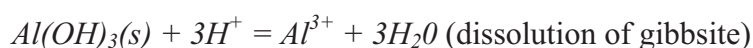
eq. 3.30



eq. 3.31



eq. 3.32



Strömberg and Banwart (Strömberg and Banwart, 1994) suggested that calcite and silicate dissolution provide two pools of different capacities and time-scales for pH buffering through reactions such as eq. 3.30 and eq. 3.31. For fresh heap sediments an initial rapid calcite dissolution buffers the pH at near neutral values. After depletion of available calcite, the relative rates of silicate dissolution and sulfide oxidation shift and keep the pH at a much lower level.

Below near neutral pH, additional sources of buffer capacity may be (hydr)oxides, carbonates other than calcite, and mixed hydroxysulphate phases that have precipitated during previous silicate dissolution and sulfide oxidation at near neutral conditions. Below a pH of 4 the dissolution of gibbsite is generally known as an almost instantaneous reaction (eq. 3.32).

Clay minerals may retard the protons by ion-exchange reactions, thus resulting in decreased acidity spread out over greater emission times.

In general, the relative amounts of acid producing and consuming minerals as well as their weathering rates determine the acidity of the water.

3.3.4 Methodology

3.3.4.1 Sediment parameters

The material used for the column experiment was taken from a core of a heap in the southern periphery of the former open-pit mine LOHSA II. The anoxic sediment was taken from the water saturated zone in a depth of 23-25 m below subsurface and has been conserved under anoxic conditions in an airtight plastic liner. The site is located in an existing dump of dominantly Quaternary material with a thickness of about 40 m. The material consisted of fine sands and lignite fragments.

The chemical characteristics of the sediment material are compiled in Tab. 3.4.

Tab. 3.4: Sediment parameters of the material used in the column study

	meq/100g sediment	analytical method
pH	4.66	CEC
sulphate	0.20	dilution with distilled water
Na	0.14	CEC (diluted with BaCl ₂)
K	0.21	CEC (diluted with BaCl ₂)
Mg	0.22	CEC (diluted with BaCl ₂)
Fe	0.02	CEC (diluted with BaCl ₂)
Mn	0.02	CEC (diluted with BaCl ₂)
Al	0.33	CEC (diluted with BaCl ₂)
Ca	0.86	CEC (diluted with BaCl ₂)
HCO ₃ ⁻	0.92	dilution with distilled water
organic carbon	22.56	Leco
pyritic sulfur	6.49	dithionite extraction
monosulfidic sulfur	0.17	dithionite extraction

The cations were analysed using BaCl₂ extractions. The sediments are characterized by a relatively low natural pyrite content. The small content of anorganic carbon indicates a low buffer capacity.

3.3.4.2 Set up of the column

A plexiglass column (200 cm length, 10 cm i.d.) was prepared along the profile with 10 suction cups, 10 TDR-probes for measuring moisture content, and 20 fiber optic oxygen probes (Fig. 3.20).

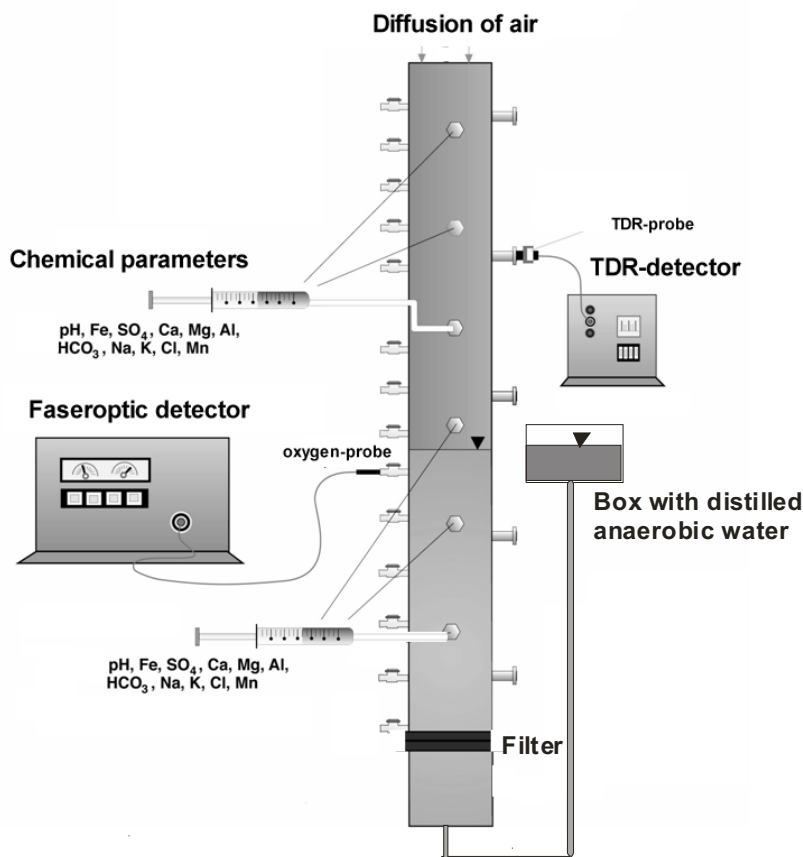


Fig. 3.20: Set up of the column for the flooding experiment.

The technique for construction of the oxygen probes was developed by H. HECHT and M. KÖLLING (Hecht and Kölling, 2001). To allow discharge and control of water level a lower outlet was prepared beyond the column. The water level was controlled by an airtight tube connected with the lower outlet. At the bottom of the column a 3 cm thick filter-layer of inert quartz sand was placed to distribute flow and to prevent obstruction by smaller particles. Before packing the columns, the sediments were homogenised. During packing with the homogenised sediment a small amount of anoxic distilled water was added to minimize contact with atmospheric oxygen. After packing the column, water was discharged from the lower outlet until a hydraulic head of 50 cm measured from the bottom of the column was reached.

To simulate the ongoing processes in the unsaturated zone of the heap during exposure to atmospheric oxygen after discharging the column it was exposed to oxygen diffusion for 100 days. To avoid transport of the originating weathering products the column was not irrigated. The oxygen saturation and moisture contents were measured at different depths in the columns.

Afterwards the column was flooded from the bottom to the top using a hydraulically connected box filled with anaerobic water. The water in the box was continuously ventilated with argon to prevent oxygen delivery.

3.3.4.3 Initial conditions of the flooding experiment

When starting the flooding experiment the pyrite bearing material of the column was partly oxidized due to the delivery of oxygen into sediment during the period of 100 after discharging the column. The resulting breakthrough curves which were measured during 100 days after discharging the column are documented in Fig. 3.21 (Kohfahl et al., 2003).

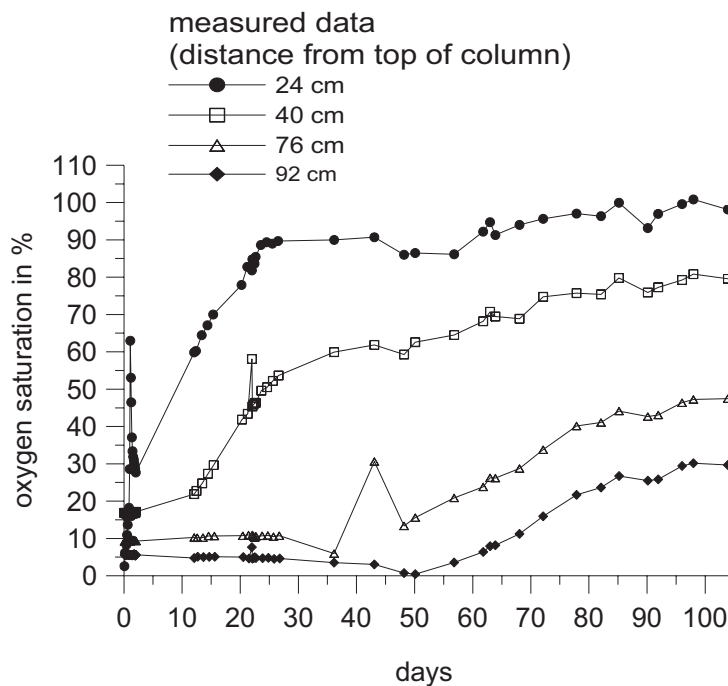


Fig. 3.21: Measured oxygen breakthrough curves of column 1 before flooding.

The oxygen breakthrough curves indicate that the oxygen front has penetrated at least 1 m into the sediment before flooding was started after 100 days. As the column was not irrigated during this time, no water samples could be taken and therefore no observation data for the hydrogeochemical evolution of the pore water exist.

However, the processes during this period and the release of weathering products were modelled in an earlier study using a one-dimensional reactive transport code SAPY (Prein, 1993). The model was calibrated on the base of the measured oxygen breakthrough curves (Kohfahl et al., 2003) using the tortuosity as calibration parameter. The results were used as

input parameters for the flooding experiment in this study. The modelled evolution of the pyrite contents calculated with the calibrated tortuosities is shown in Fig. 3.22.

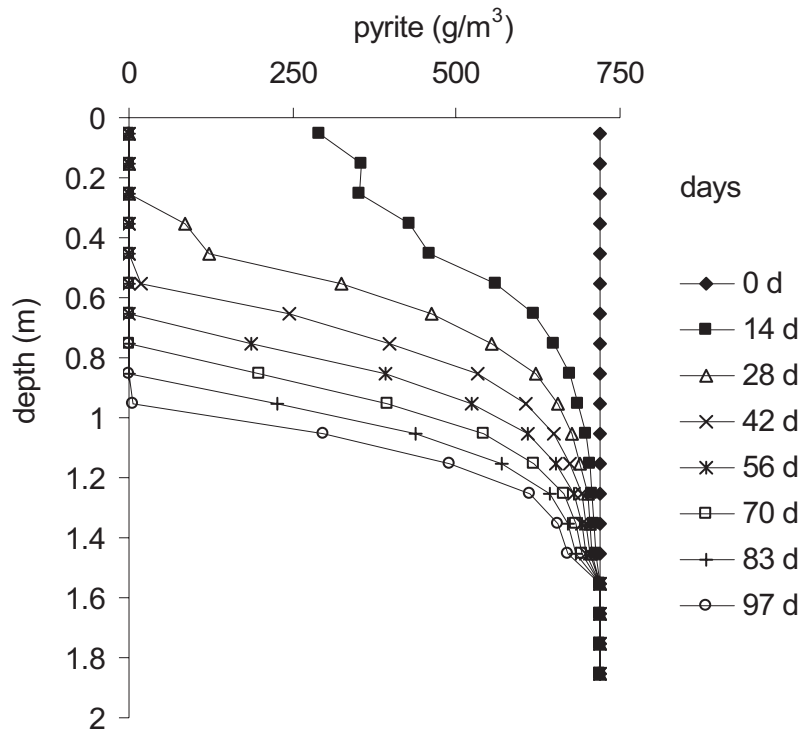


Fig. 3.22: Modelled evolution of pyrite contents with SAPY using calibrated tortuosities.

The SAPY code (Prein, 1993) is a one-dimensional reactive transport mixed cell model, which has been developed especially for the simulation of pyrite weathering. The numerical algorithm couples transport of the reactants by diffusion and advection in water and air with chemical reactions of pyrite weathering as source/sink terms including biological catalysis.

For each cell the following phases are differentiated:

- gas phase calculating convective transport of air, diffusion of oxygen and nitrogen
- water saturated phase where diffusive and convective transport of oxygen and reaction products (SO_4^{2-} , Fe^{2+} and H^+) are calculated
- solid phase with kinetically controlled chemical reactions of pyrite weathering

Diffusive and convective transport of oxygen and weathering products are calculated by eq. 3.33:

eq. 3.33

$$\frac{\partial c}{\partial t} = D_l \frac{\partial^2 c}{\partial x^2} - v_f \frac{\partial c}{\partial x} \pm Q/S$$

where c = concentration, t = time, v_f = seepage velocity, D_l = is the hydrodynamic dispersion coefficient (m^2/s , $D_l = D_e + \alpha_l v_f$, with D_e the effective diffusion coefficient, and α_l the longitudinal dispersivity [m]) and Q/S = source-sink term.

Distribution of oxygen between water and atmosphere is calculated according to Henry's Law. Source and sink terms of O_2 , Fe^{2+} , Fe^{3+} , SO_4^{2-} , FeS_2 and H^+ are calculated according to Stumm & Morgan (Stumm and Morgan, 1981) based on the available amount of oxygen in water.

The initial distribution of weathering products for the flooding experiment was derived by the modelled distribution of the pyrite after 100 days (Fig. 3.22).

3.3.4.4 Flooding of the column and sampling

After leaving the drained columns in an unsaturated state in contact to atmospheric oxygen they were flooded with anaerobic distilled water from bottom to top with an average vertical flow velocity of about 5 cm per day using the lower outlets at the base of the columns to introduce the water (Fig. 3.20). We selected distilled water to obtain a better initial estimate of the mass of weathering products which will be uptaken from the sediment. During the entire period of flooding the moisture contents, oxygen concentrations and water chemistry of the saturated zone were monitored along the profile of the column. Due to clogging of most of the suction cups after flooding the column by oxidized iron minerals water sampling could be performed only at a limited number of sampling points during that period.

3.3.5 Results

3.3.5.1 Column experiment

The uptake of weathering products of the rising water table is illustrated in Fig. 3.23. where the analyzed dissolved concentrations of Calcium and sulphate of the uppermost part of the water column during flooding are plotted.

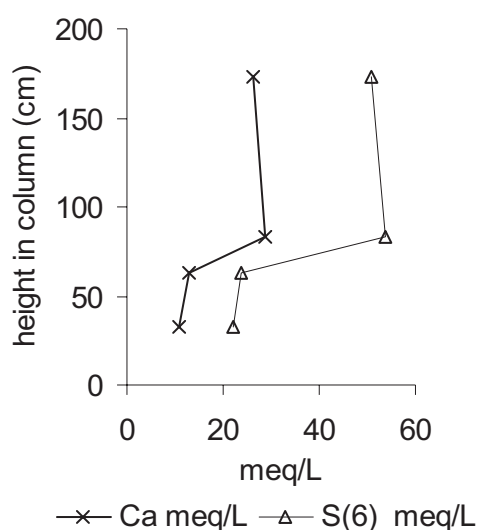


Fig. 3.23: Analyzed Ca^{2+} - and SO_4^{2-} -concentrations of the uppermost part of the water column during flooding.

The concentrations show a major increase between 60 and 80 cm height of the column, which is mainly caused by the released pyrite weathering products and dissolution of gypsum. The strong increase of calcium and sulphate between 60 and 80 cm indicates the position of the pyrite weathering front which matches quite well the modelled results shown in Fig. 3.22. The calcium and sulphate concentrations of the flooding front stay more or less constant after having passed the zone of pyrite weathering because of their control by the solubility of gypsum. Speciation calculations for the first samples taken at 83 and 173 cm height also yielded oversaturation of gypsum.

The concentrations of the other analyzed species evolved in a different way. Na^+ and Cl^- seem to have reached their maximum concentrations already after 40-50 cm height in the column and maintain roughly a Na/Cl ratio of 1 in the flooding front throughout the whole experiment (Fig. 3.24).

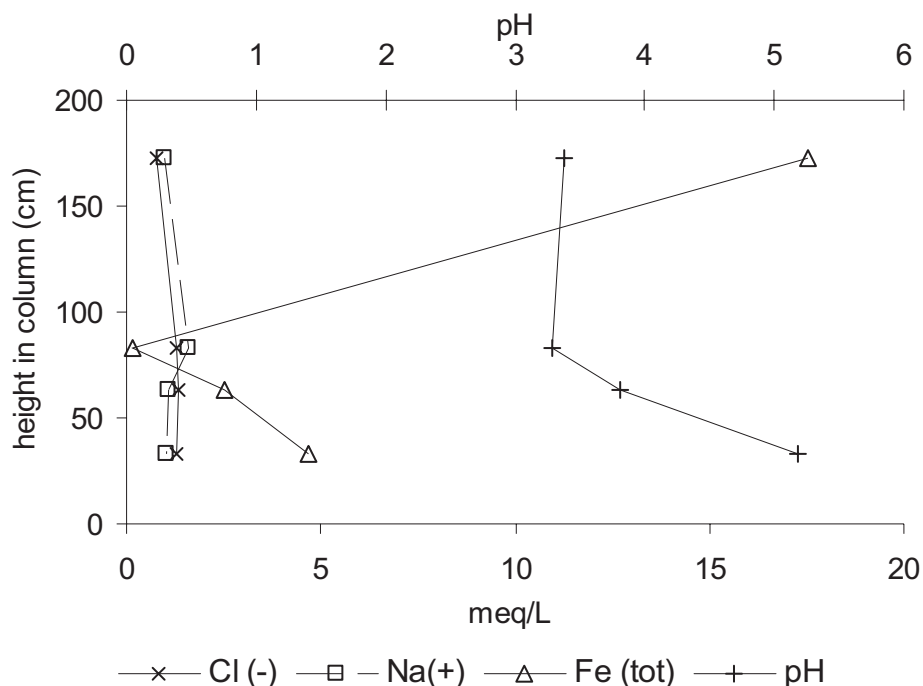


Fig. 3.24: Analyzed Na^+ - Cl^- and $\text{Fe}^{2+/3+}$ concentrations of the flooding front at different heights in the column.

The Fe concentrations at the flooding front decrease until reaching a height of 80 cm but increase between 80 cm to 170 cm to a concentration of about 17 meq/l. This leads to the conclusion that Fe is also released passing the pyrite weathering front, probably by dissolved goethite or/and other Fe-oxyhydroxides which have been originated by pyrite weathering during the period of unsaturated conditions. The solubility of Fe-species depends strongly on the ambient redox- and pH-conditions. The pH, which decreases from 5 to 3 until 80 cm height of the column should primarily lead to higher amounts of dissolved iron assuming constant pe values; however, this does not match our observations. The measured decrease of dissolved iron between 50 and 80 cm height in the column as shown in Fig. 3.24 is probably due to rising pe values in the higher parts of our column owing to rising partial pressures of oxygen which may lead to the precipitation of Fe-oxyhydroxides. This is concordant with the results of our speciation calculations with PHREEQC2 (Parkhurst, 1997) of the first water sample (first flush) at 83 cm column height. The calculations resulted in oversaturation of goethite ($\text{SI} = 4.9$) when bringing the solution into equilibrium with a partial oxygen pressure of 0.01, which seems to be a reasonable value according to our oxygen measurements (Fig. 3.21). Speciation calculations of the first water sample at 173 cm height (first flush) yielded strong oversaturation of goethite ($\text{SI} = 7.2$) and amorphous $\text{Fe}(\text{OH})_3$ ($\text{SI} = 1.42$) when bringing the solution into equilibrium even with a very small partial oxygen pressure of 0.01, which can be assumed as a minimum value in the upper part of the column. This discrepancy

is due to the fact that the precipitation of Fe-oxyhydroxides is a kinetic process which may take between minutes and years depending on ambient conditions like temperature, OH/Fe ratios, $[\text{Fe}^{3+}]$ and the nature of the anion of the salt (Cornell and Schwertmann, 1996). As the ambient parameters in our column are changing in space and time more sophisticated kinetic modelling approaches have to be applied to account for the complex chemistry of iron species in our system.

The calcium/sulphate ratios for most of the analyzed samples vary between 0.4 and 0.6 during the whole experiment as documented in Fig. 3.25.

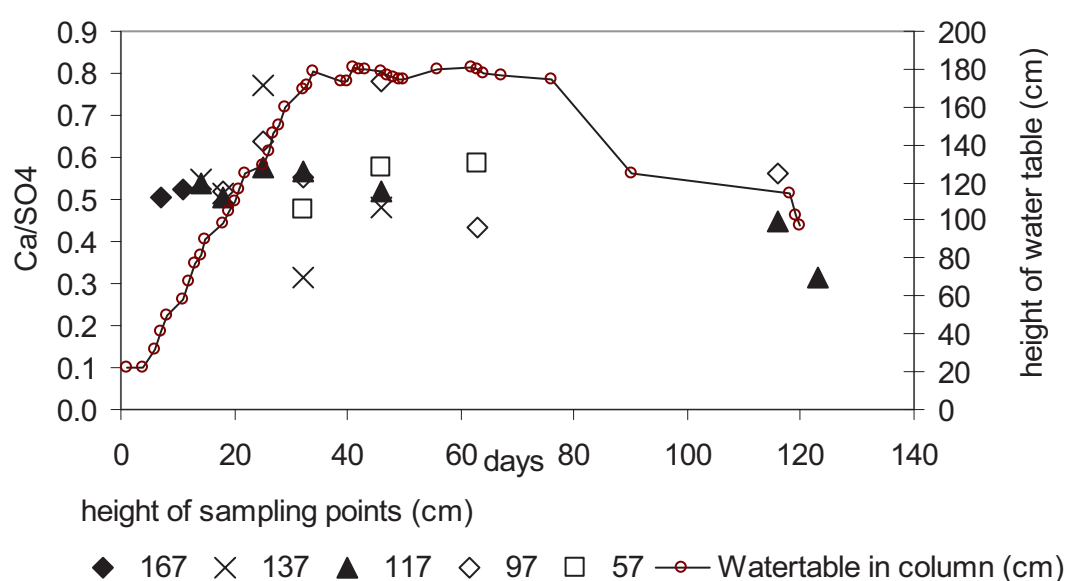


Fig. 3.25: Analyzed molar $\text{Ca}^{2+}/\text{SO}_4^{2-}$ ratios at different times and sampling points.

This leads to the conclusion that approximately 40 -60 % of the released sulphate is originated by dissolved gypsum and 60 - 40 % by oxidized pyrite respectively. Speciation calculations with PHREEQC2 (Parkhurst, 1997) for a water sample of an anoxic saturated part of the column before the unsaturated period yielded undersaturation of gypsum. Also the speciation calculation of a groundwater sample of the observation well where the sediment for our column was obtained yielded undersaturation for gypsum. Based on these results the original presence of gypsum cannot be assumed for the sediment of the entire column before the unsaturated period. Owing to the diffusive oxygen delivery during the unsaturated period, which results in the release of sulphate and the subsequent precipitation of gypsum, an increasing amount of available gypsum must be expected with rising height of the column at the beginning of the flooding experiment. Therefore the temporarily increasing amounts of

sulphate in the flooding front during its ascendance come along with increasing concentrations of Ca^{2+} originated by dissolution of previously precipitated gypsum. This may explain the more or less constant $\text{Ca}^{2+}/\text{SO}_4^{2-}$ ratios during the experiment.

Analysing the temporal hydrogeochemical evolution of the water samples only 1 sampling port at 83 cm height of column provided a sufficient number of analyzed data for a reliable interpretation based on time series. The measured results are documented in Fig. 3.26 using the normalized data sampled at 83 cm height of column.

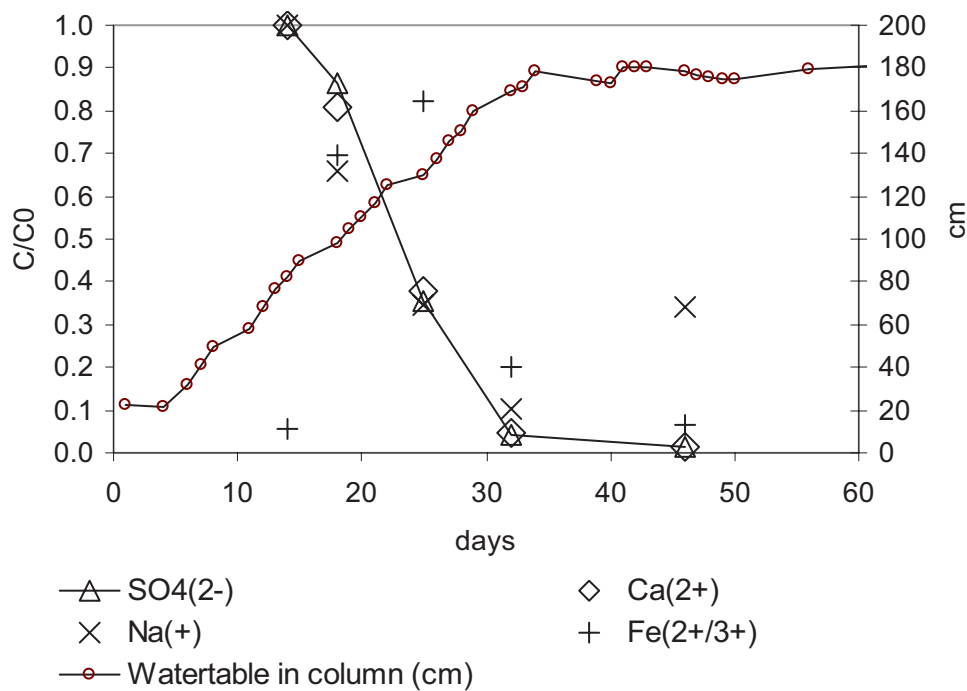


Fig. 3.26: Normalized concentrations of sulphate, Ca^{2+} , Na^+ and $\text{Fe}^{2+/3+}$ at 83 cm column height.

The concentrations of SO_4^{2-} , Ca^{2+} , Na^+ show almost identical normalized concentrations during the first 30 days indicating that predominantly dilution is taking place without chemical reactions. Possible effects of preferential sorption of higher charged cations at the exchanger due to dilution cannot be seen at this scale but will be discussed later. $\text{Fe}^{2+/3+}$ shows a completely different behaviour from that of the cations discussed before, which is the result of different counterbalancing effects concerning formation and dissolution of Fe-oxyhydroxides.

A preferential sorption at the exchanger of higher charged Ca^{2+} in this heterovalent solution can be observed by comparing the relative analyzed amounts of the cations sampled at 63 cm

height of column after 25 and 32 days of flushing as shown in Fig. 3.27. The solution after 25 days showed a measured electrical conductivity of 183 $\mu\text{S}/\text{cm}$, whereas the solution after 32 days has been diluted by flooding to 93 $\mu\text{S}/\text{cm}$ showing an increased amount Na^+ and K^+ with respect to Ca^{2+} and Mg^{2+} . The relative amounts of ions in highly diluted solutions at the other sampling points do not permit a quantitative interpretation due to analytical errors.

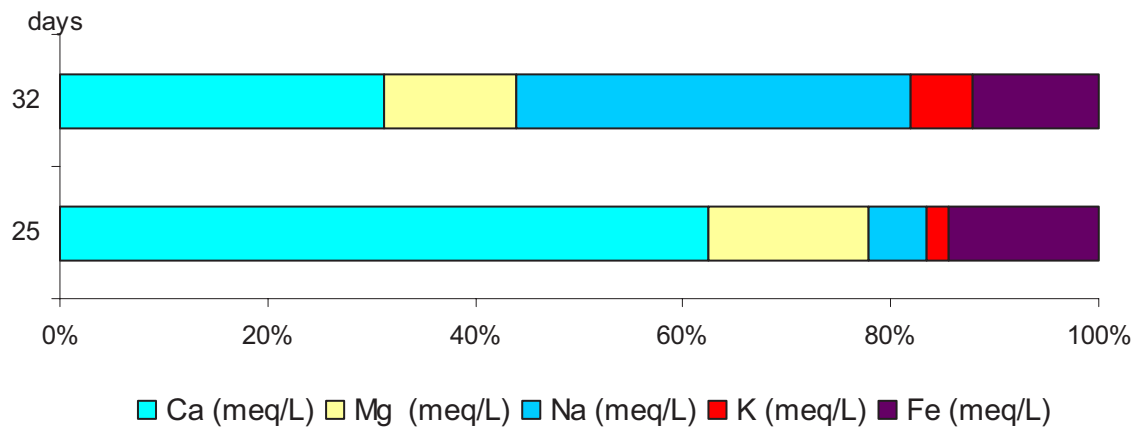


Fig. 3.27: Relative amounts of cations analyzed after 25 and 32 days of flushing at 63 cm height of column.

3.3.5.2 Boundary conditions and input parameters of the geochemical model

3.3.5.2.1 General aspects

To gain a deeper understanding of the hydrogeochemical processes going on during uptake of weathering products due to rising water levels in the heaps of decommissioned pit mines and to provide a tool for upscaling our modelling results a geochemical model was set up using PHREEQC2 (PARKHURST AND APPELO, 1999). The following processes have been implemented in the model:

- advective transport
- mixing of incoming water (mobile) with porewater (immobile)
- exchange reactions
- uptake of weathering products (gypsum, acid builders)

- equilibrium with oxygen in the upper part of the column
- equilibrium with goethite, amorphous $\text{Fe}(\text{OH})_3$ and gypsum
- Al-buffering by dissolution of gibbsite

Based on the observed data three different reactive zones of the column were distinguished (Tab. 3.5):

Tab. 3.5: Reactive zones of the column

	Height [cm]	Processes
Zone 3	100-200 cm	advective transport mixing exchange equilibrium with Fe-oxyhydroxides/gypsum equilibrium with atmospheric oxygen partial pressure strong release of acid builders $\text{Al}(\text{OH})_3$ -buffering
Zone 2	50-100 cm	advective transport mixing exchange equilibrium with Fe-oxyhydroxides/gypsum equilibrium with low oxygen partial pressure weak release of acid builders $\text{Al}(\text{OH})_3$ -buffering
Zone 1	0-50 cm	advective transport mixing exchange equilibrium with Fe-oxyhydroxides/gypsum

In the undermost part of the column (0-50 cm) no oxygen was measured therefore the implemented processes of the model are transport, mixing between mobile and immobile water and exchange. Between 50 and 100 cm these processes are completed by the uptake of weathering products and equilibrium with oxygen. The upper part of the column contains the same processes as the medium section but higher amounts of weathering products and oxygen are involved in the reactions.

A special problem of this study is that our column is partly unsaturated during the flooding experiment so many reactions in the column are limited to the saturated period of the respective cells which has been simulated using the keyword RATES in PHREEQC (Parkhurst, 1995), which provides a means to trigger reactions by statements written in the programming language BASIC.

This modelling approach does not account for:

- reduction of sulphate:

The reduction of sulphate induced by using anaerobic water in the experiment depends mainly on the reactivity of available organic matter and the amount of sulphate and may vary over orders of magnitudes (Appelo and Postma, 1993). As the groundwater samples at the observation well, where our sediment has been taken, show high sulphate concentrations of 1400 mg/l, we assumed negligible reaction rates for sulphate reduction.

- kinetics for dissolution and precipitation of Fe-oxyhydroxides and the implied changes of exchange sites because of its high complexity
- weathering of feldspar:

Na^+/Cl^- ratios were 1 or below 1 during the whole experiment (Fig. 3.24) indicating that weathering of feldspar did not take place in that time scale

3.3.5.2.2 Transport

In this study the following transport parameters were defined (Tab. 3.6):

Tab. 3.6: Transport parameters

number of cells	20
number of shifts	20
timestep (s)	172800
upper boundary flux	const. flux
upper boundary flux	const. flux
diffusion coefficient (m^2/s)	0
length of the cell (m)	0.1
longitudinal dispersivity (m)	0

The diffusion coefficient and the dispersion were set to zero in order to simplify the problem and to gain a better understanding of the ongoing chemical reactions.

After each advective shift and dispersion step, kinetic reactions and chemical equilibria are calculated. The moles of pure phases and the composition of the exchange assemblage and kinetic reactants in each cell are updated after each chemical equilibration.

3.3.5.2.3 Dual porosities

The mixing process between the flooding water and the porewater in the unsaturated zone was simulated using the dual porosity concept. This concept takes account of the dual character of water in sediments with regard to flow: part of the water is mobile and flows along the conduits, while another part remains immobile or stagnant within the structural units. The porewater in our column was modeled as a stagnant part of water, whereas the incoming flooding water represents the mobile part. As the initial solution compositions of mobile and immobile water are defined equally the composition of the water in the cells does not change until the flooding water is entering the cells.

Based on measured moisture contents by TDR probes along a profile of the column before flooding the following mixing factors were defined in this study Tab. 3.7:

Tab. 3.7: Defined mixing factors of the column for the simulation

height (cm)	Porosity mobile cells	Porosity immobile cells
0-80	0.21	0.09
80 -200	0.25	0.05

This accounts for the fact that the upper parts of the column show lower moisture contents due to evaporation than the lower parts.

3.3.5.2.4 Solutions

The initial solutions of the mobile and immobile water in the column are derived by a representative water sample of the column after packing (Tab. 3.8).

Tab. 3.8: Initial solution defined for the column

Eh (mV)	pH	temp (°C)	Na (meq/l)	K (meq/l)	Ca (meq/l)	Mg (meq/l)	Fe (meq/l)	Mn (meq/l)	Cl (meq/l)	S(6) (meq/l)
120	3.72	20	1	0.18	12.5	4.0	4.3	0.18	1.4	18.3

The definition of one homogeneous initial solution composition for the entire column is only a simple approach to understand this complex hydrogeochemical system but does not account for its heterogeneity. As PHREEQC does not provide a possibility to model the unsaturated zone, the initial solution of the column was defined not only for the immobile water (porewater) but also for the mobile water for all cells, which does not exist physically in the beginning of the experiment. Therefore only the calculated results of the flooded cells have to be regarded in the simulations. The unsaturated cells of the column are simulated by PHREEQC as a mixture of two identical solutions (porewater and mobile water) as defined in Tab. 3.7 after each shift. Thus the composition of the porewater in the respective cells does not change until these cells become flooded. The initial composition of anaerobic flooding water was defined with a pH of 7 and Eh of 0 mV.

3.3.5.2.5 Ion exchange

Ion exchange is calculated by PHREEQC in terms of association reactions of exchanger and ions, with the constraint that all the exchange sites are always occupied by ions (Parkhurst and Appelo, 1999). The association reactions take the form of half reactions. The exchanger compositions in the transport model are recalculated after each transport step for all cells.

The initial exchanger compositions of our column are a result of equilibrium with the initial porewater solution after packing the column and are assumed to be more or less similar in the entire column at the beginning of the experiment under saturated conditions. This composition was calculated by PHREEQC by equilibrating a measured exchanger assemblage of 1,22 meq/100g CEC in our sediment with the initial composition of the porewater in the column.

Our modelling approach does not consider different exchange compositions along the column at the beginning of the experiment which are a result of different oxygen concentrations in soil air. Furthermore changing sites of exchangers due to the precipitation and dissolution of goethite are not taken into account.

3.3.5.2.6 Dissolution and precipitation

The precipitation of the Fe-oxyhydroxides goethite and amorphous $\text{Fe}(\text{OH})_3$ was allowed during the simulation using the keyword EQUILIBRIUM PHASES defining an initial amount of 0 moles.

Furthermore precipitation of gypsum was allowed throughout the simulation. As the analyzed initial porewater in our column was undersaturated in gypsum, the initial amount of gypsum was set to zero. If a solution becomes oversaturated in gypsum during the simulation the precipitated amount of moles will be saved for the next transport step in the respective cells.

Dissolution of feldspar was not taken into account because of the low weathering rates which can be neglected for the time period of our experiment. Dissolution of goethite is also not implemented in our model.

3.3.5.2.7 Uptake of weathering products and oxygen

The weathering products and oxygen were implemented in PHREEQC by applying the keywords RATES and KINETICS, using BASIC statements to limit the ongoing reactions to the saturated period of the respective cells.

The release of the weathering products from the sediment matrix into the incoming water and its corresponding rate laws are compiled in Tab. 3.9.

Tab. 3.9: Compiled stoichiometries and rate laws for uptake of weathering products and oxygen (F_{O_2} [mol/m²/s]: oxygen flux; C_s : concentration of solid species [meq/100g]; λ : dissolution constant [s⁻¹]; D_e : effective diffusion coefficient [m²/s]; O_2 : oxygen concentration [mol/l]; n: effective porosity; pO_2 : partial pressure of oxygen [atm])

Process	Stoichiometry	Rate law	parameter	Initial amount of moles per l soilwater (C_0)
Gypsum dissolution	1 Ca ²⁺ 1 SO ₄ ²⁻	$\frac{dC_s}{dt} = -\lambda C_s$	$\lambda = 10^{-4} \text{ s}^{-1}$ (zone 2 and zone 3)	5 mmol gypsum
Pyrite weathering products	1 Fe, 2 SO ₄ ²⁻ , 1 H ⁺	$\frac{dC_s}{dt} = -\lambda C_s$	$\lambda = 10^{-4} \text{ s}^{-1}$ (zone 2) $\lambda = 10^{-7} \text{ s}^{-1}$ (zone 3)	4.5 mmol Pyrite (zone 2) 19.5 mmol pyrite (zone 3)
Dissolution of Al(OH) ₃	1 Al, 3 OH ⁻	Immediate uptake at flooding front		0.1 mmol
Diffusion of atmospheric oxygen into the flooding front		$F_{O_2} = D_e \frac{\partial O_2}{\partial x}$	$D_e = (D_{\text{air}} + D_{\text{water}}) * n/2$	$pO_2 = 0.21 \text{ atm}$ (zone 3) $pO_2 = 0.05 \text{ atm}$ (zone 2)

Gypsum dissolution as well as the uptake of acid builders and the release of Al³⁺ were observed during the experiment. As the porewater solution after packing the column indicated

undersaturation of gypsum, the released gypsum during the flooding experiment must have been originated only by precipitation from the porewater solution during the unsaturated period. Therefore the available amount of gypsum (C_0) was set to 5 mmol which corresponds to the initial mass of Ca^{2+} in the mobile zone of the porewater.

The available amounts of weathered pyrite were derived by sediment analysis and a previous modelling study (Kohfahl et al., 2003). The sediment is characterized by an initial pyrite content of 0.04 wt. %, which has been partly oxidized during the unsaturated time period. The amount of available weathering products in the column were derived from the remaining pyrite contents after 100 days in Fig. 3.22, which were calculated in the previous modelling study. As the column was not irrigated during the time of fully unsaturated conditions it was assumed that the released weathering products remained fixed in their cells of origin. Starting from these results, available concentrations for the upper meter of the column were set according to a complete oxidation of pyrite resulting in 19.5 mmol pyrite per l soilwater. The available amounts of weathering products in the underlying 50 cm were set to 4.5 mmol assuming a degree of 25 % weathering. The uptake of pyrite weathering products was simulated using 1st order kinetics (Tab. 3.9). X-ray diffractometry analysis of sediment samples yielded the presence of trivalent iron-sulphate minerals like jarussite.

Buffering reactions by dissolution of $\text{Al}(\text{OH})_3$ were implemented defining an immediate uptake at the flooding front based on the assumption that gibbsite dissolves instantaneously. The available amount of gibbsite was used as a fitting parameter of the pH and was verified by the calculated and measured concentrations of Al^{3+} .

The contact of the flooding front with oxygen of soil air was considered by calculating the diffusion of oxygen into the upcoming water column according to Fick's Law (Tab. 3.9). D_e was calculated by the arithmetic average over the coefficient of diffusion in air ($10^{-6} \text{ m}^2/\text{s}$) and in water ($10^{-10} \text{ m}^2/\text{s}$) corrected for a effective porosity of 0.3. The oxygen concentration in soil air was obtained by the measured oxygen profile in the unsaturated part of the column which gave a partial pressure of oxygen about 0.2 in zone 3 and 0.05 in zone 2. It is interesting to notice that the measured oxygen profile of soil air remained constant in time during the flooding experiment although the upcoming water front moves anaerobic soil air into the upper part of the column. We assume that the expected drop of oxygen was compensated by enhanced diffusion of oxygen because of the increasing gradients of oxygen concentration in the column.

3.3.5.3 Calibration

In the following the main results of the geochemical model described in chap. 3.3.5.2 are compared with the results of the column study. In all figures the parameters are plotted versus the number of shifts during the saturated period of the respective cell, where each shift represents a rise of the waterlevel of 10 cm in the column. The lower part of the column is represented by data taken from a suction cup at 83 cm height, which provides the greatest number of data. To verify the results concerning the upper part of the column a sample taken at 173 cm height is included in the plots.

The calculated data were fitted to the observed pH values using an available amount of 0.1 mM $\text{Al}(\text{OH})_3$ (Fig. 3.28). Analyzed Al^{3+} concentrations of 3 mM were reproduced by a calculated concentration of 3 mM in the flooding front at 83 cm height of the column.

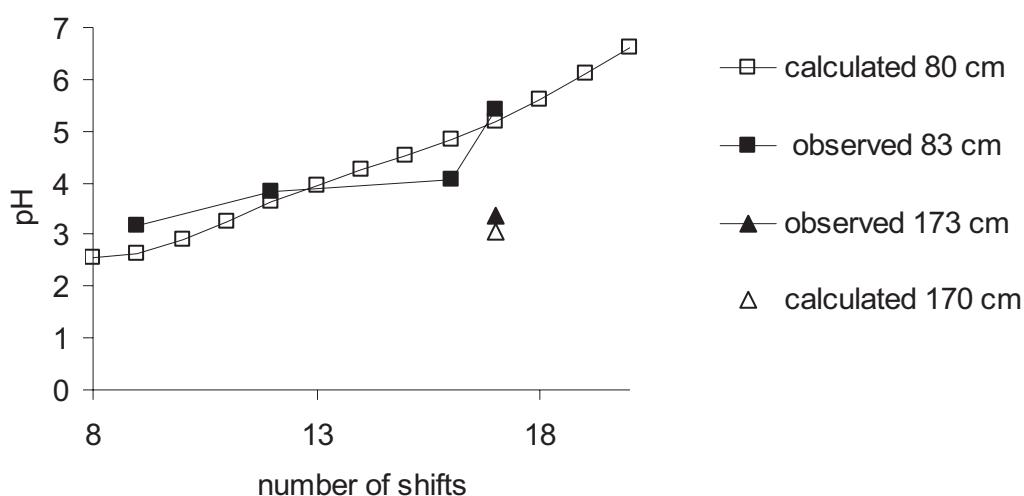


Fig. 3.28: Observed and calculated pH values.

Fig. 3.29 shows the observed and calculated concentrations of sulphate at two different heights of the column indicating consistent results.

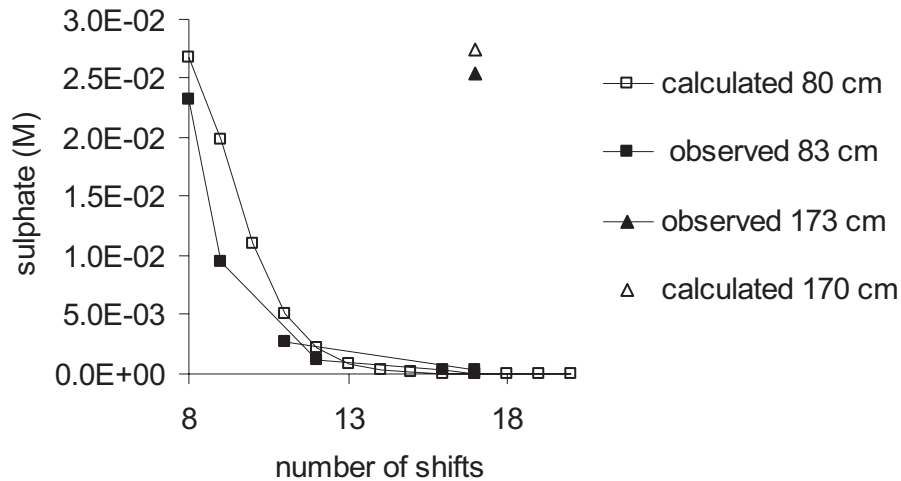


Fig. 3.29: Observed and calculated sulphate concentrations.

For both the observed and the calculated data the values at 80 cm and 83 cm height respectively indicate an exponential decline of the concentrations due to the dilution by the incoming water. The calibration yielded an almost immediate uptake of the available pyrite weathering products in zone 2 corresponding to a value for λ of 10^{-4} s^{-1} . For zone 3 a slow diffusion rate had to be defined to reproduce the sulphate concentrations measured at 173 cm height (Tab. 3.9). This is likely due to the clogging effects of pore spaces by precipitated Fe-oxyhydroxides in the aerobic part of the column.

The concentrations of iron in the solution are predominantly controlled by the pe and pH conditions of the solution and do not show a satisfying fit due to the fact that the kinetics of dissolution of goethite are not considered in our simulations (Fig. 3.30).

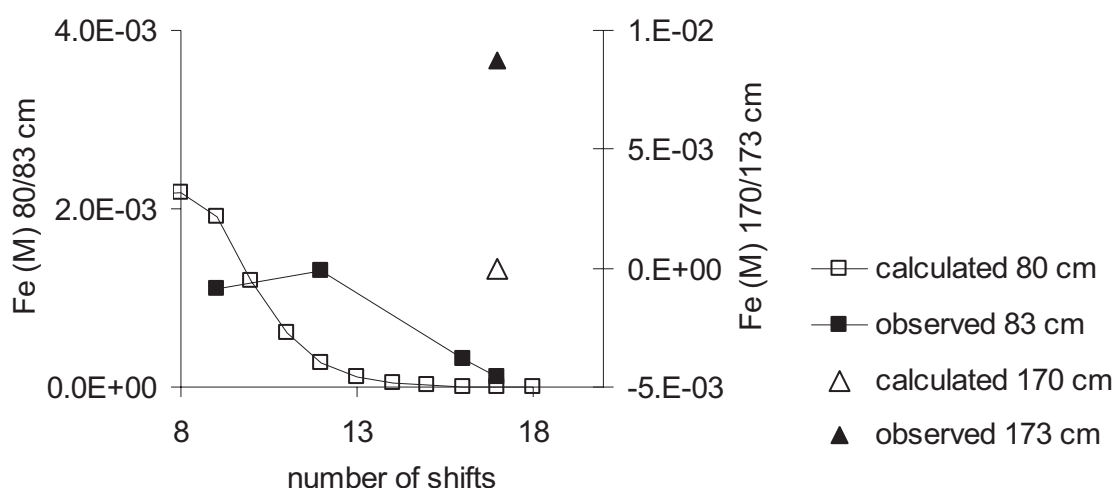


Fig. 3.30: Observed and calculated iron concentrations.

The analyzed sample yields strong oversaturation for goethite and also oversaturation of amorphous $\text{Fe}(\text{OH})_3$ indicating that no equilibrium was achieved during the experiment.

The plotted concentrations of Na (Fig. 3.31) illustrate the dilution of the original water of the column by the incoming flooding water.

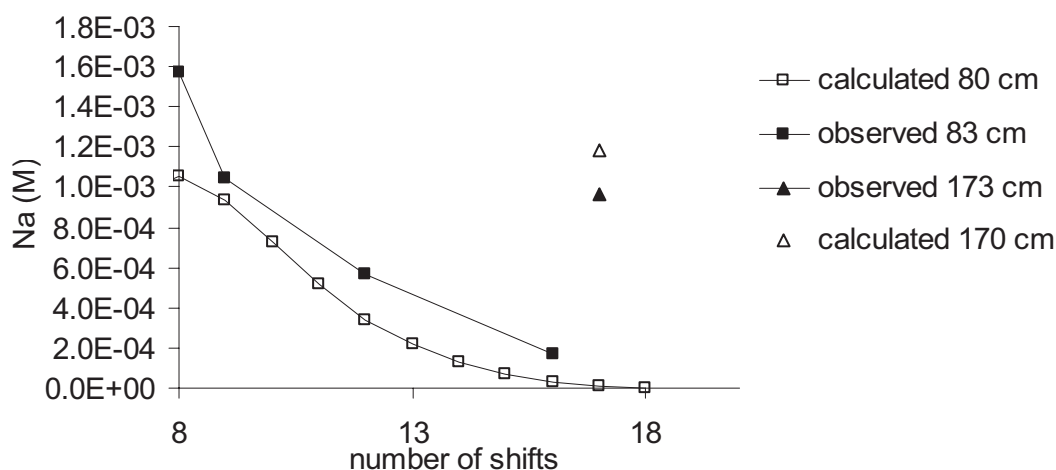


Fig. 3.31: Observed and calculated concentrations of Na.

The difference of the concentrations at shift 8 are likely due to the definition of one homogeneous initial composition for the entire column, which gave lower concentrations of sodium than the analysis at 83 cm at shift 8 and disregarded possible heterogeneities in the column. Measured and calculated concentrations at 173 cm height indicate that the max. concentrations of Na^{1+} are already obtained after less than 80 cm travel path.

The model calculated reasonable Ca concentrations with regard to the measured data (Fig. 3.32).

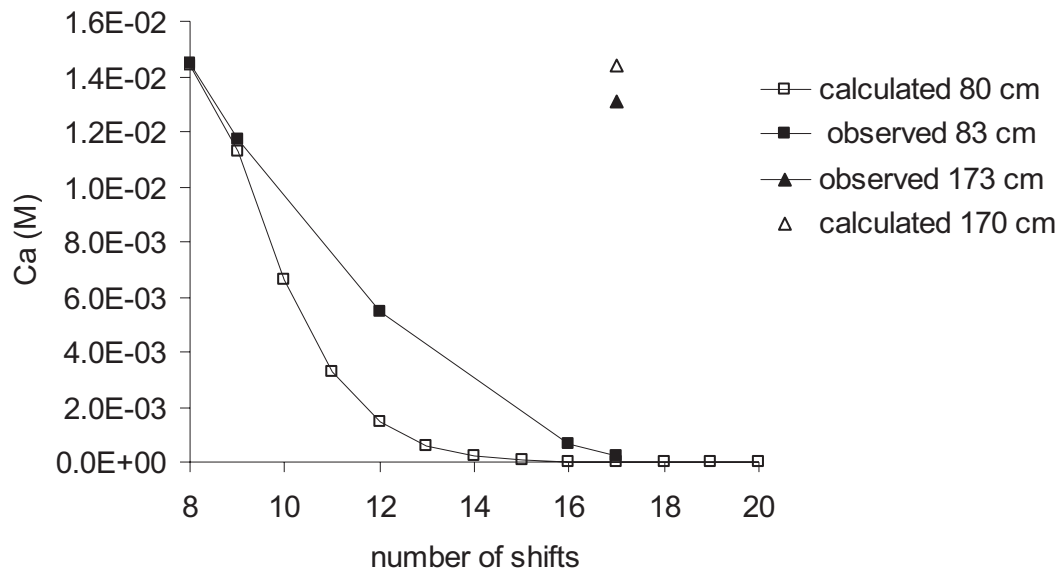


Fig. 3.32: Observed and calculated Ca^{2+} concentrations.

The slower decline of the observed data indicates that delivery of Ca^{2+} by gypsum dissolution is underestimated in our model. The max. concentrations are limited by the solubility of gypsum which is verified by observed and calculated data at 170/173 cm height.

3.3.5.4 Simulated results

The results of the geochemical model are documented based on three breakthrough curves of sulphate at different heights of the column (Fig. 3.33)

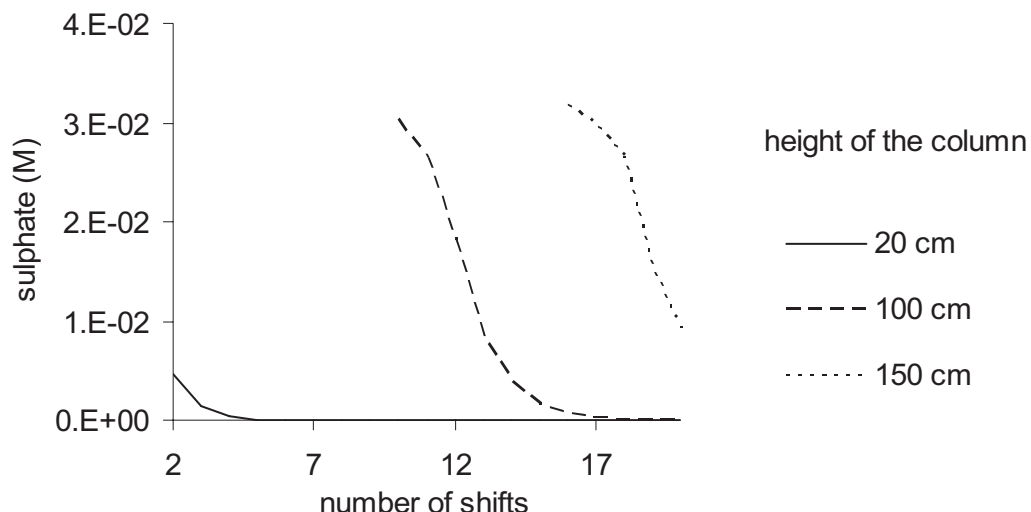


Fig. 3.33: Calculated breakthrough curves of sulphate at different heights of the column.

The undermost part of the column shows low sulphate concentrations which increase significantly until reaching 100 cm height, where gypsum saturation controls already the maximum concentration for sulphate, which remains more or less constant until reaching 150 cm. The slower decline of sulphate at 150 cm height is due to the higher amount of available weathering products which are released into the solution during more than one shift.

3.3.6 Conclusions and Outlook

In this study the uptake of weathering products by a rising watertable was modelled in a simplified approach using distilled water as flooding water. It was shown that the entire process could be described as a mixing process considering equilibria with Fe-oxyhydroxides minerals, uptake of weathering products and buffering reactions. Due to the lack of components in the flooding water exchange reactions had a negligible influence in this study. A complex kinetic control of dissolution and precipitation of Fe-oxyhydroxide by redox and pH conditions produced major differences between observed and calculated data of iron concentrations.

It is of interest to consider how far the capacity of this model is sufficient for a real mining environment, where in principle two different scenarios take place after decommissioning a mine. One of them is the rise of acid highly mineralised groundwater into partly oxidized unsaturated sediments, the second one is the elution of pyrite bearing sediments close to the shoreline of flooded lakes. Due to water oscillations in these lakes surface water infiltrates

into the sediments with rising surface water levels and exfiltration occurs during descending periods. In these scenarios exchange reactions become more important because of the different ionic compositions of the mixed types of water. Lower pH values may cause the dissolution of clay minerals and the release of aluminium, which was not taken into account in this study. Therefore future work will focus on adjusting this simple approach to more realistic conditions using data of further column experiments and field observations and to upscale the results to field conditions.

3.4 Estimating the effect of water table oscillations on acidification using a hydraulic model

3.4.1 Abstract

During and after the process of artificial recharge by flooding of former pit mines, oscillations of the water level, caused by seasonal effects or management strategies, are often inevitable. In the study area LOHSA in the new eastern federal states of Germany, the annual water oscillations due to management strategies are predicted to range between 5 and 8 m. This leads to oxygen input by freshwater and air, which causes pyrite oxidation in the surrounding sediments and leads to additional acidification of both groundwater and the flooded lakes. To quantify the contribution of water oscillations to the acidification processes in the flooded lignite mine LOHSA II, a two-dimensional vertical model was built up using PROCESSING MODFLOW. The strong lateral migration of the shoreline due to the low morphologic gradient was simulated by the reservoir package. The modeled transient water fluxes were used to estimate the discharge of acid builders from the water-saturated part of the heap into the lake. The contribution of acidification due to the continuous release of weathering products in the unsaturated zone was calculated separately. The modeled scenarios indicate that the contribution to acidification by release of weathering products from the unsaturated zone is small in comparison to the mass input by acid mine drainage from the saturated zone of the heap.

3.4.2 Introduction

Brown coal surface mining pits are anthropogenically disturbed geological systems. In the Lusatian region of eastern Germany, brown coal (lignite) has been extracted from large open-pit mines for over 50 years. The study area is the LOHSA II lignite mine near Hoyerswerda in southeastern Germany and belongs to the Lusatian Zone and is situated in the new federal states of Germany (Fig. 3.34).



Fig. 3.34: Study area.

It forms part of the NORTH GERMAN LOWLANDS and was dominantly shaped during the Pleistocene epoch by glacial and glaciofluvial processes. The exploited lignite is of Lower Tertiary age and is covered by 40 to 60 m of overburden of Quaternary sediments, which constitute mainly the material of the present heaps.

LOHSA II is to be flooded mainly with surface water until 2005 and will afterwards be used as a reservoir basin for the river SPREE (LmbV and Cottbus, 1996). To equilibrate the hydraulic head of the river, present management strategies are predicting annual surface water oscillations in LOHSA II between 5 and 8 m. This may lead to enhanced oxygen delivery by convection and diffusion providing optimal conditions for the oxidation of pyrite and subsequent leaching of associated weathering products.

Different models have already been applied to study geochemical processes at mine sites (Foos, 1997; Strömberg and Banwart, 1994). All these models usually consider equilibrium reactions, reaction kinetics. Some of them include diffusion of oxygen and reactive transport (Hecht et al., in press; Prein and Mull, 1995; Wunderly et al., 1996) but normally they are based on simulations assuming time-constant moisture contents of the sediment and disregard the effect of watertable oscillations

The aim of this research is to study the influence of watertable oscillations on the formation of acid mine drainage for the LOHSA storage system using a hydraulic model.

3.4.3 Hydrogeological frame

The general hydrogeological situation caused by surface water oscillations may be illustrated by Fig. 3.35 using a north-south orientated vertical profile.

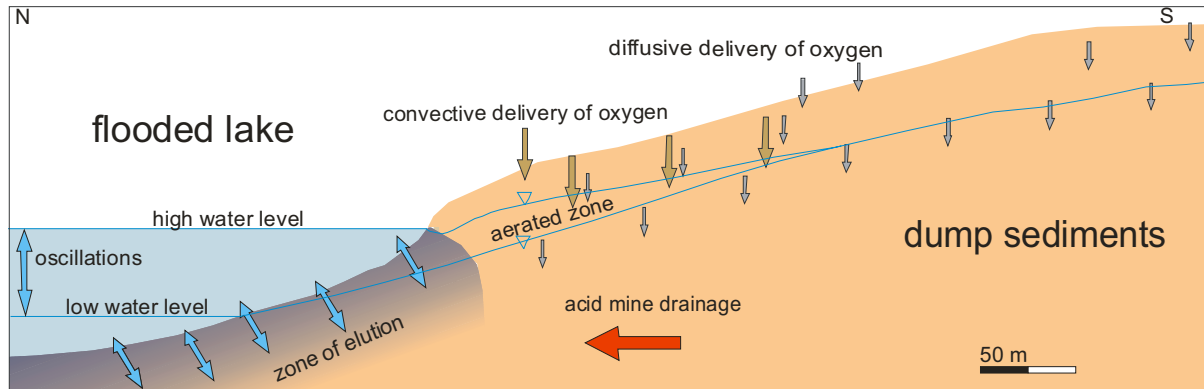


Fig. 3.35: Hydrogeological sketch.

The general groundwater flow is directed towards the north from the heap into the lake. This groundwater flow is superposed by annual oscillations of the surface water. During the ascending periods the aerobic surface water infiltrates into the sediment and leads to oxygen input into the heap. The descending period leads at first to the exfiltration of the previously infiltrated surface water. Afterwards the original groundwater from the heap, which is called here acid mine drainage (AMD) will also be discharged into the lake. The sediment area which is infiltrated by surface water is called here the eluated zone and the infiltrated water is named here elution water.

So the total input of acid builders into the lake depends on the following points:

- Volumes of exfiltrating water
- Acid charges of exfiltrating water
- Oxygen delivery in the unsaturated zone with subsequent pyrite weathering and release of acid builders

The volumes of exfiltrating groundwater into LOHSA II are strongly dependent on the water table oscillations and were calculated with PROCESSING MODFLOW.

3.4.4 Volumes of exfiltrating water

3.4.4.1 The hydraulic model

The volumes of exfiltrating water were calculated building up a transient, two-dimensional vertical model with PROCESSING MODFLOW (Chiang and Kinzelbach, 1998). The strong lateral migration of the shoreline due to the low morphologic gradient was simulated by the reservoir package. As the watersides in the study area have low morphologic gradients, water oscillations produce strong lateral flow components. To model these effects of periodic inundations, the computer program RES1 (Fenske et al., 1996), which is implemented in PROCESSING MODFLOW (Chiang and Kinzelbach, 1998), has been applied.

3.4.4.2 Model structure, boundary conditions and flow parameters

The model profile represents a 4.5 km long section of the pyrite-bearing dump south and upstream of LOHSA II and was oriented parallel to the groundwater flow direction (Fig. 3.36).

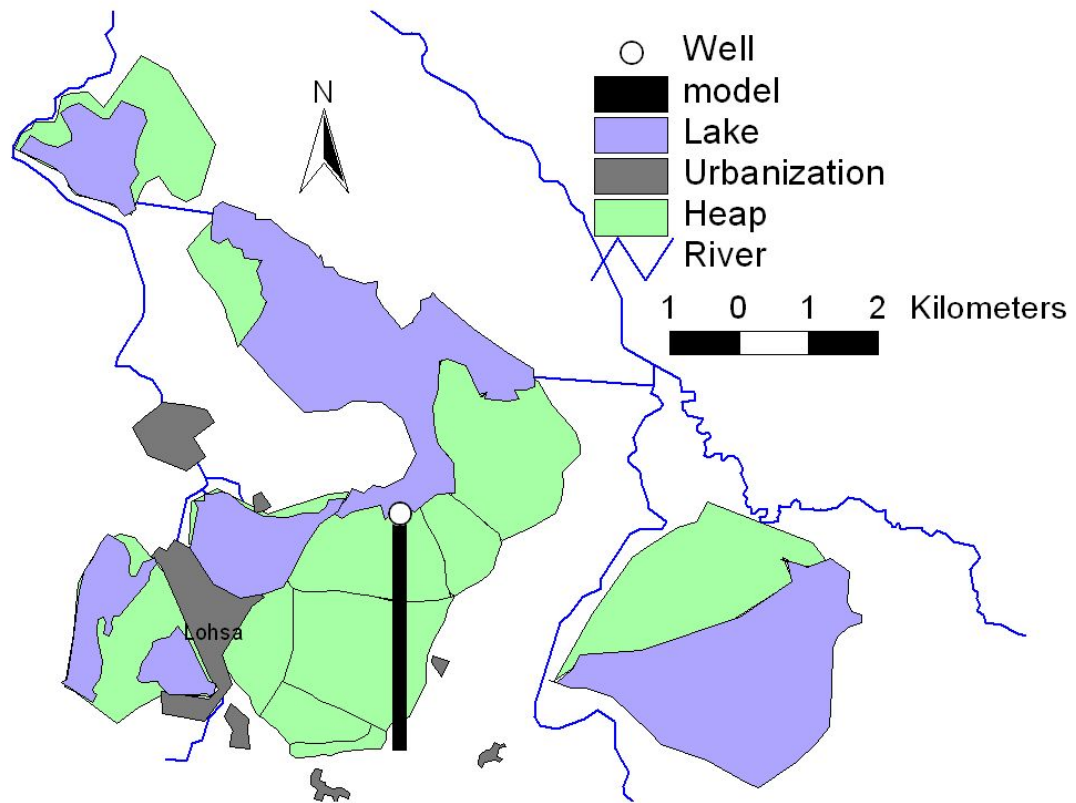


Fig. 3.36: Location of the vertical hydraulic model.

The model was discretized in 1635 cells with cell lengths between 100 m in the southern part and 10 m in the northern part near the surface water(Fig. 3.37).

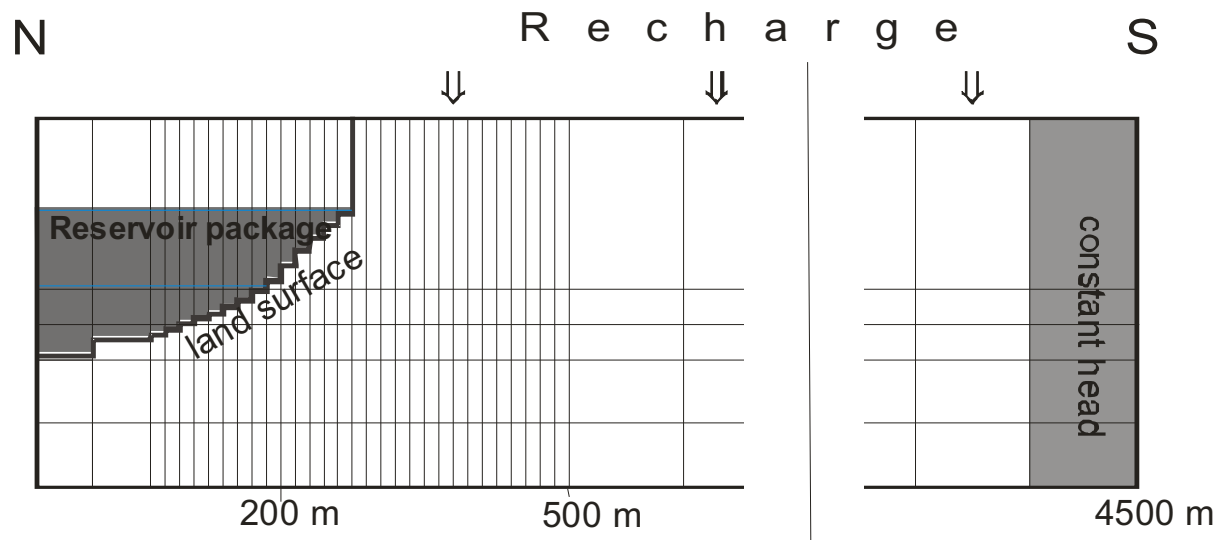


Fig. 3.37: Schematic sketch of the model structure (not scaled). The left part represents the area near Lohsa II and the right part documents the southern part of the model.

The base of the model corresponds to the base of the dump, where horizontal flow was assumed. To account for vertical flow components and to optimize particle tracking calculations, the model was divided into 5 layers, representing a total thickness of 85 m. The bottom elevation of the uppermost layer was defined beyond the lowest water level in the lake to avoid drying of cells. The uppermost layer was defined as unconfined.

The boundary conditions for the flow simulation are as follows:

- The southern model boundary has been modeled with fixed heads (Dirichlet-type) corresponding to measured piezometric heads of adjacent observation wells. The measured piezometric heads have not been influenced by flooding and are assumed to have reached their hydrostatical equilibrium.
- The region of temporal inundation due to surface water level oscillations in the north has been simulated with the reservoir package RES1 (Fenske et al., 1996) for the uppermost 3 layers, which considers lateral changes of shorelines typical for flooding scenarios. In this way water exchange for inundated regions between surface water and groundwater is computed in a manner identical to the Dirichlet-type boundary. To distinguish inundated and dry seasons, the land surface elevation and reservoir stages have to be defined for the individual cells in the region of potential inundation.

- The northern boundaries of the undermost 2 layers are simulated by no-flow boundaries (Neumann-type), assuming a water divide in the centre of the flooded lake. The laterals and the basement are set to no-flow boundaries.

As the dump consists mainly of polymixed fine-grained Quaternary sand with varying amounts of silt and gravel, for large scales it can be considered as homogeneous and therefore a unique k_f -value was specified for the whole model. Corresponding to the results of a pumping test and grain fractionation analysis an initial value of $k_f = 1 \times 10^{-5}$ m/s was defined. Groundwater recharge was set to 190 mm/year according to representative measured field data. The storage coefficient was set to 0.25 according to the results of our pumping test conducted in 2001.

3.4.4.3 Calibration

As hydrodynamics in the investigated area are strongly transient due to the groundwater rise in recent years, a transient calibration has been performed. Therefore measured piezometric heads of October 1997 have been defined as initial heads and the groundwater rise has been simulated by specified measured time-variant fixed heads (Dirichlet-type) and surface-water-stages of the reservoir (RES1) at the northern model boundary. The model was fitted to observed piezometric heads October 2000 by adjusting the k_f -value. The best fit between observed and calculated data was achieved when using a k_f -value of 4×10^{-5} m/s.

3.4.4.4 Scenarios

Corresponding to the above mentioned management strategy for LOHSA II the following scenarios have been simulated using the calibrated parameters:

- Scenario 1: Steady state high surface water level of 116 m NN in LOHSA II
- Scenario 2: Steady state low surface water level of 109.5 m NN in LOHSA II
- Scenario 3: annual oscillations of surface water between 109.5 and 116 m NN in LOHSA II for a time of 30 years. The initial heads for this scenario were calculated by a transient simulation of flooding starting with a surface water level of LOHSA II of 107 m measured in October 2000, which rises up to a reservoir stage of 116 m above sea level in 2005. The

time variant heads between low- and high level reservoir stage were always divided into 20 time-steps within a half year and interpolated linearly.

The evaluation of these scenarios aims to estimate the influence of changing water levels in comparison to a water management with a constant water table in LOHSA II with respect to acidification.

3.4.4.5 Evaluation of the scenarios with respect to discharge of elution water and AMD

To quantify the exfiltrating fluxes of water into LOHSA II, the following factors were taken into account:

- Discharge of acid mine drainage (AMD) from the heap into the lake
- Discharge of water from the heap into the lake, which has been infiltrated in the previous ascending period of surface water oscillation (elution water)

These factors refer to the discharge of water from the heap during the descending period of the surface water and. This water is mainly composed of two different types which are the original groundwater of the heap (AMD) and the elution water that infiltrated from the lake into the heap during the former ascending period (Fig. 3.35).

Scenarios 1-3 have been evaluated with regard to the discharge of the two different water types from the heap into the lake. The total discharge of elution water and AMD has been calculated based on flow balances with PROCESSING MODFLOW.

As the budget calculator of PROCESSING MODFLOW does not provide the direct calculation of fluxes along the reservoir package boundaries, the corresponding fluxes were computed based on the in- and exfiltrating volumes through the top of the adjacent cells below the RES1- boundary. These fluxes are equivalent to the in- and exfiltration rates respectively. Fig. 3.38 illustrates the situation for an ascending and a descending period leading to in- and exfiltration.

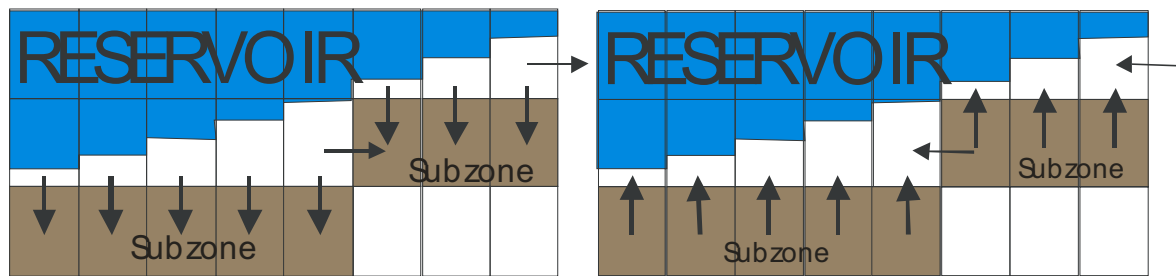


Fig. 3.38: Schematic sketch for the definition of subzones to calculate fluxes along RES1 boundaries (left: ascending surface water levels; right: descending surface water levels.

The lateral fluxes which occur at the displacements of the subzones have been disregarded due to its small amounts of less than 1% of the total fluxes.

The total exfiltration from the heap into the lake is composed of AMD and of infiltrated surface water of the previous ascending period. The amount of discharged elution water of the corresponding period is derived from the infiltrated volumes of the surface water of the preceding ascending phase. The resulting volumes for infiltration water, acid mine drainage and elution water are documented in Fig. 3.39.

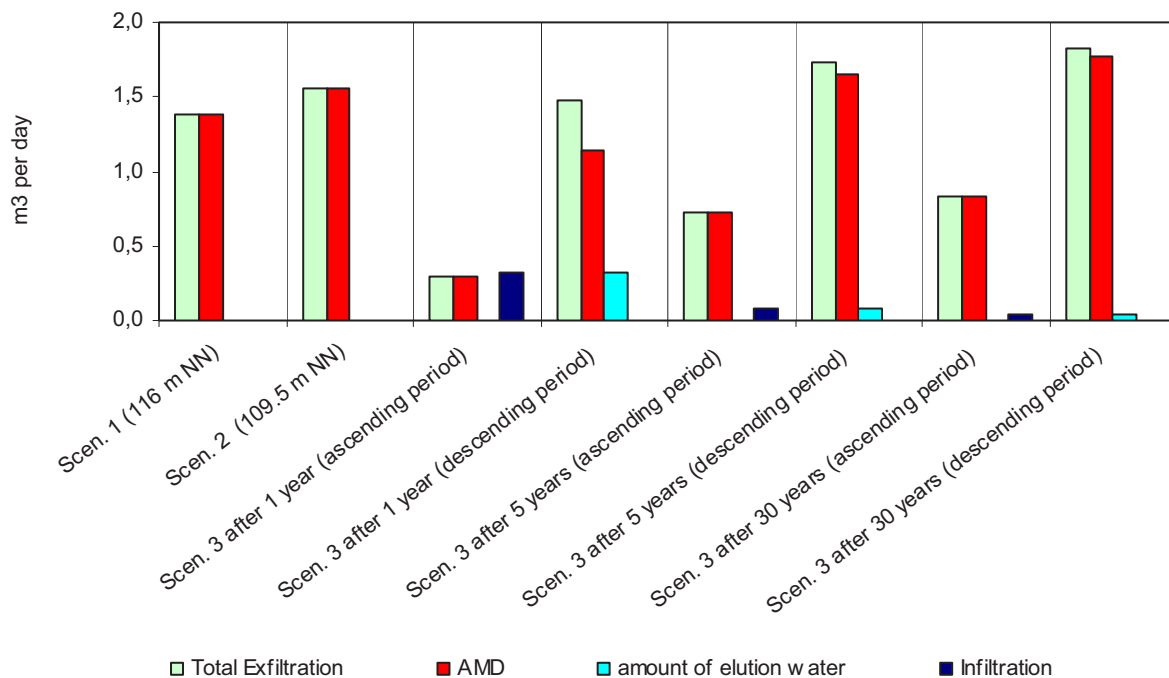


Fig. 3.39: Water discharge from the heap into the lake.

The first two columns represent the steady state scenarios resulting in higher exfiltration rates for low surface water levels due to the higher hydraulic gradient into the lake. Infiltration and elution water does not exist due to the lack of oscillations.

The following six groups of columns show the evolution of the respective water fluxes of the transient scenarios after one, five and thirty years in the corresponding ascending and descending periods. Fig. 3.39 shows that the total exfiltration during the descending periods of scenario 3 rises with time. This is due to the general trend of rising groundwater levels more distant to the lake, which is not directly influenced by surface water oscillations. This trend is related to the part of the former regional drawdown cone, which due to pumping during mining activities and has not recovered completely so far (Fig. 3.40). According to the simulation the greatest rise of groundwater takes place during the first 5 years until the potentials are getting close to hydrostatic equilibrium. After 5 years the total exfiltration rates in the descending period of scenario 3 show even higher exfiltration rates than the steady state scenarios, which is owing to the strong local hydraulic gradients near the surface water.

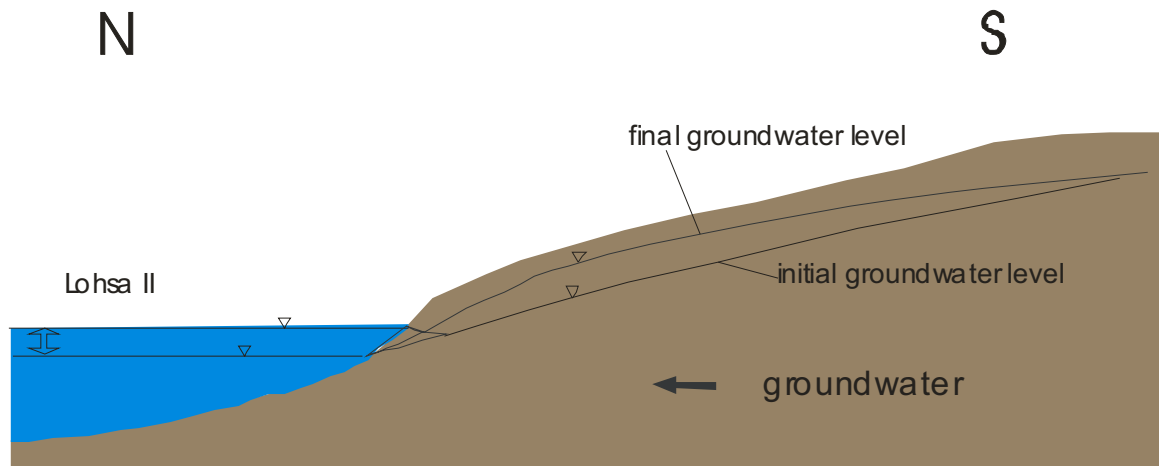


Fig. 3.40: schematic sketch of the simulated evolution of distant groundwater levels.

Another effect of the rising groundwater levels distant to the lake are descending infiltration rates with time in scenario 3. This leads to increasing amounts of acid mine drainage during the descending periods and to rising input of acids into the lake within the time of simulation.

3.4.4.6 Comparative calculations with respect to the elution zone

According to Schöpke et al. (1999) the depth of the elution zone can be calculated based on the following equation:

eq. 3.34

$$x_{ELU} = 2A \sqrt{\frac{k_f}{SH \omega}}$$

where:

- k_f - hydraulic permeability [m/s]
- x_{ELU} - maximum range of the elution zone [m]
- A - half amplitude of oscillation [m]
- S - storage coefficient [-]
- H - thickness of layer [m]
- ω - angular frequency ($= 2\pi/t$) [1/s]

The eq. 3.34 is based on the following assumptions:

- Vertical slope of the lakefront
- No hydraulic gradient between ground- and surface water

The resulting maximum range of the elution zone for an amplitude of 7 m and a storage coefficient of 0.25 is about 40 m. The real value in LOHSA II should be smaller because of the general hydraulic gradient towards the lake. It was estimated on the basis of the following equation, which results from a mass balance:

eq. 3.35

$$x_{ELU} = Q/b/l/n$$

where

Q: total infiltration volume

b: width of the model

l: horizontal distance between the lakefront at high water level and low water level

n: porosity

Defining the values 0.25 for n, 100 m for l, 1 m for b and 100 m³ for Q results in a value of 4 m for the thickness of the elution zone. The value for Q was set to 100 m³ assuming an infiltration rate about 0.6 m³/d during the ascending period (Fig. 3.39). The calculated thickness is only an average value, which can vary considerably along the elution zone.

3.4.5 Acid charges of the exfiltrating water

The estimation of acid charges is based on the previous computation of the fluxes of AMD and elution water and was completed by input sources from the unsaturated zone.

The acid charges that will result from the exfiltrating water volumes of the corresponding scenarios were calculated as follows:

eq. 3.36

$$\sum Ac = Q_1 * NP_1 + Q_2 * NP_2$$

where:

Ac: Acid builders

Q₁: Exfiltrated volume of AMD per year (summed up over 40 timesteps)

Q₂: Exfiltrated volume of elution water per year (summed up over 40 timesteps)

NP₁: neutralization potential of AMD

NP₂: neutralization potential of elution water

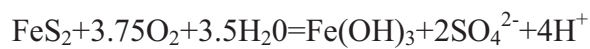
The total neutralization potentials NP₁ and NP₂ were calculated with reference to their contribution to acidity applying the concept of neutralization potential (NP) developed by Evangelou (Evangelou, 1995):

eq. 3.37

$$NP \text{ [meq/l]} = -[H^+] - 2[Fe^{2+}] - 2[Mn^{2+}] - 3[Al^{3+}] + [HCO_3^-]$$

The stoichiometric factors for pyrite weathering in our calculations are based on eq. 3.38.

eq. 3.38



NP₁ was calculated from analysis of groundwater in the heap (Tab. 3.10).

Tab. 3.10: Neutralization potential of acid mine drainage according to eq. 3.37 using analyzed groundwater samples

pH	5.50E+00
Concentration of protons (mmol/l)	3.16E-06
Alkalinity (meq/l)	2.1
Fe (meq/l)	7.5
Mn (meq/l)	2.00E-01
Al (meq/l)	0.023
NP₁ (meq/l)	-5.62E+00

NP₂ was defined according to eq. 3.37 and eq. 3.38. based on the release of acid builders which would result if an assumed oxygen content in the surface water of 10 mg/l would react with pyrite (Tab. 3.11).

Tab. 3.11: Assumed neutralization potential NP₂ according to eq. 3.37

dissolved O ₂ (mg/l)	1.00E+01
dissolved O ₂ (mmol/l)	3.13E-01
oxidated pyrite (mmol/l)	8.33E-02
released protons (mmol/l)	3.33E-01
released Fe ²⁺ (meq/l)	1.67E-01
NP₂ (meq/l)	-5.00E-01

The neutralization potential of the AMD (NP₁) has been assumed as constant during the period of the scenario. This assumption is based on column experiments with saturated dump sediments which have been flushed several times with different types of water (Gruetzmacher, 2001). The concentrations in the outlet of the columns declined considerably after 2-3 flushed pore volumes. Based on these results and assuming a travel velocity of 50 m per year in the heap and a travel length of 4.5 km, one pore volume would be completely flushed after 90 years.

The resulting acid charges of the corresponding scenarios are shown in Fig. 3.41.

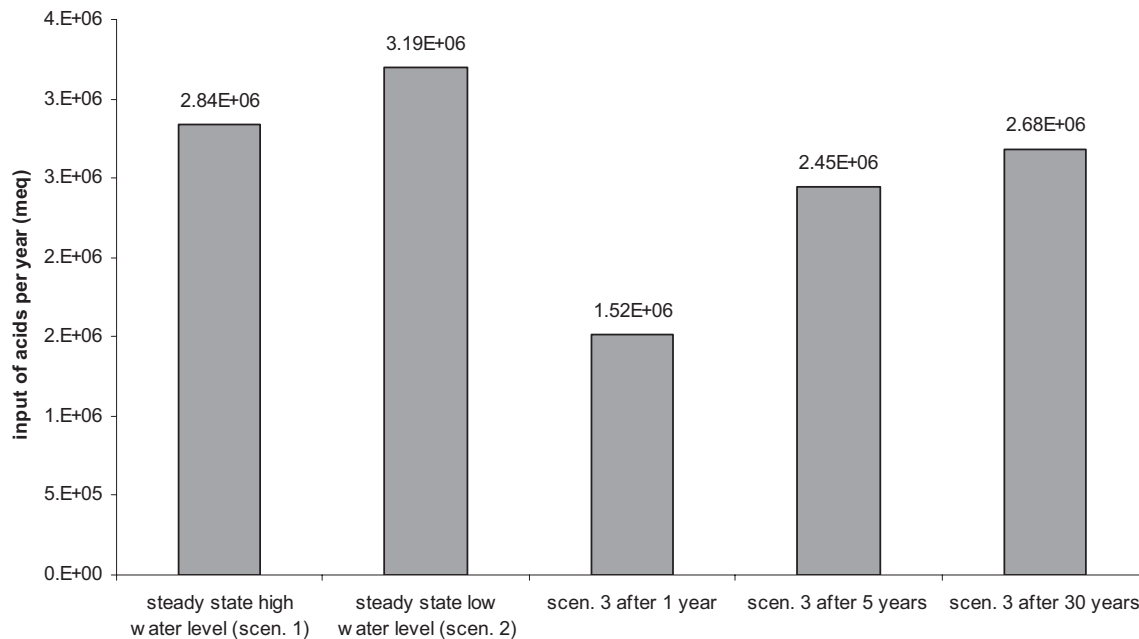


Fig. 3.41: Annual acid charges of the groundwater.

As the amounts of AMD in the exfiltrating periods are rising with time predominantly during the first 5 years (Fig. 3.39) the input of charges will rise analogically in this period. The fact that the total annual input of the transient scenarios is always smaller than the corresponding input of the steady state scenarios, is due to the ascending periods in the transient scenarios.

3.4.6 Input of acids from the unsaturated zone

The unsaturated zone represents a source term with respect to acid inputs, which is due to pyrite weathering caused by oxygen delivery. The released weathering products may reach the groundwater by vertical seepage water percolation or by rising groundwater levels. The actual quantity of weathering products in the unsaturated zone is a result of oxygen delivery into the sediment during recent decades. During the flooding period and the first 5 years of water management a great part of these weathering products will be taken up by the rising groundwater, which discharges with a certain retardation into the lake LOHSA II.

Furthermore the continuous delivery of oxygen into the sediment leads to ongoing pyrite weathering processes with subsequent release of acids.

On the basis of the following calculations some rough estimates with respect to the source terms in the unsaturated zone have been made. The assumptions for these calculations are:

- an annual oscillation amplitude of 7 m (assumed for present management strategies)
- an annual groundwater travel path of 50 m (derived from hydroisolines and available data of permeabilities)
- the zone where pyrite weathering processes take place has a vertical thickness of 3 m (estimated based on results of column experiments and similar studies in the literature)
- the distance of hydraulic influence by surface water oscillations in the heap is 500 m (calculated with the hydraulic model)
- the dry density of overburden material = 1850 kg/m^3

3.4.6.1 Uptake of weathering products

The quantity of existing weathering products in the unsaturated zone was derived from analyzed sediment parameters of a representative heap in our study area. The concentrations of H^+ , Al^{3+} , Fe^{2+} , and Mn^{2+} have been analyzed by Cation Exchange Capacity experiments (CEC) applying the BaCl_2 exchange procedure. Sulphate and alkalinity were analyzed based on batch experiments using distilled water(Tab. 3.12). The neutralization potential was calculated using eq. 3.37.

Tab. 3.12: Analyzed sediment parameters

	mmol per kg dry substrate	meq per kg dry substrate
$\text{H}^+(\text{CEC})$	0.13	0.13
$\text{Al}^{3+}(\text{CEC})$	12.57	37.71
$\text{Fe}(\text{CEC})$	0.13	0.26
$\text{Mn}^{2+}(\text{CEC})$	0.09	0.18
$\text{SO}_4^{2-}(\text{H}_2\text{O})$	0.85	1.70
HCO_3^-	4.44	4.44
neutralization potential		-33.84

Assuming an increase of the saturated sediment volume of 2000 m^3 after flooding LOHSA II, which was calculated by the hydraulic model in former studies (Hamann, 2002), this would lead to a total charge of $1.26\text{E}+08$ meq of acid species, which will travel with an average

velocity of 50 m per year towards the lake and cause considerable additive acidification of the surface water.

When interpreting these rough estimates it must be considered that the release of weathering products analyzed in the laboratory is much higher than in nature and represents a maximum value. The natural additional acidification by uptake of weathering products will act with smaller concentrations but for a longer period. The uptake of weathering products is therefore mainly owing to the rising groundwater level distant to the lake until hydraulic equilibrium will be reached.

3.4.6.2 Diffusive oxygen delivery in the gas phase

The estimation of acidification caused by oxygen delivery in the gas phase was performed using Fick's Law:

eq. 3.39

$$F = D_0 * n_a * \frac{\Delta C}{z} * \frac{1}{Tort^2}$$

where:

F : oxygen flux in $\text{mol s}^{-1} \text{m}^{-2}$

D_0 : molecular diffusion coefficient in $\text{m}^2 \text{s}^{-1}$ (25°C and 1 atm)

C : concentration of oxygen in mol m^{-3}

n_a : airfilled porosity

$Tort$: tortuosity

z : vertical distance in m

It was assumed that all the available oxygen reacts with pyrite and that all the released weathering products are transported into the groundwater by sewage water. The following input data have been defined in Tab. 3.13:

Tab. 3.13: Input data for calculation of oxygen diffusion

Average annual travel distance of groundwater	50	m
Area of the heap influenced by oscillations	500	m ²
Tortuosity (Tort)	4	
Depth of weathering front (z)	10	m
Airfilled porosity (n _a)	0.05	
change of oxygen concentration from surface to pyrite	8.7	mol/m ³
Molecular diffusion coefficient of oxygen in air	77	m ² /a

The average annual travel distance of groundwater of 50 m was derived using k_f -values (pumping test, grain fractionation analysis) and hydroisolines, which were constructed based on measured groundwater levels. The boundary condition for oxygen concentration was fixed by a partial pressure of 0.2 at the top of the heap which corresponds to a concentration of 8.7 mol oxygen per cbm atmosphere. Assuming that the oxygen concentration at the pyrite weathering front is zero the change of oxygen concentration along a vertical profile is 8.7 mol oxygen per cbm atmosphere. The depth of the pyrite weathering front where all oxygen is consumed was derived by analysis of sediment parameters and oxygen measurements of soil air in our study area. The airfilled porosity is a typical value measured for our periodically rewetted sediments which are characterized by high amounts of silt. The molecular diffusion coefficient of 77 m²/a is a widespread value in the literature. The tortuosity is defined as the quotient of real and direct travel length of a particle through the sediment and was derived by data taken from in-situ measurements of oxygen and sulphate profiles in the sediments of the study area (measured data provided by the Faculty of Environmental Sciences and Process Engineering of the University of Cottbus). The stoichiometric factors are based on eq. 3.38.

Based on these input parameters a total flux of 209.3 mmol oxygen per sqm and year was calculated using eq. 3.39. This leads to a release of 223.3 mmol protons per year and sqm according to eq. 3.38. The charges have been upscaled to a distance of 500 m, which is influenced by hydraulic oscillations. Assuming a groundwater travel distance of 50 m per year this results in an annual input of 1.12E+05 meq of acids into the lake. This value has to be interpreted as a maximum value, because the lowering flux of oxygen due to the migration of the pyrite weathering is not considered in these calculations. Furthermore we assumed that the total amount of oxygen in the sediment would react with pyrite, without considering the thickness of the pyrite weathering front. In spite of this the importance of diffusive oxygen

delivery in this case is small in comparison with the acid charges due to acid mine drainage as shown in Fig. 3.42.

3.4.6.3 Convective delivery of oxygen in gas phase

The calculation of convective oxygen delivery into the heap caused by water oscillations also assumes the complete reaction of the available oxygen amount with pyrite. The following parameters were defined:

Tab. 3.14 Input parameters for convective oxygen delivery in gas phase

Average annual travel distance of groundwater	50	m
Area of the heap influenced by oscillations	500	m ²
Vert. thickness of the pyrite weathering front	3	m
Aerated volume due to oscillations	1500	m ³
Airfilled porosity (n_a)	0.05	-
Partial pressure of oxygen in ground air (pO_2)	0.1	-

The partial pressure of oxygen was set to 0.1 in our calculations regarding biologic degradation and oxygen consumption in the subsurface.

The annual release of protons was calculated according to:

eq. 3.40

$$nH(+) = \frac{V * n_a * pO_2 * 4}{CF * 3.75}$$

where:

V : aerated volume of sediment

n_a : airfilled porosities

pO_2 : partial pressure of oxygen in soil air

CF : conversion factor from volume of gas to moles of gas (0.0224 for 10° C)

$nH(+)$: number of protons (moles)

The coefficient 4/3.75 regards the stoichiometric factors of the pyrite weathering reaction (eq. 3.38).

The defined aerated volume of pyrite bearing sediments results from the vertical thickness of the pyrite weathering front and the area of the heap influenced by oscillations. According to eq. 3.40 this would lead to an annual input of $3.57 \text{ E}+05$ meq protons assuming an average groundwater travel length of 50 m. The importance of convective oxygen delivery in this case is small in comparison to the acid charges due to acid mine drainage as shown in Fig. 3.42.

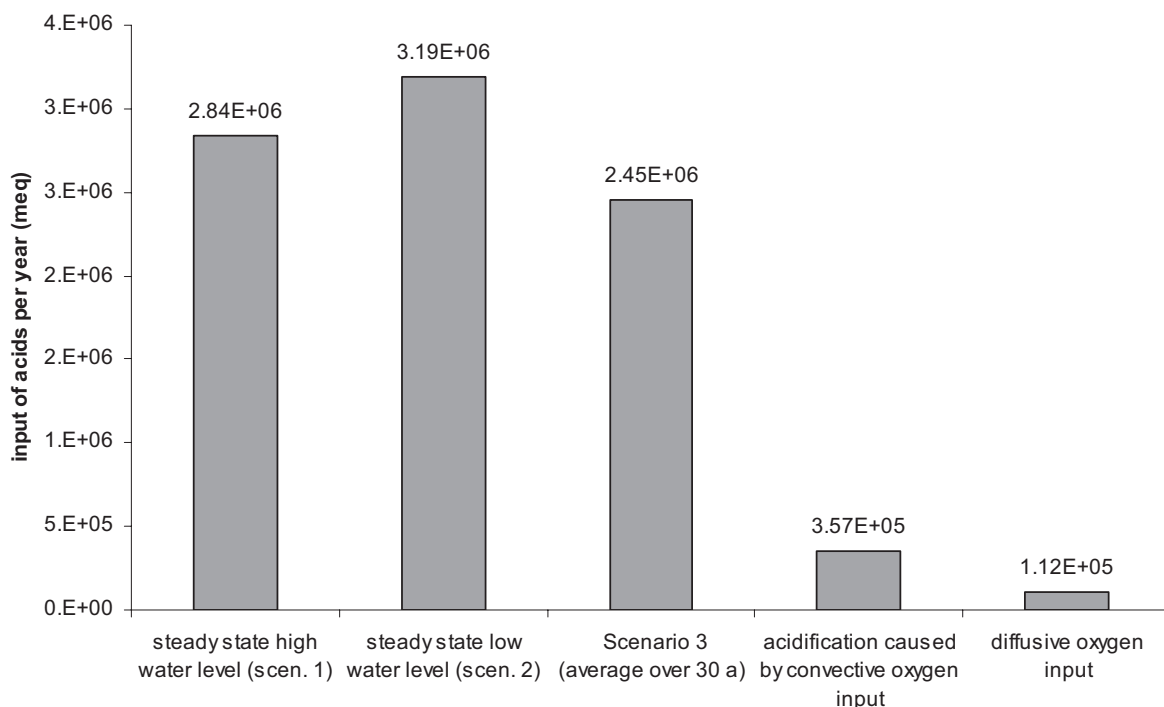


Fig. 3.42: Compiled amounts of acid input due to groundwater discharge and ongoing weathering processes.

3.4.6.4 Oxygen delivery by seepage water

The calculation of the oxygen delivery by seepage water is based on the assumption that 1 liter water contains 10 mg of oxygen which corresponds approximately to the maximum saturation index of oxygen in water. Regarding the average annual groundwater recharge of 200 mm this leads to an input of 2 g or 62.5 mmol oxygen per sqm. Upscaling this input to the hydraulically influenced area of 500 sqm and an average groundwater flow velocity of 50 m/a

this results in an annual oxygen input of $3.125 \text{ E}+04 \text{ mmol}$ which, according to eq. 3.38, corresponds to an annual acid charge of $3.3 \text{ E}+04 \text{ meq}$ into the lake. As these charges are not influenced by hydraulic oscillations they are not relevant to estimates of the influence of water oscillations on acidification.

3.4.7 Conclusions and outlook

This study indicates that by 2005 the uptake of weathering products owing to the rising groundwater table will cause strong acidification of the ground- and surface water. The ongoing weathering processes during the next decades will have a comparatively small influence on acidification in comparison to the mass input caused by the discharge of already generated AMD from the heap into the lake. The resulting water quality in the flooded lake will be controlled predominantly by the amounts of uncontaminated surface water which will be available for the recovery of LOHSA II during flooding and subsequent management of the storage basin. Future water oscillations will partly control the amounts of different water fluxes into the lake. Therefore their control on acidification is rather due to their influence on the amount of discharged acid mine drainage from the heap into the lake than to ongoing weathering processes.

The simulation approach demonstrated in the present paper provides a helpful tool for an initial estimate of the effect of surface water level oscillations on groundwater acidification due to pyrite weathering. However, because the regional water balance has not been taken into account, the quantitative results obtained from this study should be interpreted in a relative sense only. Much further work, including regional studies based on a 3-dimensional numerical transport model and its calibration using site-specific field and laboratory data, is necessary before quantitative predictions at a regional scale can be made.

4 Combined conclusions and outlook

The present studies show in which way the prognostic of acidification of a natural system depends both on hydraulic and on geochemical issues. In this case the oxygen delivery seems to be the limiting factor for the production rates of acids whereas the amounts of acid builders which are released into the surface depend strongly on hydraulic issues and on the water budget of the lake.

This study is again an example that a deeper understanding of the ongoing processes in nature only can be achieved using a combination of different methods and scales. The greatest challenge is the simplification of nature with its great number of parameters and uncertainties. Simplification is essential for a deeper comprehension but at the same time requires comprehension. Here a model can do a good job because it helps to separate important and less important parameters and enables to reduce complexity to its essential determining variables. Under this perspective the combination of field studies, laboratory experiments and modelling could lead us a step closer to reality.

The main results and also the remaining uncertainties of this study will be summarized in the following. All prognostic results enumerated in the following are based on the assumption that flooding of LOHSA II will continue until 2005 and afterwards water management will lead to periodic annual surface water oscillations of 7 m in the lake.

4.1 Field studies

- The exploited coal seam in the study area is of Lower Tertiary age and is covered by 40 to 60 m of overburden of predominantly Quaternary sediments, which constitute mainly the material of the present heaps. These heaps have an average thickness of 30-40 m and are characterized by a low acidification potential due to low pyrite contents about 0.04-wt-%.
- Nevertheless there are local heap areas showing higher acidification potential due to higher amounts of Tertiary sediments. This material is located predominantly southeast of LOHSA II and shows pyrite contents up to 25 %.
- The biggest heap areas are upstream of LOHSA II and have a max. extension of 4 km from north to south.

- The fault zone LAUSITZER HAUPTABBRUCH northeast to LOHSA II has uplifted some Tertiary sediments, leading to sporadic outcrops of this material, which is characterized by a high acidification potential.
- The aquifer system can be subdivided in 6 different aquifers. Only the two uppermost Quaternary aquifers are directly connected hydraulically with the surface water. The groundwater flow in these uppermost aquifers is orientated roughly from south to north.
- The sulphate concentrations of the groundwater show a clear dependency on the Tertiary amount of the surrounding sediments. The highest values between 2500 and 4000 mg/l (50-80 meq/l) were analysed southeast of LOHSA II, where the heap shows a Tertiary amount of 25 %. The surface water quality depends mainly on the amount of surface water used for flooding, which leads to sulphate concentrations of about 2500 mg/l in LOHSA II, where flooding had been realised exclusively by rising groundwater until the date of sampling. The lowest sulphate concentrations of about 200 mg/l have been measured in DREIWEIBERN, which had been flooded with great amounts of surface water.
- The analysed pH values can be interpreted analogue to the sulphate concentrations. The pH of groundwater shows a high dependency on the Tertiary amount of the surrounding sediments and the pH of the surface water depends on the amount of SPREE-water used during flooding. The pH of the surface water in LOHSA II shows values between 3.5 and 2.9 and the groundwater of the catchment area is characterized by a pH between 3.9 and 5.5. This is due to the release of protons during the formation of Fe-hydroxides when the groundwater exfiltrates into the surface water with aerobic conditions.

4.2 Main results concerning column studies and geochemical modelling

- The modelling approach of the column study revealed strongly reduced oxygen delivery for the sediment of our study area, leading to a penetration depth of less than 2 m after half a year of exposition to atmospheric oxygen. The high heterogeneity of the sediment and the elevated amount of silt are the determining factors for this result. Applied to field conditions the penetration depth of less than 2 m has to be interpreted as a maximum value considering the elevated moisture contents of the sediments in our study area. Therefore even high annual amplitudes of water oscillations about 7-8 m will cause oxygen penetration into the sediment of less than 2 m.
- The dependency of tortuosities on moisture content which has been revealed by our column study could not be upscaled to field conditions. This can be originated from the

different ranges of moisture contents in our column (0.05-0.1) and in the field (ca. 0.2). Furthermore preferential pathways may occur in the heaps due to its artificial deposition leading to higher permeabilities for gas flow. Also the local variability of the heap material may influence the tortuosity in a major way.

- The modelling approach of our column study could be upscaled using the dependency of tortuosities on moisture content, which was originally implemented in the source code of the Fortran code SAPY. The results could be verified using oxygen and sulphate measurements along a profile of 10 m in the unsaturated zone of the heap.
- Using the upscaled model, time dependent source terms for mass input of sulphate from the unsaturated zone into the groundwater could be derived for different depths of the groundwater table and for different amounts of natural recharge. The results indicate that the maximum input of sulphate into the groundwater - assuming an average depth of 12-15 m of the future groundwater table – are predicted between 20 and 40 years after the formation of the heap in the early 70's of the last century, depending on the amount of natural recharge.
- Oscillating water levels in the column during flooding did not influence the measured oxygen profiles in the unsaturated part. This may be due to the increasing concentration gradients of oxygen during flooding which lead to higher diffusive oxygen delivery and compensate the convective displacement of anaerobic ground air into higher parts of the column. This means applied to field conditions that oscillating water levels below the pyrite weathering front will not have a measurable influence on acidification. Also oscillating water levels above the pyrite weathering front do not have a measurable influence on acidification because no acid builders are generated by oxidation anymore. Therefore the greatest influence of water oscillations on acidification must be expected when the oscillations are occurring within the front of pyrite weathering.
- The measured uptake of weathering products by a rising watertable in a column study could be modelled with respect to sulphate in a simplified approach with PHREEQC. It could be illustrated that the entire process can be described as a mixing process in a double porosity medium considering kinetically controlled uptake of weathering products.

4.3 Main results concerning hydraulic modelling

- The annual surface water oscillations of 7 m will lead to a maximum infiltration depth of 40 m of surface water into the heap sediments upstream of LOHSA II.

- The surface water oscillations will be recognizable in the groundwater with descending amplitudes up to a distance of approximately 500 m to LOHSA II.
- Within the first years of periodic annual oscillations in LOHSA II the total annual exfiltration volumes of AMD in the descending periods into the lake will rise. This is due to the general trend of rising groundwater levels more than 500 m distant to the lake as retarded hydraulic response to the flooding of the lake. In this area the groundwater oscillations caused by water management are negligibly small. The trend of the rising groundwater table is expected to continue during the first 5 years until the conditions get close to hydraulic equilibrium.
- The rising volumes of AMD lead to rising input of acid builders within the first years of management.
- The hydrogeochemical evolution of the surface water depend predominantly on the relative amounts of surface water and acid mine drainage used for flooding. The influence of water table oscillations is comparatively small.

4.4 Outlook

However beside all these results there are a couple of questions which have to be solved in future and these questions are mostly related to the regionalization of the ongoing processes and the regional water budget. As the regional water balance has not been taken into account, the quantitative results obtained from this study can be interpreted in a relative sense only. So future investigations should focus on coupling the geochemical models developed in the present study with a calibrated regional hydraulic model, to account for the regional water budgets for different management scenarios. The developed geochemical models can be used to define temporal source terms for acidification in different regions of our study area in dependence on the type of sediment and the vertical thickness of the unsaturated zone. The results of the coupled modelling approach should be calibrated and verified using laboratory data and field data before quantitative predictions for the hydrogeological system can be made at a regional scale.

References

- Ahonen, L. and Tuovinen, O.H., 1989. Microbiological Oxidation of Ferrous Iron at Low Temperatures. *Applied and Environmental Microbiol.*, 2: 312-316.
- Albertsen, M., 1977. Labor- und Felduntersuchungen zum Gasaustausch zwischen Grundwasser und Atmosphäre über natürlichen und verunreinigten Gewässern. PhD thesis Thesis, Christian-Albrechts-Universität zu Kiel, Kiel, 145 pp.
- Appelo, C.A.J. and Postma, D., 1993. *Geochemistry, groundwater and pollution*. Balkema, Rotterdam, 536 pp.
- Bigham, J.M., Schwertmann, U., Traina, S.J., Winland, R.L. and Wolf, M., 1996. Schwermannite and the chemical modeling of iron in acid sulfate waters. *Geochemica et Cosmochimica Acta*, 60(12): 2111-2121.
- Brand, T., 1996. Numerische Simulation dreidimensionaler Strömungs,- Transport- und hydrogeochemischer Reaktionsprozesse um Grundwasserabstrom von Braunkohletagebaukippen. Besondere Mitteilung zum Deutschen Gewässerkundlichen Jahrbuch, 59. Landesumweltamt Essen, Essen.
- Bronswijk, J.J.B., Nugoroho, K., Aribawa, I.B., Groenenberg, J.E. and Ritsema, C.J., 1993. Modeling of oxygen transport and pyrite oxidation in acid sulphate soils. *J. Environ. Qual.*, 22: 544-554.
- Chiang, W.H. and Kinzelbach, W., 1998. *Aquifer Simulation Model for Windows - Groundwater flow and transport modeling, an integrated program*. Gebrueder Borntraeger, Berlin, Stuttgart.
- Cornell, R.M. and Schwertmann, U., 1996. *The Iron Oxides*, Weinheim, 573 pp.
- Currie, J.A., 1970. Movement of gases in soil respiration. In: S.C. Ind. (Editor), *Sorption and transport processes in soils.*, London, pp. 152-171.
- Davis, G.B. and Ritchie, A.I.M., 1986. A model of oxidation in pyritic mine waste. Part I: equations and approximate solutions. *Appl. Math.*, 10: 314-322.

- Dullien, F.A.L., 1991. Porous Media. Fluid Transport and Pore Structure. Academic Press, Inc., Boston, 574 pp.
- Elberling, B., Nicholson, R.V. and Scharer, J.M., 1994. A combined kinetic and diffusion model for pyrite oxidation in tailings: a change in controls with time. *J. Hydrol.*, 157: 47-60.
- Epstein, N., 1989. On tortuosity and the tortuosity factor in flow and diffusion through porous media. *Chem. Eng. Sci.*, 44(3): 777-779.
- Erikson, N., 1997. Coupling hydrological and chemical processes that affect field scale metal leaching from mining waste rock. *J. Hydrol.*, 194: 143-163.
- Evangelou, V.P., 1995. Pyrite oxidation and its Control. Boca Raton, Florida, C.L. Press, 293 pp.
- Fenske, J.P., Leake, S.A. and Prudic, D.E., 1996. Documentation of a computer program (RES1) to simulate leakage from reservoirs using the modular finite-difference ground-water flow model (MODFLOW). U.S. Geological Survey Open-File Report 96-364, U.S. Geological Survey.
- Foos, A., 1997. Geochemical modelling of coal mine drainage, Summit County, Ohio. *Environmental Geology*, 31(3/4): 205 - 210.
- Gerke, H., 1998. Modelling the effect of chemical heterogeneity on acidification and solute leaching in overburden mine spoils. *Journal of Hydrology*, 209: 166-185.
- Greskowiak, J., 2002. Sauerstoffeintrag und Pyritverwitterung in Braunkohlekippensedimenten (Säulenversuch und Modellierung). Diplomarbeit, unpublished Thesis, Freie Universität, Berlin, 66 pp.
- Gruetzmacher, G., 2001. Untersuchung zur Grundwassergüteentwicklung in der Bergbaufolgelandschaft. *Geologisches Jahrbuch Sonderhefte*, Reihe C, Heft SC 2, Hannover, B.f.G.u. Rohstoffe, 124 pp.
- Hamann, E., 2002. Bewertung des Einflusses von Seespiegelschwankungen auf den Sauerstoffeintrag in Kippensedimente des Tagebaurestloches Lohsa II (Niederlausitz) anhand einer instationären hydraulischen Modellierung. Diplomarbeit, unpublished Thesis, Freie Universität, Berlin.

- Hecht, H. and Kölling, M., 2001. A low-cost optode array measuring system based on 1 mm plastic optical fibers - new technique for in situ detection and quantification of pyrite weathering processes. *Sensors and Actuators, B* 81: 76-82.
- Hecht, H., Kölling, M. and Geissler, N., in press. DiffMod7 - modeling oxygen diffusion and pyrite decomposition in the unsaturated zone based on ground air oxygen distribution. *Geochemical Processes- Concepts for Modeling Reactive Transport in Soils and Groundwater*. Wiley-VCH, Weinheim.
- Herbert, R.B., 1996. Metal retention by iron oxide precipitation from acid groundwater in Dalarna, Sweden. *Appl. Geochim.*, 11: 229-235.
- Karathanasis, A.D., Thompson, Y.L. and Evangelou, V.P., 1990. Temporal solubility of aluminium and iron leached from coal spoils and contaminated soil materials. *J. Environ. Qual.*, 19: 389-395.
- Karavaiko, G.I., Kovalenko, T.V. and Piskunov, V.P., 1982. Effect of Fe(III)-Ions in the Oxidation of Ferrous Iron by *Thiobacillus Ferrooxidans* at Various Temperatures. *Microbiology*, 51: 156-160.
- Kleinmann, R.L.P. and Crerar, D.A., 1979. *Thiobacillus ferrooxidans* and the Formation of Acidity in Simulated Coal Mine Environments. *Geomicrobiology Journal*, 1 (4): 373-387.
- Kleinmann, R.L.P., Crerar, D.A. and Pacelli, R.R., 1981. Biogeochemistry of acid mine drainage and a method to control acid formation. *Mining Engng.*, 33 (3): 300-305.
- Kohfahl, C., Greskowiak, J. and Pekdeger, A., 2003. Modeling oxygen diffusion and acidification for extremely heterogeneous pyrite bearing sediments based on a column study. In: H.D.S.a.A. Haderl (Editor), *Geochemical Processes in Soil and Groundwater, Measuring-Modelling-Upscaling*. Wiley-VCH, pp. 640.
- Kölling, M., 1990. Modellierung geochemischer Prozesse im Sickerwasser und im Grundwasser. no. 8, Fachbereich Geowissenschaften der Universität Bremen, Bremen.
- Kölling, M. and Schüring, J., 1994. Pyrite weathering in coal mine tailings, 25th Congress of the IAH/IHWRS IEAust; Sydney. The Institution of Engineers, Australia, pp. 545-550.

- LMBV, 1997. Geotechnisch-hydromechanisches Grundsatzgutachten für die zweckmäßige Gestaltung von Böschungen an Tagebaurestseen am Beispiel des Wasserspeichers Lohsa II, Lausitzer und Mitteldeutsche Bergbau-Verwaltungsgesellschaft mbH, Berlin (not published).
- LmbV and Cottbus, B., 1996. Wissenschaftlich-technisches Projekt: Erfassung und Vorhersage der Gewässergüte in Tagebaurestseen der Lausitz als Basis für deren nachhaltige Steuerung und Nutzung., Cottbus, 56 pp.
- Marshall, T.J., 1959. The diffusion of gases through porous media. J. Soil Sci., 10: 79-82.
- Mayer, K.U., 2002. Multicomponent reactive transport modeling in variably saturated porous media using a generalized formulation for kinetically controlled reactions. Water Resources Research, 38 (9): 1174-1195.
- Millington, R.J., 1960. Transport in porous media, Trans. 7th Int. Congr. Soil Sci., pp. 97-106.
- Nordstrom, D.K., 1982. The effect of sulfate on aluminium concentrations in natural waters: some stability relations in the system $\text{Al}_2\text{O}_3\text{-SO}_3\text{-H}_2\text{O}$ at 298 K. Geochim. Cosmochim. Acta, 46: 681-692.
- Nowel, W., Bönisch, R., Schneider, W. and Schulze, H., 1994. Geologie des Lausitzer Braunkohlenreviers. c-macs publishing service Dresden, Senftenberg, L.B. Aktiengesellschaft, 102 pp.
- Parkhurst, D.L., 1995. PHREEQC - A computerprogram for speciation, reaction-path, advective-transport and inverse geochemical calculations. 95-4227, U.S. Geological Survey Water-Resources, Lakewood, Colorado.
- Parkhurst, D.L., 1997. Geochemical mole-balance modeling with uncertain data. Water Resources Research, 33(8): 1957 - 1970.
- Parkhurst, D.L. and Appelo, C.A.J., 1999. User's guide to Phreeqc (Version 2)- A computer program for speciation, batch-reaction, one dimensional transport, and inverse geochemical calculations. Water-Resources Investigations Report 99-4259, U.S. Geological Survey, Denver, Colorado.
- Penman, H.L., 1940. The diffusion of vapours through porous solids. J. Agric. Sci., 30: 437-463.

- Prein, A., 1993. Sauerstoffzufuhr als limitierender Faktor für die Pyritverwitterung in Abraumkippen, Mitt. des Inst. Wasserwirtsch., Hydrologie und landwirtsch. Wasserbau Univ. Hannover. Inst. Wasserwirtsch., Hydrologie und landwirtsch. Wasserbau Univ. Hannover, Hannover, pp. 126.
- Prein, A. and Mull, R., 1995. Pyritverwitterung in den Abraumkippen des Braunkohlebergbaus - die Sauerstoffnachlieferung als limitierender Faktor. In: L. Luckner and E. Föhl (Editors), Fachtagung: Rezente Flutungsprobleme mitteldeutscher und Lausitzer Tagebaurestlöcher. Dresdner Grundwasserforschungszentrum e.V., Coswig, pp. 93-109.
- Refsgaard, J.C., Christensen, T.H. and Ammentorp, H.C., 1991. A model for oxygen transport and consumption in the unsaturated zone. *Journal of Hydrology*, 129: 1350-1369.
- Rogowski, A.S., Pionke, H.B. and Broyan, J.G., 1977. Modeling the impact of strip mining and reclamation processes on quality and quantity of water in mined areas: a review. *J. Environ. Qual.*, 6: 237-244.
- Schwan, M., Fischer, R. and Dybek, K., 1988. Prognose von Acidität, Eisen- und Sulfatkonzentration im Grundwasser von Bergbaugebieten. *Acta Hydrochim. Hydrobiol.*, 16(6): 579-588.
- Sigg, L. and Stumm, W., 1991. *Aquatische Chemie*. Teubner Verlag, 388 pp.
- Strömberg, B. and Banwart, S., 1994. Kinetic modeling of geochemical processes at the Aitik mining waste rock site in northern Sweden. *Applied Geochemistry*, 9: 583-595.
- Stumm, W. and Morgan, J.J., 1981. *Aquatic Chemistry*. Wiley Interscience, New York, 780 pp.
- Stumm, W. and Morgan, J.J., 1996. *Aquatic Chemistry*. Wiley Interscience, New York, 1022 pp.
- Troeh, F.R., Jalal, D.J. and Kirkham, D., 1982. Gaseous diffusion equations for porous materials. *Geoderma*, 27: 239-253.
- van Breemen, N. and Harmsen, K., 1975. Translocation of iron in acid sulfate soils: I. Soil morphology and the chemistry and mineralogy of iron in a chronosequence of acid sulfate soils. *Soil Sci. Soc. Am. Proc.*, 39: 1140-1148.

- Walter, A.L., Frind, E.O., Blowes, D.W., Ptacek, C.J. and Molson, J.W., 1994a. Modeling of multicomponent reactive transport in groundwater, Model development and evaluation. *Water Resources Research*, 30(11): 3137 - 3148.
- Walter, A.L., Frind, E.O., Blowes, D.W., Ptacek, C.J. and Molson, J.W., 1994b. Modeling of multicomponent reactive transport in groundwater, Metal mobility in aquifers impacted by acidic mine tailings discharge. *Water Resources Research*, 30(11): 3149 - 3158.
- Wisotzky, 1996. Hydrogeochemische Reaktionen im Sicker- und Grundwasserbereich von Braunkohletagebaukippen. *Grundwasser*, 3-4: 129-136.
- Wunderly, M.D., Blowes, D.W., Frind, E.O. and Ptacek, C.J., 1996. Sulfide mineral oxidation and subsequent reactive transport of oxidation products in mine tailings impoundments - a numeric model. *Water Resources Research*, 32: 3173-3187.

Appendix

The following data were archived on a CD-ROM, which is deposited at the Hydrogeology Working Group of the Free University of Berlin (Prof. Pekdeger):

- digital text version

- laboratory data of the column studies

- sediment parameters

- hydraulic model (processing modflow)

- input files of the geochemical models (SAPY, PHREEQC)

Danksagung

Zuerst möchte ich mich sehr herzlich bei Herrn Prof. Pekdeger für die hervorragende Betreuung meiner Arbeit bedanken. Seine stete Gesprächsbereitschaft sowie seine fachliche Unterstützung trugen viel zu dem Gelingen dieser Arbeit bei. Dr. habil. Ekkehard Holzbecher danke ich für die freundliche Übernahme des Zweitgutachtens.

Großer Dank gilt Tony Appelo für seine vielen konstruktiven Hinweise. Bei Paul Brown und Claire Linklater der Arbeitsgruppe SULFIDE SOLUTIONS der AUSTRALIAN NUCLEAR SCIENCE & TECHNOLOGY ORGANISATION (Sydney) möchte ich mich vielmals für die nette Zusammenarbeit und Unterstützung bedanken.

Besonderer Dank gilt Ulrike Maiwald, Maja Tesmer und Andreas Winkler für die hilfreiche Unterstützung in dem Projekt.

Der Arbeitsgruppe des Lehrstuhls für Hydrologie und Wasserwirtschaft der Brandenburgischen Technischen Universität Cottbus und der Lausitzer und Mitteldeutschen Bergbau-Verwaltungsgesellschaft mbH (LMBV) danke ich für die freundliche Bereitstellung der Daten und die Einführung in das Untersuchungsgebiet. Herrn Dr. Benthaus danke ich für seine kompetente Zusammenarbeit und Projektkoordination.

Für die äußerst kompetente technische und auch fachliche Unterstützung bei der Fertigstellung der Sauerstoffsonden bedanke ich mich herzlich bei Henrik Hecht und Martin Kölling der Arbeitsgruppe Geochemistry and Hydrogeology der Universität Bremen.

Ich bedanke mich bei Michael Facklamm des Fachgebietes Standortkunde und Bodenschutz der TU Berlin für die Untersuchung der Sedimentdurchlässigkeiten. Herrn Torsten Schäfer des FZK Karlsruhe danke ich für die röntgendiffraktometrischen Analysen.

Den Diplomanden Janek Greskowiak, Martin Recker und Enrico Hamann danke ich für ihre selbständige und einsatzfreudige Arbeit! Janek möchte ich ganz besonders für die vielen anregenden Diskussionen danken. Frau Anne Beck danke ich vielmals für die Korrektur des englischen Textes.

Bei Herrn Prof. Günter Voigt bedanke ich mich für die Einführung in die Geologie und Problematik des Untersuchungsgebietes.

Und natürlich bedanke ich mich bei den zahlreichen Mitarbeitern des Arbeitskreises von Prof. Pekdeger. Ich danke Achim Bartels und Elke Weiss für die Durchführung der zahlreichen

Analysen, sowie Dietrich Lange für die professionelle Anfertigung der Säulen. Insbesondere gilt mein Dank Gudrun Massmann für die nette Zusammenarbeit während meiner Arbeit. Ich danke den Hiwis Martin Recker und Doreen Richter für ihren kompetenten Einsatz und ihre stets gute Laune. Mein Dank gilt außerdem Bettina Ohm, Andrea Knappe, Christian Sommer von Jamerstedt und allen anderen.

Mein allergrößter Dank gilt meiner Frau Susana für ihre Unterstützung und die vielen Tipps zum Layout, sowie meiner lieben Mutter.

Lebenslauf

Persönliche Daten

Familienstand: verheiratet

Nationalität: deutsch

Geburtsdatum: 09.07.1965

Berufliche Tätigkeit

seit 2000	Freie Universität Berlin (AG Hydrogeologie)
1996-2000	Grundwasser Consulting Ingenieurgesellschaft mbH Königs Wusterhausen
1995-1996	Stadtwerke Karlsruhe Abt. Grundwasserschutz und Hydrologie

Ausbildung

1986-1995	Universitäten Würzburg, Granada, Karlsruhe Geologiestudium (Diplom 1995)
1985-1986	Christian Albrecht Universität Kiel Chemiestudium (2 Sem.)
1985	Jürgen-Fuhlendorf-Gymnasium Bad Bramstedt Abitur

Ersatzdienst

1990-1991